

RESISTIVITY AND INDUCED-POLARIZATION RESPONSES
OVER TWO DIFFERENT EARTH GEOMETRIES

by

Hulya Hayriye Akman

A Thesis Submitted to the Faculty of the
DEPARTMENT OF GEOSCIENCES
In Partial Fulfillment of the Requirements
For the Degree of
MASTER OF SCIENCE
In the Graduate College
THE UNIVERSITY OF ARIZONA

1 9 8 8

STATEMENT BY AUTHOR

This thesis has been submitted in partial fulfillment of requirements for an advanced degree at The University of Arizona and is deposited in the University Library to be made available to borrowers under rules of the library.

Brief quotations from this thesis are allowable without special permission, provided that accurate acknowledgement of source is made. Requests for permission for extended quotation from or reproduction of this manuscript in whole or in part may be granted by the head of the major department or the Dean of the Graduate College when in his or her judgment the proposed use of the material is in the interests of scholarship. In all other instances, however, permission must be obtained from the author.

SIGNED: *H. Akmar*

APPROVAL BY THESIS DIRECTOR

This thesis has been approved on the date shown below:

James R. Wait
James R. Wait
Regents Professor of Electrical & Computer
Engineering and of Geosciences

24 June 1988
Date

ACKNOWLEDGMENTS

The author wishes to acknowledge her appreciation to Professor James R. Wait for his direction and supervision of this thesis. I would like to thank Professor J.S. Sumner and Professor M.N. Nabighian for their help. The author also wishes to thank Professor B. Sternberg for his useful comments.

In addition, I would like to thank the Turkish Government for the scholarship I was awarded which made it possible for me to attend graduate school. I thank Dr. T.P. Gruszka for his timely encouragement and helpful advice. The author also thanks to H.R. Houck for her helpful criticisms.

Finally, I would like to thank John Saba for \TeX typesetting assistance.

TABLE OF CONTENTS

	page
LIST OF ILLUSTRATIONS	6
LIST OF TABLES	9
ABSTRACT	10
1. INTRODUCTION	11
2. ANALYSIS OF APPARENT RESISTIVITY FOR DIFFERENT EARTH GEOMETRIES	14
2.1 Two-layer Horizontal Earth Model	14
2.1.1 Basic Derivation of Resistivity Formulas for Pole-Pole Array	15
2.1.2 Thin-sheet Limit for Pole-Pole Array	20
2.1.3 Basic Derivation of Resistivity Formulas for Dipole-Dipole Array	22
2.1.4 Thin-sheet Limit for Dipole-Dipole Array	24
2.2 Two Vertical Boundary Planes (Dike Model)	25
2.2.1 Use of Method of Images	26
2.2.1.1 Use of Method for Pole-Pole Array	27
2.2.1.2 Use of Method for Dipole-Dipole Array	31
2.2.2 Use of Bessel Integral Formulation for Thin-dike Limit	34
2.2.3 Numerical Examples	36
3. IP DILUTION AND DISTORTION PARAMETERS FOR DIFFERENT EARTH GEOMETRIES	63
3.1 IP Parameters over Thin Horizontal Layer	64
3.2 IP Parameters over Dike Model	69
3.3 Numerical Examples	74

TABLE OF CONTENTS—continued

4. CONCLUSIONS	93
APPENDIX A. CALCULATION OF POTENTIAL BY USING IMAGE METHOD	95
APPENDIX B. COMPUTER PROGRAMS	99
REFERENCES	117

LIST OF ILLUSTRATIONS

Figure	page
2-1 Resistivity Arrays and resistivity technique: a) Pole-pole array, b) Dipole-dipole array, c) Plan views of the resistivity technique	41
2-2 The geometry of a) Two-layer horizontal earth model, b) Thin horizontal layer	42
2-3 Ratio of apparent resistivity to the second-layer resistivity as a function of $r\rho_1/d\rho_2$ over thin horizontal layer a) for pole-pole array, b) for dipole-dipole array	43
2-4 Dike model	44
2-5 Some image points a) when current and potential electrodes are located left of dike b) when current electrode is left of dike and potential electrode is on dike	45
2-6 Some image points when both electrodes are on dike	46
2-7 Ratio of apparent resistivity to resistivity of surrounding material vs. distances d/a for pole-pole array when $b = 4a$	47
2-8 Ratio of apparent resistivity to resistivity of surrounding material vs. d/a for pole-pole array when $b = 2a$, a) over dike, b) over hemispherical sink (A. Peters, 1988)	48
2-9 Ratio of apparent resistivity to resistivity of surrounding material vs. d/a for pole-pole array when $b = a$	49
2-10 Ratio of apparent resistivity to resistivity of surrounding material vs. d/a for pole-pole array when $b = 0.5a$ and a) $\rho_2/\rho_1 = 10, 5, 1, 0.5, 0.1, 0.01$ over the dike b) $\rho_2/\rho_1 = 10$ over the dike (Dakhnow, 1962) c) $\rho_2/\rho_1 = 10, 5, 2, 0.5, 0.2, 0.1$ over hemispherical sink (Peters, 1988) . .	50

LIST OF ILLUSTRATIONS—continued

2-11	Ratio of apparent resistivity to resistivity of surrounding material vs. d/a for pole-pole array when a) $b = 0.25a$ and $\rho_2/\rho_1 = 10, 5, 1, 0.5, 0.1, 0.01$ b) $b = 0.5a$ and $\rho_2/\rho_1 = 5.67$ (Telford, 1976) c) $b = 0.25a$ and $\rho_2/\rho_1 = 5.67$ (Telford, 1976)	51
2-12	Ratio of apparent resistivity to resistivity of surrounding material vs. d/a when thicknesses of dike goes to infinity a) for pole-pole array, b) for dipole-dipole array	52
2-13	Ratio of apparent resistivity to resistivity of surrounding material vs. d/a for dipole-dipole array when $b = 4a$ and a) $\rho_2/\rho_1 = 10, 5, 1, 0.5, 0.1, 0.01$ on dike b) $\rho_2/\rho_1 = 10, 5, 2, 0.5, 0.2, 0.1$ on hemispherical sink (Peters, 1988) . . .	53
2-14	Ratio of apparent resistivity to resistivity of surrounding material vs. d/a for dipole-dipole array when $b = 2a$	54
2-15	Ratio of apparent resistivity to resistivity of surrounding material vs. d/a for dipole-dipole array when $b = a$ and a) $\rho_2/\rho_1 = 10, 5, 1, 0.5, 0.1, 0.01$ on dike b) $\rho_2/\rho_1 = 10, 5, 2, 0.5, 0.2, 0.1$ on hemispherical sink (Peters, 1988) . . .	55
2-16	Ratio of apparent resistivity to resistivity of surrounding material vs. d/a for dipole-dipole array when a) $b/a = 0.5$, b) $b/a = 0.25$	56
2-17	Ratio of apparent resistivity to resistivity of surrounding material vs. d/a for dipole-dipole array when a) $n = 1$, b) $n = 2$, c) $n = 3$, d) $n = 4$	57
2-18	Ratio of apparent resistivity to resistivity of surrounding material vs. d/a , a) for pole-pole array when $b = a$ and $\rho_2/\rho_1 = 100$, b) for pole-pole array when $b = a$ and $\rho_2/\rho_1 = 100$ (Dakhnow, 1962), c) for dipole-dipole array when $b/a = 0.25$ and $\rho_2/\rho_1 = 0.1$ (x: the curve we obtained, Δ : Ludwig's curve, 1967)	58
3-1	Dilution factor of thin layer, B_1 , and of second-layer, B_2 , vs. $r\rho_1/d\rho_2$ a) for pole-pole array, b) for dipole-dipole array	80
3-2	Distortion factor, a) for pole-pole array, b) for dipole-dipole array	81

LIST OF ILLUSTRATIONS—continued

3-3	When $b/a = 4$, a) dilution factor of dike for pole-pole array, b) distortion factor of dike for pole-pole array, c) dilution factor of dike for dipole-dipole array, d) distortion factor of dipole-dipole array	82
3-4	When $b/a = 2$, a) dilution factor of dike for pole-pole array, b) dilution factor of hemispherical sink for pole-pole array, c) distortion factor of dike for pole-pole array	83
3-5	When $b/a = 2$, a) dilution factor of dike for dipole-dipole array, b) distortion factor of dike for dipole-dipole array	84
3-6	When $b/a = 1$, a) dilution factor of dike for pole-pole array, b) dilution factor of hemispherical sink for pole-pole array (Peters, 1988), c) distortion factor of dike for pole-pole array	85
3-7	When $b/a = 1$, a) dilution factor of dike for dipole-dipole array, b) distortion factor of dike for dipole-dipole array	86
3-8	When $b/a = 0.5$, a) dilution factor of dike for pole-pole array, b) dilution factor of hemispherical sink for pole-pole array, c) distortion factor of dike for pole-pole array	87
3-9	When $b/a = 0.5$, a) dilution factor of dike for dipole-dipole array, b) distortion factor of dike for dipole-dipole array	88
3-10	When $b/a = 0.25$, a) dilution factor of dike for pole-pole array, b) distortion factor of dike for pole-pole array, c) dilution factor of dike for dipole-dipole array, d) distortion factor of dike for dipole-dipole array	89

LIST OF TABLES

Table	page
2-1 Numerical values of Struve function and Bessel function of second kind of order zero as a function of $x = r\rho_1/d\rho_2$	59
2-2 Numerical values of Struve function and Bessel function of second kind of order zero as a function of $2x, 3x, 4x$	60
2-3 Numerical convergence of ρ_a/ρ_1 for pole-pole array	61
2-4 Numerical convergence of ρ_a/ρ_1 for dipole-dipole array	62
3-1 Numerical convergence of B_2 and B_{22} for dipole-dipole array	90
3-2 Numerical examples to show effect of distortion term to apparent complex resistivity	91
3-3 Numerical examples to show effect of distortion term to apparent complex resistivity	92

ABSTRACT

The object of the thesis is to obtain the apparent-resistivity curves and induced-polarization (IP) effects that are utilized in geophysical exploration. Two different earth geometries, the thin horizontal conductive layer and vertical dike, were studied. The solution for both cases is identical. First, quasi-static electrical conditions were assumed, so that the problem could be solved using potential fields. The exact solution to the problem was obtained by using the Bessel integral formulation. Also, the image method was employed to find the potential fields. We noticed that the image-type series converges best when the dike or layer was thick (ratio of thickness to electrode spacing, b/a , is large) and the reflection coefficient was not near ± 1 . Otherwise, it is preferable to employ the thin conductive sheet model. The next step was to determine the dilution and distortion factors which are relevant to the induced polarization response. Finally, numerical results were obtained using a Fortran computer program. These calculations were compared with some results taken from the literature and good agreement is seen.

CHAPTER 1

INTRODUCTION

The induced-polarization (IP) method of geophysical exploration started with the work of Schlumberger in 1920. It has been developed for field exploration by Brant and his group at Newmont Exploration Limited during the late 1950s (Brant, 1981). The IP method is a special case of the complex-resistivity method, which is an extension of the resistivity technique. In the resistivity technique the voltage or potential difference is measured between two electrodes when an electric current is injected into the earth formations at two different electrodes. The current is then suddenly turned off, but the difference of potential does not immediately drop to zero in the IP technique. It will decay slowly over a period of time. During this phenomenon, when current flows from an electrolyte into a metal, chemical processes are involved (electrode polarization and overvoltage). Such processes can take place in rocks containing grains of conductive minerals, such as sulfides and oxide minerals, dispersed through the rock. At the boundary between the electrolyte and the metal, polarization effects are produced. When an electric current is passed through an electrolyte bounded by metal electrodes, the accumulation of the ions at the electrodes produces the phenomenon called polarization, which consists of an electromotive force acting in the opposite direction to the current, and producing an apparent increase of the resistance (Maxwell, 1892).

An important paper about the theoretical basis of the IP technique was published by Seigel in 1959. He formulated a relationship based on the proportionality of polarization with current density and defined chargeability, m , in terms of a change in resistivity. Then, he determined the apparent chargeability, m_a , for any

polarizable body and any electrode array. The apparent chargeability is a summation of all chargeabilities, m_i , times the weighting function or dilution factor, B_i . The dilution factors are obtained by simply differentiating the logarithm of the apparent-resistivity expression with respect to the logarithm of the resistivity of the medium that is polarizable. Such a result was obtained by Seigel (1959) using only first-order theory. Wait (1959) in the same year showed that a similar formulation could be developed in the frequency domain by admitting the possibility that the complex resistivities of the region are complex and frequency dependent. Also, he has showed that the higher order terms for the apparent resistivity may be important, particularly for highly polarizable media (Wait, 1981). He indicated that the apparent resistivity is complex and frequency dependent for time harmonic current sources to analyze IP responses. The second-order terms, which might be called distortion factors, involve double differentiation in the dc formulation.

In this thesis, we review an exact solution for the apparent resistivity and IP parameters, dilution and distortion factors, over a thin overburden layer, vertical dike, and single contact models. To introduce a family of dimensionless dilution and distortion functions, a two-electrode system (pole-pole) and a four electrode system (dipole-dipole) arrays are considered. First, the potential field of a pole-pole and dipole-dipole arrays, located on the surface of a thin horizontal conductive layer, is determined exactly by using the Bessel integral method. From the potential solution, dilution B_1 , B_2 , etc. and distortion factors B_{11} , B_{12} , etc. are derived for this earth geometry. The image technique is a relatively simple means of finding solutions to Laplace's equation for certain special but useful geometries. For this reason, the second part of this study deals with the apparent resistivity and dilution, and distortion factors observed on the surface due to an outcropping dike of any width, by using the image method. An electrical image is an electrified point or

system of points on one side of a surface which would produce on the other side of that surface the same electrical action which the actual electrification of that surface really does produce (Maxwell, 1892). Electrical images correspond to virtual images in optics in being related to the space on the other side of the surface. The method of images allows the removal of discontinuities in resistivity by introducing fictitious image current sources of the proper strengths (Ludwig, 1967). Although the image method gives the correct solution, the convergence of the series may be very poor for a thin dike that is highly conductive. Fortunately, the highly conducting thin dike case can be handled directly using a Bessel function transform model such as discussed by Wait (1982) and Aguirre (1986).

In this presentation, we assumed that a dike consists of a vertical slab of material bounded by two parallel planes and surrounded on both sides with a material whose resistivity is different from that of the dike itself. We solved the dike problem, because in geophysics two vertical contacts are a model for two parallel faults. The dike is assumed to be of infinite length in the direction of strike and of infinite depth extent. We also assumed that the electrodes are located on the surface of the dike. Such a dike formation and a borehole in an infinite formation are actually equivalent (Wait, 1986 and 1987).

The resistivity effect of a hemispherical sink should have some similarity with the resistivity effect of a vertical dike or a pair of vertical faults. So, it is useful to compare the results with Peters' (1988) computed resistivity and IP dilution curves for a hemispherical body for pole-pole and dipole-dipole configurations. Finally, the theoretical results of apparent resistivity and IP effects are compared the results of Dakhnov (1962), Ludwig (1967), Telford (1976), and Keller (1970).

CHAPTER 2

ANALYSIS OF APPARENT RESISTIVITY FOR DIFFERENT EARTH GEOMETRIES

2.1 Two-layer Horizontal Earth Model

Pole-pole and dipole-dipole arrays, as indicated in Figures 2-1a and b, at the surface of a two-layer earth model, are considered in this presentation. There is only one current, C , and one potential, P , electrode for a pole-pole array. In the field investigation, this is not possible. The second current and potential electrodes are placed at a large distance; they have practically no influence on the measurements. This array is also called half-Wenner. The second electrode array used is a dipole-dipole which has two current, C_1 and C_2 , and two potential, P_1 and P_2 , electrodes. The distance between electrodes is a . However, the distance between the first current and first potential electrodes depends on n which is any integer. When n is increased, deeper information is obtained. For this investigation, we chose n is 2. We also did some calculations for different ratio of resistivities of layers when n is 1, 3, and 4.

The potential field of these two arrays for electric direct current (dc) flow through the earth is determined by solving Laplace's equation for an appropriate set of boundary conditions. The purpose here is to examine an apparent resistivity for a two-layer earth model by using such potential equations. We also assumed that the thickness of slab is sufficiently small and can be represented as a thin sheet. Here the dc method is discussed to illustrate the use of the thin-sheet approximation (Fig. 2-2b). The kernel function and limiting case are used to solve this approximation over the thin-layer horizontal earth structure. In this geometry, let ρ_1 and

ρ_2 be the resistivities of the upper and lower horizontal layers, respectively, and d be the thickness of the first layer.

2.1.1 Basic Derivation of DC Resistivity Formula for Pole-Pole Array

The potential equation about a single point source of current above a homogeneous, isotropic earth can be developed from two basic considerations which are Ohm's law,

$$\mathbf{J} = \frac{\mathbf{E}}{\rho}, \quad (2.1)$$

and the divergence condition (Keller and Frischknecht, 1970),

$$\nabla \cdot \mathbf{J} = 0, \quad (2.2)$$

where the potential gradient $\mathbf{E} = -\text{grad}U$, \mathbf{J} is the current density, and ρ is the resistivity of the medium. These two equations may be combined to obtain Laplace's equation

$$\nabla^2 U = 0, \quad (2.3)$$

where U is a scalar potential function.

A Cartesian coordinate system is placed with its origin at C, x-axis parallel to the surface, positive y-axis downwards, and positive z-axis perpendicular to and out of the plane of the paper. The formal mathematical solutions for this medium must satisfy Laplace's equation (2.3) everywhere except at the point C. The solution of Laplace's equation in geophysical problems was first given by Stefanescu et al. during the late 1930s (Wait, 1982). In this part of the chapter, we will follow his steps for the mathematical solution of two-layer earth model. These mathematical solutions must meet the following boundary conditions.

- a) The potential is continuous at $z = d$

$$U_1 = U_2. \quad (2.4)$$

b) The normal current density is continuous at $z = d$

$$\frac{1}{\rho_1} \frac{\partial U_1}{\partial z} = \frac{1}{\rho_2} \frac{\partial U_2}{\partial z}. \quad (2.5)$$

c) The vertical current density must be zero at the surface of the earth

$$\frac{\partial U_1^s}{\partial z} = 0. \quad (2.6)$$

In cylindrical coordinates, U is a function of (r, z) . Because of a symmetry of the solution with respect to the vertical coordinate axis, the derivative of the potential with respect to ϕ must be zero. Therefore, there is no ϕ dependence in this geometry. In dc conditions, U satisfies the differential equation of Laplace's equation in cylindrical coordinates except at the source.

$$\frac{\partial^2 U}{\partial r^2} + \frac{1}{r} \frac{\partial U}{\partial r} + \frac{\partial^2 U}{\partial z^2} = 0. \quad (2.7)$$

This equation may be solved by separation of variables. Then, the solution of equation (2.7) can be written as

$$U(r, z) = R(r)Z(z). \quad (2.8)$$

Substituting equation (2.8) into (2.7), gives two ordinary differential equations for $R(r)$ and $Z(z)$:

$$\frac{\partial^2 R}{\partial r^2} + \frac{1}{r} \frac{\partial R}{\partial r} + \lambda^2 R = 0, \quad (2.9a)$$

$$\frac{\partial^2 Z}{\partial z^2} - \lambda^2 Z = 0, \quad (2.9b)$$

where λ is a separation variable.

The solutions of equation (2.9a) are Bessel functions of the first, $J_0(\lambda r)$, and second, $Y_0(\lambda r)$, kinds.

$$R(r) = AJ_0(\lambda r) + BY_0(\lambda r). \quad (2.10)$$

The Bessel function of the second kind, $Y_0(\lambda r)$, is infinite as r goes to zero. For this reason, it cannot appear in the present problem ($B = 0$). So $J_0(\lambda r)$ is the only solution of R . The solution of equation (2.9b) is

$$Z(z) = Ce^{\lambda z} + De^{-\lambda z}. \quad (2.11)$$

Using equation (2.10) and (2.11), the secondary potential U^s is obtained since it vanishes if the thickness of the layer goes to infinity (Wait, 1982).

$$U^s(r, z) = A' J_0(\lambda r) e^{-\lambda z} + B' J_0(\lambda r) e^{\lambda z}. \quad (2.12)$$

The secondary potential when $0 < \lambda < \infty$ is

$$U^s(r, z) = \int_0^\infty [A' J_0(\lambda r) e^{-\lambda z} + B' J_0(\lambda r) e^{\lambda z}] d\lambda. \quad (2.13)$$

We normalize the two coefficients by

$$A' = A \frac{I \rho_1}{2\pi}, \quad (2.14a)$$

and

$$B' = B \frac{I \rho_1}{2\pi}. \quad (2.14b)$$

If the potential electrode P is very close to the current source ($r \rightarrow 0$), the effect of the second layer can not be seen. Therefore, the ground seems to be homogeneous in all direction. When the current I is injected into the earth at the origin of the cylindrical coordinates, the potential can be taken to be

$$U^p = \frac{I \rho_1}{2\pi} \frac{1}{(r^2 + z^2)^{\frac{1}{2}}}, \quad (2.15)$$

where U^p is the primary potential. Then, the primary potential can be written in a form similar to the secondary potential by using the Weber-Lipschitz integral (Watson, 1944).

$$U^p = \frac{I\rho_1}{2\pi} \int_0^\infty J_0(\lambda r) e^{-\lambda z} d\lambda. \quad (2.16)$$

Finally, the resultant potential in the upper layer should be a summation of primary and secondary potentials:

$$U = U^p + U^s. \quad (2.17)$$

For a horizontally bedded earth, the resultant potential at $0 < z < d$ is determined by using equations (2.16), (2.13), (2.14a), and (2.14b)

$$U_1 = \frac{I\rho_1}{2\pi} \left[\int_0^\infty \left[(1 + A(\lambda)) e^{-\lambda z} + B(\lambda) e^{+\lambda z} \right] J_0(\lambda r) d\lambda \right]. \quad (2.18)$$

The appropriate form for the potential in the lower layer at $z > d$:

$$U_2 = \frac{I\rho_1}{2\pi} \left[\int_0^\infty C(\lambda) e^{-\lambda z} J_0(\lambda r) d\lambda + \int_0^\infty D(\lambda) e^{+\lambda z} J_0(\lambda r) d\lambda \right]. \quad (2.19)$$

In equation (2.19), the function $D(\lambda)$ must be zero because U_2 is finite as z becomes infinite. So equations (2.18) and (2.19) contain three unknown functions $A(\lambda)$, $B(\lambda)$, and $C(\lambda)$. The functions can be determined by applying boundary conditions equations (2.4), (2.5), and (2.6). Then, the constants A, B, and C are computed with Cramer's rule:

$$A = \frac{ke^{-\lambda d}}{(1 - ke^{-2\lambda d})}, \quad (2.20)$$

$$B = A, \quad (2.21)$$

$$C = 1 + \left(\frac{ke^{-2\lambda d}}{1 - ke^{-2\lambda d}} \right) (1 + e^{2\lambda d}), \quad (2.22)$$

where $k = (\rho_2 - \rho_1)/(\rho_2 + \rho_1)$ is defined as the reflection coefficient, which varies between +1 and -1. If the second layer is a pure insulator, i.e., $\rho_2 = \infty$, then $k = +1$ and if the second layer is a perfect conductor, i.e., $\rho_2 = 0$, then $k = -1$.

Hence, the potentials at $0 < z < d$ may be expressed by

$$U_1 = \frac{I\rho_1}{2\pi} \left[\int_0^\infty e^{-\lambda z} J_0(\lambda r) d\lambda + \int_0^\infty \frac{ke^{2\lambda d}}{1 - ke^{-2\lambda d}} (e^{-\lambda z} + e^{+\lambda z}) J_0(\lambda r) d\lambda \right]. \quad (2.23)$$

The surface potential U_1 at any point on the surface due to a current I is introduced (Wait, 1982).

$$U_1(r, 0) = \frac{I\rho_1}{2\pi} \left[\int_0^\infty J_0(\lambda r) d\lambda + \int_0^\infty [A(\lambda) + B(\lambda)] J_0(\lambda r) d\lambda \right]. \quad (2.24)$$

Using the Bessel integral identity (Watson, 1944)

$$\int_0^\infty J_0(\lambda r) d\lambda = \frac{1}{r}. \quad (2.25)$$

Then, the surface potential is obtained by

$$U_1(r, 0) = \frac{I\rho_1}{2\pi r} G(r, k), \quad (2.26)$$

where $G(r, k)$ is defined as a Green is function

$$G(r, k) = 1 + 2rk \int_0^\infty \frac{e^{-2\lambda d}}{1 - ke^{-2\lambda d}} J_0(\lambda r) d\lambda. \quad (2.26a)$$

or by

$$2\pi r \frac{U_1}{I} = \rho_1 G(r, k). \quad (2.27)$$

Now in the quantity on the left-hand side of equation (2.27), the ratio U/I is the resistance R , and so the left-hand side of the equation becomes $2\pi r R$ (Tagg, 1964). But this is the expression which when the pole-pole array is used in homogeneous soil gives the resistivity. Now, if the simple expression is used in the two-layer

problem, it gives an “apparent resistivity,” which is designated by ρ_a . So equation (2.27) can be written,

$$\rho_a = \rho_1 G(r, K). \quad (2.28)$$

From equation (2.28), it is possible to calculate ρ_a/ρ_1 for any given value of k .

2.1.2 Thin-sheet Limit for Pole-Pole Array

If the thickness of a slab is sufficiently small, it may be represented as a thin-sheet problem. The expression for the potential due to a point source of current on the surface of a layered earth is

$$U(r) = \frac{I\rho_1}{2\pi} \left[\int_0^\infty J_0(\lambda r) d\lambda + 2k \int_0^\infty \frac{e^{-2\lambda d}}{1 - ke^{-2\lambda d}} J_0(\lambda r) d\lambda \right]. \quad (2.29)$$

The solution of the first integral in equation (2.29) is, as already indicated, $1/r$. The second integral times the reflection coefficient is called the Stefanescu’s kernel function (Koefoed, 1979). It is controlled by the resistivities of the layers, ρ_1, ρ_2 , and by the depth of the boundary planes, d . The integral in equation (2.29) can be numerically evaluated by the kernel function. Substituting k into equation (2.29), we obtain

$$U(r) = \frac{I\rho_1}{2\pi} \int_0^\infty \left[\frac{(1 + \frac{\rho_1}{\rho_2}) + (1 - \frac{\rho_1}{\rho_2})e^{-2\lambda d}}{(1 + \frac{\rho_1}{\rho_2}) - (1 - \frac{\rho_1}{\rho_2})e^{-2\lambda d}} \right] J_0(\lambda r) d\lambda. \quad (2.30)$$

or

$$U(r) = \frac{I\rho_1}{2\pi} \int_0^\infty \left[\frac{1 + \frac{\rho_1}{\rho_2} \left(\frac{1 - e^{-2\lambda d}}{1 + e^{-2\lambda d}} \right)}{\frac{1 - e^{-2\lambda d}}{1 + e^{-2\lambda d}} + \frac{\rho_1}{\rho_2}} \right] J_0(\lambda r) d\lambda. \quad (2.31)$$

In this expression, $\frac{1 - e^{-2\lambda d}}{1 + e^{-2\lambda d}}$ is equal to $\tanh(\lambda d)$. Then, the surface potential is

$$U = \frac{I\rho_1}{2\pi} \int_0^\infty \left[\frac{1 + \frac{\rho_1}{\rho_2} \tanh(\lambda d)}{\tanh(\lambda d) + \frac{\rho_1}{\rho_2}} \right] J_0(\lambda r) d\lambda. \quad (2.32)$$

In equation (2.32), the term in bracket is the resistivity transform, $T(\lambda)$, introduced by Koefoed in 1970. The resistivity transform is defined by the equation

$T(\lambda) = \rho_1 K$, which has the same meaning as the subscript of the Slichter kernel function.

$$U = \frac{I\rho_1 d}{2\pi d} \int_0^\infty T(\lambda) J_0(\lambda r) d\lambda. \quad (2.33)$$

The resistivity transform has the physical dimension of a resistivity. The resistivity transform is also a function of the layer parameters and of λ , which has the dimension of a reciprocal length. There are some interesting analogies between the resistivity transform as a function of the length, $1/\lambda$, and the apparent resistivity as a function of the electrode spacing. In the analysis presented here, we assume that the slab is a thin conductive sheet. Therefore, as λd approaches zero, the hyperbolic tangent approaches λd , and equation (2.33) takes the form for a thin sheet

$$U = \frac{I}{2\pi g} \int_0^\infty \left[\frac{d + d^2 \lambda \frac{\rho_1}{\rho_2}}{\lambda d + \frac{\rho_1}{\rho_2}} \right] J_0(\lambda r) d\lambda \quad (2.34)$$

where,

$$g = \frac{d}{\rho_1} = \sigma_1 d \quad (2.34a)$$

where σ_1 is the conductivity of the surface layer, which is $1/\rho_1$.

Because the thickness of the conductive surface layer, d , is sufficiently thin ($d \rightarrow 0$), higher order terms of d are neglected. Thus, (Aguirre and Wait, 1985),

$$U = \frac{I}{2\pi g} \int_0^\infty \frac{1}{\lambda + \frac{\sigma_2}{g}} J_0(\lambda r) d\lambda. \quad (2.35)$$

where σ_2 is the second-layer conductivity, equal to $1/\rho_2$. By using the following identity,

$$\frac{1}{\lambda + \frac{\sigma_2}{g}} = \int_0^\infty e^{-(\lambda + \frac{\sigma_2}{g}x)} dx \quad (2.36)$$

and the Bessel integral identity given by Watson (1944, p. 331, #3 with $\omega = 0$ and $\nu = 0$),

$$\int_0^\infty \frac{1}{z + \lambda} J_0(\lambda r) d\lambda = \frac{\pi}{2} [\mathbf{H}_0(rz) - Y_0(rz)] \quad (2.37)$$

where $z = \sigma_2/g$, \mathbf{H}_0 is the Struve function, and Y_0 is the Bessel function of the second kind of order zero, the potential U is now written in terms of conductivity

$$U = \frac{I}{4g} \left[\mathbf{H}_0 \left(\frac{r\sigma_2}{g} \right) - Y_0 \left(\frac{r\sigma_2}{g} \right) \right]. \quad (2.38)$$

From equation (2.38), the apparent-resistivity formula over a thin horizontally bedded earth is evaluated (Aguirre and Wait, 1985):

$$\frac{\rho_a}{\rho_2} = \frac{\pi r \rho_1}{2 d \rho_2} \left[\mathbf{H}_0 \left(\frac{r \rho_1}{d \rho_2} \right) - Y_0 \left(\frac{r \rho_1}{d \rho_2} \right) \right]. \quad (2.39)$$

Figure 2-3a shows ρ_a/ρ_2 plotted as a function of $r \rho_1/d \rho_2$ on semi-logarithmic paper. It is computed by using Table 2-1.

2.1.3 Basic Derivation of Resistivity Formulas for Dipole-Dipole Array

The next system to look at is the dipole-dipole electrode system. Two of the electrodes (C_1 and C_2) are used to inject current into the earth and the other two electrodes (P_1 and P_2) are used to measure the potential difference (Fig. 2-1b). The dipole-dipole array has several advantages over most other expanding arrays. Many field geophysicist believe that the dipole-dipole array is logistically more efficient than the Schlumberger array. For this reason, the dipole-dipole electrode array is sometimes preferred in the field investigation. Disadvantages include sensitivity to unwanted lateral variations and relatively low signal levels (Ludwig, 1967).

Now, the general potential equation for this array should be written by using equation (2.24). The resultant potential U_1 measured at the first potential electrode, P_1 , for $n = 2$ can be found by using the expression for a general four-electrode array (Wait, 1982):

$$U_{1P_1} = \frac{I \rho_1}{2\pi} \left(\frac{G(3r, k)}{3r} - \frac{G(2r, k)}{2r} \right), \quad (2.40)$$

where,

$$G(3r, k) = 1 + 6rk \int_0^\infty \frac{e^{-2\lambda d}}{1 - ke^{-2\lambda d}} J_0(3\lambda r) d\lambda, \quad (2.40a)$$

and

$$G(2r, k) = 1 + 4rk \int_0^\infty \frac{e^{-2\lambda d}}{1 - ke^{-2\lambda d}} J_0(2\lambda r) d\lambda. \quad (2.40b)$$

The resultant potential U_1 for $n = 2$ at P_2 (Wait, 1982) is:

$$U_{1_{P_2}} = \frac{I\rho_1}{2\pi} \left[\frac{G(4r, k)}{4r} - \frac{G(3r, k)}{3r} \right], \quad (2.41)$$

where,

$$G(4r, k) = 1 + 8rk \int_0^\infty \frac{e^{-2\lambda d}}{1 - ke^{-2\lambda d}} J_0(4\lambda r) d\lambda. \quad (2.41a)$$

The voltage V between the electrodes is now given by:

$$V = U_{1_{P_1}} - U_{1_{P_2}}. \quad (2.42)$$

$$V = \frac{I\rho_1}{2\pi} \left[\frac{2G(3r, k)}{3r} - \frac{G(2r, k)}{2r} - \frac{G(4r, k)}{4r} \right]. \quad (2.43)$$

Thus, the apparent resistivity for a dipole-dipole array over a two-layer earth model is:

$$\begin{aligned} \rho_a = \rho_1 & \left[1 + 24kr \int_0^\infty \frac{e^{-2\lambda d}}{1 - ke^{-2\lambda d}} J_0(2\lambda r) d\lambda \right. \\ & - 48kr \int_0^\infty \frac{e^{-2\lambda d}}{1 - ke^{-2\lambda d}} J_0(3\lambda r) d\lambda \\ & \left. + 24kr \int_0^\infty \frac{e^{-2\lambda d}}{1 - ke^{-2\lambda d}} J_0(4\lambda r) d\lambda \right]. \quad (2.44) \end{aligned}$$

The integral in equation (2.44) can be evaluated numerically for an inhomogeneous ground.

2.1.4 Thin-sheet Limit for Dipole-Dipole Array

The surface potential for a thin-layer earth model can also be obtained by following same steps as was done by using a pole-pole array in section 2.1.2. One can obtain the resulting expression for V by assuming $\sigma_1 \rightarrow \infty$, $d \rightarrow 0$, but $\sigma_1 d = g$. After employing the identities given by equation (2.36) and (2.37), the potential can be written

$$V = \frac{I}{2\pi g} \int_0^\infty \frac{1}{\lambda + \frac{\sigma_2}{g}} \left[2J_0(3\lambda r) - J_0(2\lambda r) - J_0(4\lambda r) \right] d\lambda. \quad (2.45)$$

or

$$\begin{aligned} V = \frac{I}{2g} & \left[\mathbf{H}_0 \left(3r \frac{\sigma}{g} \right) - Y_0 \left(3r \frac{\sigma}{g} \right) \right. \\ & - \frac{1}{2} \mathbf{H}_0 \left(2r \frac{\sigma}{g} \right) + \frac{1}{2} Y_0 \left(2r \frac{\sigma}{g} \right) \\ & \left. - \frac{1}{2} \mathbf{H}_0 \left(4r \frac{\sigma}{g} \right) + \frac{1}{2} Y_0 \left(4r \frac{\sigma}{g} \right) \right]. \quad (2.46) \end{aligned}$$

Finally, the apparent-resistivity formula for a dipole-dipole array over a thin conductive sheet can be written as

$$\begin{aligned} \frac{\rho_a}{\rho_2} = \frac{\pi r \rho_1}{2 d \rho_2} & \left[2\mathbf{H}_0 \left(3 \frac{r \rho_1}{d \rho_2} \right) - 2Y_0 \left(3 \frac{r \rho_1}{d \rho_2} \right) \right. \\ & - \mathbf{H}_0 \left(2 \frac{r \rho_1}{d \rho_2} \right) + Y_0 \left(2 \frac{r \rho_1}{d \rho_2} \right) \\ & \left. - \mathbf{H}_0 \left(4 \frac{r \rho_1}{d \rho_2} \right) + Y_0 \left(4 \frac{r \rho_1}{d \rho_2} \right) \right]. \quad (2.47) \end{aligned}$$

The computed curve for ρ_a/ρ_2 as a function of $r\rho_1/d\rho_2$ for a dipole-dipole array, as indicated in Figure 2-3b, is computed by using Table 2-2.

Figures 2-3a and b show the apparent-resistivity anomalies for the thin-sheet layer situation. In both anomalies, ρ_a/ρ_2 begins at 0 for small values of distance $r\rho_1/d\rho_2$, then increase rapidly with a steep gradient towards 1.

2.2 Two Vertical Boundary Planes (Dike Model)

This thesis also deals with the apparent resistivity as observed on the surface of a dike. A dike is assumed to consist of a vertical slab of material bounded by two parallel planes and surrounded on both sides with a material whose resistivity is different from that of the dike itself. It is also assumed to be of infinite length in the direction of strike and of infinite depth. Consider the problem shown in Figure 2-4, that of a vertical dike of width $2b$. In this geometry, d is the distance from a current point to a midpoint of a dike and a is the distance between the current and potential electrodes. In the field investigation, the second current and the second potential electrodes are placed so far away (at infinity) that they have practically no influence on the measurements. The current electrode C is moved along a profile normal to the dike, and the potential V is measured at a point P a distance from the current electrode.

It is possible to mathematically determine the potential field above this medium with a half-Wenner array by solving Laplace's equation for the boundary conditions as was done for a two-layer earth in section 2.1. However, we first present a series of apparent-resistivity curves for a dike model by using the image method. The method of images is a relatively simple means of finding solutions of Laplace's equation along a profile that crosses a vertical contact. This method presents the resulting potential function in a manner that can be easily visualized (Ludwig, 1967). However, the image-type series converges very poorly when the dike is very thin and when it is highly conducting or very resistive.

We also solve the dike problem for a dipole-dipole array as in section 2.1.3.

2.2.1 Use of Method of Images

An electrical image is an electrified point or system of points on one side of a dike surface that would produce on the other side of the dike the same electrical action which the actual electrification of that surface of dike. In optics, points on one side of a mirror or lens, which if they existed, would emit the system of rays that actually exists on the other side of the mirror or lens, is called a virtual image (Maxwell, 1892). Electrical images correspond to virtual images in optics by being related to the space on the other side of the surface. They do not correspond to them in actual position, or in the merely approximate character of optical foci. There are no real electrical images, that is, imaginary electrified points that would produce in the region on the same side of the electrified surface an effect equivalent to that of the electrified surface (Maxwell, 1892). This method allows the removal of discontinuities in resistivity by introducing fictitious image current sources of the proper strengths (Ludwig, 1967). We shall now consider the solution of Laplace's equation in a medium with two vertical interfaces by using the method of images. Following the boundary conditions will be satisfied at two plane parallel boundaries

- a) $U \rightarrow 0$ as $r \rightarrow \infty$,
- b) $U_1 = U_2$ at ρ_1, ρ_2 and ρ_2, ρ_1 interfaces,
- c) $\frac{1}{\rho_1} \frac{\partial U_1}{\partial r} = \frac{1}{\rho_2} \frac{\partial U_2}{\partial r}$ at interfaces.

It can be shown that the boundary conditions at a vertical contact plane can be satisfied by placing an image source at the mirror point of each of the real sources with respect to this contact plane; the current intensity assigned to this image source should be kI , where k is the reflection coefficient and I is the current intensity of the real source (Koefoed, 1979).

Using this image method, we will solve the thin- and thick-dike models for pole-pole (half-Wenner) and dipole-dipole arrays. One can also use the two-layer

horizontal earth model to find image points for dike model, because the dike and two-layer models are the same type of problem.

2.2.1.1 Use of Method for Pole-Pole Array

As the pole-pole array crosses the dike at right angles, we have five possible situations, depending on electrode positions with respect to the contact. For this derivation, we again keep V to the right of I . The distance a between C and P is always constant in every position; we just move the electrodes from left to right on the profile.

In the first case, we will assume both the current and measuring electrodes are to the left of the dike (Fig. 2-5a). An electric current of I (amperes), introduced into the earth with resistivity ρ_1 (ohm-meters) through a point electrode C placed on the surface of the earth and another electrode placed at infinity, will give the potential function as if the earth were homogeneous

$$V_1^0 = \frac{I\rho_1}{2\pi a}, \quad (2.48)$$

Having image current sources whose resulting potentials are added to the real current source potential. The current source I at C has an image in the dike at C' caused by reflection in the first boundary. This image point can be written as $k_{21}I$, where k_{21} is the reflection coefficient from the first boundary, if the origin of coordinates is taken to be at the measuring electrode and this is located a distance $(2d - 2b - a)$ from the potential electrode. The current from this image source gives rise to a potential in medium 1 as follow:

$$V_1' = \frac{I\rho_1}{2\pi} \frac{k_{21}}{(2d - 2b - a)}. \quad (2.49)$$

There is a second image of C reflected in the second boundary at C'' , which is located in medium 3. The second image point is obtained by transmitting the current from the first medium to the second medium, τ' , and reflecting in the second boundary, k_{12} . Then the potential from the electrodes, located over the first medium, is measured from the second image point at distance $(2d + 2b - a)$ which is also transmitted from the second medium to the first medium, τ , and the current from image C'' gives the potential in medium 1 as

$$V_1'' = \frac{I\rho_1}{2\pi} \frac{k_{12}\tau\tau'}{(2d + 2b - a)}, \quad (2.50)$$

where

$$\tau = (1 - k_{21}) = \frac{2\rho_1}{\rho_1 + \rho_2}, \quad (2.51)$$

$$\tau' = (1 + k_{21}) = \frac{2\rho_2}{\rho_1 + \rho_2}, \quad (2.52)$$

and

$$k_{12} = \frac{\rho_1 - \rho_2}{\rho_1 + \rho_2}. \quad (2.53)$$

τ is the transmission coefficient from medium 2 into medium 1, τ' is the transmission coefficient from medium 1 into medium 2, and k_{12} is the reflection coefficient in the second medium which is equal to $-k_{21}$. Then,

$$V_1'' = \frac{I\rho_1}{2\pi} \frac{(-k_{21})(1 - k_{21}^2)}{2d + 2b - a}. \quad (2.54)$$

The last image causes another image C''' in medium 1 at a distance $(4b + a)$ from point P . To balance the effect of the third image, we must now introduce the fourth image, C' , at a distance $(2d + 6b - a)$ from point P which can be shown by $I\tau\tau'(-k_{21})^3$. So, the potential equation is

$$V_1''' = \frac{I\rho_1}{2\pi} \frac{(-k_{21})^3(1 - k_{21}^2)}{2d + 6b - a}. \quad (2.55)$$

By repeated reflection in the two boundary planes, we thus get an infinite series of images. All of image current source potential equations like equations (2.49), (2.54), and (2.55) are added to the real current source potential equation (2.48) to give the following expression for the potential in a point on the surface of the medium 1.

$$V_1 = \frac{I\rho_1}{2\pi a} \left(1 + \frac{k_{21}}{2\left(\frac{d}{a} - \frac{b}{a}\right) - 1} - k_{21}(1 - k_{21}^2) \sum_{m=0}^{\infty} \frac{k_{21}^{2m}}{2\left((2m+1)\frac{b}{a} + \frac{d}{a}\right) - 1} \right). \quad (2.56)$$

From the relation of potential formulas, one can obtain, in the usual way, the value of ρ_a in terms of ρ_1 for complete profiles across the dike.

$$\frac{\rho_a}{\rho_1} = 1 + \frac{k_{21}}{2\left(\frac{d}{a} - \frac{b}{a}\right) - 1} - k_{21}(1 - k_{21}^2) \sum_{m=0}^{\infty} \frac{k_{21}^{2m}}{2\left((2m+1)\frac{b}{a} + \frac{d}{a}\right) - 1}. \quad (2.57)$$

When the potential electrode is in medium 2 and the current electrode is in medium 1, image sources are located in media 1 and 3 (Fig. 2-5b). By the same reasoning, we get as an expression for the real current source and image current sources potentials

$$V_2^0 = \frac{I\rho_1\tau}{2\pi a}, \quad (2.58)$$

$$V_2^1 = \frac{I\rho_1}{2\pi} \frac{\tau(-k_{21})}{2d + 2b - a}, \quad (2.59)$$

$$V_2^2 = \frac{I\rho_1}{2\pi} \frac{\tau(-k_{21})^2}{4b + a}. \quad (2.60)$$

By adding the image current sources potential equations (2.59) and (2.60) into the real current source potential, equation (2.58), we can get as an expression for the potential in a point on the surface of the medium 2.

$$V_2 = \frac{I\rho_1}{2\pi a} (1 + k) \left(\sum_{m=0}^{\infty} \frac{k^{2m}}{4m\frac{b}{a} + 1} - k \sum_{m=0}^{\infty} \frac{k^{2m}}{2\left((2m+1)\frac{b}{a} + \frac{d}{a}\right) - 1} \right), \quad (2.61)$$

where k is same as k_{21} . Having expressions for the potential functions, we may find an equation for the apparent resistivity.

$$\frac{\rho_a}{\rho_1} = (1 + k) \left(\sum_{m=0}^{\infty} \frac{k^{2m}}{4m\frac{b}{a} + 1} - k \sum_{m=0}^{\infty} \frac{k^{2m}}{2\left((2m+1)\frac{b}{a} + \frac{d}{a}\right) - 1} \right). \quad (2.62)$$

The other case can be obtained from the relation of potential equations when the current electrode is on the first medium and the potential electrode is on the third medium by following the same procedure for the method of images . All calculations for this case and next three cases are given in the Appendix A. These results compare with Dakhnov's results (1962). The value of ρ_a for this case in terms of ρ_1

$$\frac{\rho_a}{\rho_1} = (1 - k^2) \sum_{m=0}^{\infty} \frac{k^{2m}}{4m\frac{b}{a} + 1}. \quad (2.63)$$

The fourth case we will consider is that in which both the current and potential electrodes are on the dike. In this geometry (in Fig. 2-6), some of image points appear to be to the right of the dike and some of them to the left of it. The effect of one or two sets of images caused by reflections in two boundaries can give the expression for potential of the fourth case.

$$\begin{aligned} V_3 = & \frac{I\rho_1}{2\pi a} \left(\frac{1+k}{1-k} \right) \left(1 + k^2 \left(\sum_{m=0}^{\infty} \frac{k^{2m}}{4(m+1)\frac{b}{a} + 1} + \sum_{m=0}^{\infty} \frac{k^{2m}}{4(m+1)\frac{b}{a} - 1} \right) \right. \\ & \left. - k \left(\sum_{m=0}^{\infty} \frac{k^{2m}}{2((2m+1)\frac{b}{a} + \frac{d}{a}) - 1} + \sum_{m=0}^{\infty} \frac{k^{2m}}{2((2m+1)\frac{b}{a} - \frac{d}{a}) + 1} \right) \right). \quad (2.64) \end{aligned}$$

Apparent resistivity may be computed using the last expression for the potential field in the appropriate defining equation for the half-Wenner array.

$$\begin{aligned} \frac{\rho_a}{\rho_1} = & \left(\frac{1+k}{1-k} \right) \left(1 + k^2 \left(\sum_{m=0}^{\infty} \frac{k^{2m}}{4(m+1)\frac{b}{a} + 1} + \sum_{m=0}^{\infty} \frac{k^{2m}}{4(m+1)\frac{b}{a} - 1} \right) \right. \\ & \left. - k \left(\sum_{m=0}^{\infty} \frac{k^{2m}}{2((2m+1)\frac{b}{a} + \frac{d}{a}) - 1} + \sum_{m=0}^{\infty} \frac{k^{2m}}{2((2m+1)\frac{b}{a} - \frac{d}{a}) + 1} \right) \right). \quad (2.65) \end{aligned}$$

By a similar analysis, we can obtain the potential when the current electrode is on the dike and the potential electrode is on the right side of the dike. At this position, image points of current source are located on media 1 and 3 with strengths

$I(1-k)(-k)^{2m-1}$ and $I(1-k)(-k)(-k)^{2m-1}$. So the potential function of a series of image sources is:

$$V_4 = \frac{I\rho_1}{2\pi a}(1+k)\left(\sum_{m=0}^{\infty} \frac{k^{2m}}{4m\frac{b}{a}+1} - k \sum_{m=0}^{\infty} \frac{k^{2m}}{2\left(\left(2m+1\right)\frac{b}{a} - \frac{d}{a}\right)+1}\right). \quad (2.66)$$

The apparent-resistivity formula for this case is:

$$\frac{\rho_a}{\rho_1} = (1+k)\left(\sum_{m=0}^{\infty} \frac{k^{2m}}{4m\frac{b}{a}+1} - k \sum_{m=0}^{\infty} \frac{k^{2m}}{2\left(\left(2m+1\right)\frac{b}{a} - \frac{d}{a}\right)+1}\right). \quad (2.67)$$

Finally the potential for the last case is obtained when both electrodes are on the right side of the dike.

$$V_5 = \frac{I\rho_1}{2\pi a}\left(1+k \sum_{m=0}^{\infty} \frac{k^{2m}}{2\left(\left(2m-1\right)\frac{b}{a} - \frac{d}{a}\right)+1} - k \sum_{m=0}^{\infty} \frac{k^{2m}}{2\left(\left(2m+1\right)\frac{b}{a} - \frac{d}{a}\right)+1}\right). \quad (2.68)$$

From the last equation (2.68), the apparent resistivity in terms of ρ_1 is obtained.

$$\frac{\rho_a}{\rho_1} = 1+k \sum_{m=0}^{\infty} \frac{k^{2m}}{2\left(\left(2m-1\right)\frac{b}{a} - \frac{d}{a}\right)+1} - k \sum_{m=0}^{\infty} \frac{k^{2m}}{2\left(\left(2m+1\right)\frac{b}{a} - \frac{d}{a}\right)+1} \quad (2.69)$$

All these equations are used if I is to the left of V . Otherwise, if I is to the right of V , reciprocity can be used plus transforming the measurement of d from I to V .

Apparent-resistivity anomalies for pole-pole array over the dike model obtained by using the image method are shown by Figures 2-7 through 2-11.

2.2.1.2 Use of the Method for Dipole-Dipole Array

Because of the complexity of the dike model, we first derived the pole-pole expressions crossing this model. For the dipole-dipole array crossing the dike we considered fourteen cases. Using the number of equation of ρ_a in terms of ρ_1 for pole-pole array, we should have new equations for dipole-dipole array. To write the

general potential equation for the dipole-dipole array, consider the plan view of the ground surface (Fig. 2-1c), showing the locations of the current and the potential electrodes (Wait,1982). The potential difference V between an pair of electrodes is obtained by following the same steps as we covered in section 2.1.3.

$$V = \frac{I\rho_1}{2\pi} \left[\frac{G(a_{11}, k)}{a_{11}} - \frac{G(a_{12}, k)}{a_{12}} - \frac{G(a_{21}, k)}{a_{21}} + \frac{G(a_{22}, k)}{a_{22}} \right], \quad (2.70)$$

where the a represent the locations of the potential electrodes with respect to the current electrodes. G is the solution to Laplace's equation as a function of the resistivity of each layer and the a . Then, an apparent resistivity as a function of the geometry of the array can be written for each case as follows.

For the thin-dike model $b < a$, adding the apparent resistivity as was done for pole-pole array, we should have nine cases involved. The apparent resistivity for $n = 2$ is written using the potential equation (2.70) and the relation between the potential and the apparent resistivity.

$$\frac{\rho_a}{\rho_1} = G_1(2a, d) - G_1(3a, d + a) - G_1(3a, d) + G_1(4a, d + a). \quad (2.71)$$

We have already shown that $G_1(a, d)$ for the pole-pole array is equal to equation (2.57). By changing a in this equation, we can obtained G_1 for the different locations of the electrodes. When two current electrodes, C_1 and C_2 , and one potential, P_1 , electrode are on the left side of the dike, but the second potential electrode, P_2 , is on the dike, the apparent resistivity is obtained by following the same procedure.

$$\frac{\rho_a}{\rho_1} = G_1(2a, d) - G_1(3a, d + a) - G_2(3a, d) + G_2(4a, d + a) \quad (2.72)$$

where $G_2(a, d)$ is equal to equation (2.62). When C_1 , C_2 , and P_1 are still on the left side of the dike, but P_2 is on the third medium, the apparent resistivity is

$$\frac{\rho_a}{\rho_1} = G_1(2a, d) - G_1(3a, d + a) - G_3(3a, d) + G_3(4a, d + a) \quad (2.73)$$

where $G_3(a, d)$ is equal to equation (2.63). When C_1 and C_2 are on the left side of the dike, P_1 is on the dike, and P_2 is right side of the dike, the apparent resistivity is

$$\frac{\rho_a}{\rho_1} = G_2(2a, d) - G_2(3a, d + a) - G_3(3a, d) + G_3(4a, d + a). \quad (2.74)$$

When C_1 and C_2 are on the left side of the dike and P_1 and P_2 are on the right side of the dike, the apparent resistivity is

$$\frac{\rho_a}{\rho_1} = G_3(2a, d) - G_3(3a, d + a) - G_3(3a, d) + G_3(4a, d + a). \quad (2.75)$$

When C_2 is on the first, C_1 is on the second, and P_1 and P_2 are on the third medium, the apparent resistivity is

$$\frac{\rho_a}{\rho_1} = G_4(2a, d) - G_3(3a, d + a) - G_4(3a, d) + G_3(4a, d + a) \quad (2.76)$$

where G_4 is equal to equation (2.67). When C_2 is on the first medium and others are on the third medium, the apparent resistivity is

$$\frac{\rho_a}{\rho_1} = G_5(2a, d) - G_3(3a, d + a) - G_5(3a, d) + G_3(4a, d + a) \quad (2.77)$$

where G_5 is equal to equation (2.69). When the C_2 is on the dike and others are on the right side of it, the apparent resistivity is

$$\frac{\rho_a}{\rho_1} = G_5(2a, d) - G_4(3a, d + a) - G_5(3a, d) + G_4(4a, d + a). \quad (2.78)$$

When whole electrodes are on the third medium, the apparent resistivity for the last case is

$$\frac{\rho_a}{\rho_1} = G_5(2a, d) - G_5(3a, d + a) - G_5(3a, d) + G_5(4a, d + a). \quad (2.79)$$

For a thick-dike model, $b > a$, there are eight cases, but only the following four cases are different from the thin-dike model. When C_1 and C_2 are on the first medium and P_1 and P_2 are on the dike,

$$\frac{\rho_a}{\rho_1} = G_2(2a, d) - G_2(3a, d + a) - G_2(3a, d) + G_2(4a, d + a). \quad (2.80)$$

When C_2 is on the first medium and C_1 , P_1 , and P_2 are on the dike,

$$\frac{\rho_a}{\rho_1} = G_{3A}(2a, d) - G_2(3a, d + a) - G_{3A}(3a, d) + G_2(4a, d + a) \quad (2.81)$$

where G_{3A} is equal to equation (2.65). When C_1 , C_2 , and P_1 are on the dike, P_2 is the left of it,

$$\frac{\rho_a}{\rho_1} = G_{3A}(2a, d) - G_{3A}(3a, d + a) - G_4(3a, d) + G_4(4a, d + a). \quad (2.82)$$

When C_1 and C_2 are on the dike, P_1 and P_2 are left of it,

$$\frac{\rho_a}{\rho_1} = G_4(2a, d) - G_4(3a, d + a) - G_4(3a, d) + G_4(4a, d + a). \quad (2.83)$$

A profile plots of ρ_a/ρ_1 from the five derived cases for ρ_2/ρ_1 as a function of d/a are shown by Figures 2-13 through 2-16. We also solved the dike problem for n is 1, 2, 3, and 4 cases when the thickness of the dike is $4a$ (Fig. 2-17).

2.2.2 Use of the Bessel Integral Formulation for Thin-dike Limit

The thin-dike limit is $\sigma_2(= \frac{1}{\rho_2}) \rightarrow \infty$, $2b \rightarrow 0$, but $2\sigma_2 b = g$ which is finite. The potential field for this limiting case can be found by applying the Bessel integral formulation. The Bessel integral formulation and image series are the same for the limiting case.

The potentials on the right and left side of the thin dike were obtained by using the thin-sheet boundary conditions. These boundary conditions are that the

potentials on the right and left side of the thin dike be continuous through the thin dike and the normal currents to the dike are discontinuous by the amount of change of transverse current.

$$U_1 = U_3 \quad \text{at } x = -d \quad (2.84)$$

$$\frac{1}{\rho_1} \frac{\partial U_1}{\partial x} - \frac{1}{\rho_1} \frac{\partial U_3}{\partial x} = \frac{2b}{\rho_2} \frac{\partial^2 U_3}{\partial x^2} \quad (2.85)$$

where U_1 is the potential of the formation adjacent to a dike on the left side, U_3 is the potential of the formation adjacent to a dike on the right side, d is the distance from C to the boundary of the dike, and x is the axis parallel to the surface. The potentials at both sides of the dike can be found by following the Bessel integral formulation as in section 2.1.1. At $-d < x < 0$, the potential equation is

$$U_1 = \frac{I\rho_1}{2\pi} \int_0^\infty (e^{\lambda x} + Ae^{-\lambda x}) J_0(\lambda r) d\lambda. \quad (2.86)$$

At $x < -d$, the potential equation is

$$U_3 = \frac{I\rho_1}{2\pi} \int_0^\infty B e^{\lambda x} J_0(\lambda r) d\lambda. \quad (2.87)$$

By applying boundary conditions to equations (2.86) and (2.87), one obtains unknown constants, A and B , which are

$$A = -\frac{\lambda\rho_1 b e^{-2\lambda d}}{\rho_2 + \lambda\rho_1 b}, \quad (2.88)$$

$$B = -\frac{\rho_2}{\lambda b\rho_1 + \rho_2}. \quad (2.89)$$

Substituting equations (2.88) and (2.89) into (2.86) and (2.87), equations (2.86) and (2.87) at $r = 0$ are obtained. At $0 > x > -d$,

$$U_1 = \frac{I\rho_1}{2\pi} \left[\int_0^\infty e^{\lambda x} d\lambda - \int_0^\infty \frac{\lambda\rho_1 b e^{-2\lambda d}}{\rho_2 + \lambda\rho_1 b} e^{-\lambda x} d\lambda \right] \quad (2.90)$$

and at $x < -d$,

$$U_3 = \frac{I\rho_1}{2\pi} \int_0^\infty -\frac{\rho_2}{\lambda b\rho_1 + \rho_2} e^{\lambda x} d\lambda. \quad (2.91)$$

For use in the numerical examples, the integral expression for the potentials will be written in terms of the exponential integrals $Ei(-x)$ (Abramowitz and Stegun, 1970).

$$Ei(-x) = -\int_x^\infty \frac{e^{-t}}{t} dt. \quad (2.92)$$

If we define $\alpha(x) = \rho_2 x / \rho_1 b$ and use the following exponential integral identity given by Abramowitz and Stegun (1965):

$$\int_0^\infty \frac{e^{-at}}{t+b} dt = -e^{ab} Ei(-ab), \quad (2.93)$$

potential equations can be computed as

$$U_1 = \frac{I\rho_1}{2\pi} \left[\frac{1}{x} - \frac{1}{x} \left(\frac{1}{\frac{2d}{x} + 1} \right) - \alpha \exp\left(\left(\frac{2d}{x} + 1\right)\alpha\right) Ei\left(-\alpha\left(\frac{2d}{x} + 1\right)\right) \right], \quad (2.94)$$

$$U_3 = -\frac{I\rho_1}{2\pi} \frac{\alpha}{x} \exp(\alpha) Ei(-\alpha). \quad (2.95)$$

2.2.3 Numerical Examples

The ratios of the apparent resistivity ρ_a to the resistivity ρ_1 of the surrounding material of the dike was plotted on semi-logarithmic paper as a function of d/a for various values of ρ_2/ρ_1 . The apparent resistivities are obtained for different values of thickness of dike and shown in Figures 2-7 through 2-11 and 2-13 through 2-16. These curves are obtained for pole-pole (half-Wenner) and dipole-dipole arrays. The apparent resistivity on either side of the dike depends not only the resistivity contrast between the dike and the surrounding rock, but also the width of the dike. The apparent resistivities can be compared to field data and can thus assist in interpretations.

In numerical examples, consideration will be given to investigating how the apparent resistivities change with the thickness of the dike and the resistivity ratio of material surrounding the dike. The solutions are obtained for different thickness of dike ($b = 4a, 2a, a, 0.5a, 0.25a$) and for various values of resistivity ratios ($\rho_2/\rho_1 = 10., 5., 1., 0.1, 0.01$). For each value of resistivity ratio, we used 10, 20, 30, 40, 50, 60, and 80 terms to check the convergence of the series. Finally, we saw that the results did not change after 30 terms when $b/a = 4, 2, 1$. However, the result for the thin dike ($b/a = 0.25$) changed up to 300 terms for pole-pole and dipole-dipole arrays. Here we computed the series with 300 terms to obtain the apparent-resistivity curves by using the Fortran computer program shown in the Appendix B. The numerical convergence of ρ_2/ρ_1 for pole-pole and dipole-dipole arrays are given in Table 2-3 and Table 2-4 when $b/a = 0.25$. The group of curves for resistive dikes are usually charted separately from those for conductive dikes. With both arrays over the resistive and conductive dike models, a symmetric profile is obtained. Here, the axis of symmetry is $d/a = 1$, because we chose distance d from the current electrode C_1 to the middle of dike. If the distance, d , were from C_1 to the first boundary of the dike, the axis of symmetry would be $d/a = 0$.

Attention will first be directed to the case $b = 4a$. The apparent resistivities as a function d/a are plotted in Figures 2-7 and 2-13 for the pole-pole and dipole-dipole arrays, respectively. For the dipole-dipole array, there are two maximum points on the resistive dike contrast ($\rho_2/\rho_1 = 10, 5$), shown in Figure 2-13a. Over the conductive dike, the horizontal positions of the apparent-resistivity twin peaks shift toward the center of the dike. On the other hand, for pole-pole array (Fig. 2-7), the high apparent-resistivity anomaly is occurring when the dike is perfectly resistive ($\rho_2/\rho_1 = 10., 5.$). For the conductive dike, a low anomaly is obtained. The width of the anomaly for the pole-pole array is larger than that for the dipole-dipole

array. However, the peak values of resistive anomalies for the pole-pole array are smaller than those for the dipole-dipole array.

The apparent-resistivity (ρ_a/ρ_1) plots as a function of d/a are shown in Figures 2-8 and 2-14 for pole-pole and dipole-dipole arrays, respectively, when the dike is resistive and conductive. In this particular case, the width of dike ($2b$) is $4a$. For the pole-pole array, the similar structure as shown in Figure 2-7 is obtained. The widths of the anomalies and the maximum values are smaller as the dike becomes smaller. For the dipole-dipole array, the apparent-resistivity anomaly has only one peak. For a very resistive dike ($\rho_2/\rho_1 = 10.$), the distance of the highest peak is approximately 19, which is larger than the peak values of a wider dike. As the dike becomes thinner, the distance over the anomaly becomes smaller.

We also considered the case in which the thickness of the dike is $2a$ ($b = a$). In this situation, for the dipole-dipole array, there are two peaks on the apparent-resistivity curve near the right and left edges of the dike which is shown in Figure 2-15a. The distance between these peaks flanking either side of the main anomaly is $3a$. For a conductive dike, there is only one small peak over the dike. This anomaly is in the shape of a W for small ρ_2/ρ_1 values. In Figure 2-9, the resistive dike for the pole-pole array gives anomalously high trend pointing over the dike, whereas the conductive dike gives a very slight low trend.

Other calculations were conducted and results are presented in Figures 2-10a and 2-16a for pole-pole and dipole-dipole arrays. Here, we selected thinner dikes ($2b = a$). When the dike is resistive, the apparent-resistivity anomalies for both arrays have two high peaks and show pronounced resistivity lows over the dike. The apparent-resistivity values have a flat low area over the dike for dipole-dipole array, as shown in Figure 2-16a. The width of the flat area is the same as the width of the dike. When the dike is conductive, the apparent-resistivity values rise over the

dike. The apparent resistivities for the conductive dike look like W-shaped curve. The peak values of the apparent resistivity are much larger for dipole-dipole array.

When the dike is very thin ($b = 0.25a$), the apparent-resistivity curve for the resistive dike model has two maximum points for both arrays, as shown in Figures 2-11a and 2-16b. It is accompanied by a significant minimum value over the dike. The two highest points of the dike for ρ_2/ρ_1 (10, 5) for dipole-dipole array rise to apparent-resistivity values of approximately 2.5 and 2 (Fig. 2-16b). However, for the pole-pole array, they rise to approximately 1.6 and 1.4 (Fig. 2-11a). The distances between these two peaks are wider than the dike for both arrays. When the dike is conductive, the apparent-resistivity anomaly has a W shape a for pole-pole array, however, the middle of the W shape is flat for the dipole-dipole array and the width of the flat region is larger than the thickness of the dike. The flat area is obtained on the curve because the current and potential electrodes are not located together on the dike when the dike is very thin.

We also consider the case in which the width of the dike is infinitely large. The apparent resistivities as a function of d/a are plotted in Figures 2-12a and b for pole-pole and dipole-dipole arrays. Here, the distance d is measured from the current electrode C_1 to the first boundary of the dike. We obtained the half of symmetrical profiles of a thick dike model for both arrays when the thickness of dike is infinite.

To complete the numerical examples, we also calculated the case for various values of distances between C_1 and P_1 (for different numbers of n) for the dipole-dipole array. In this case, n is an integer from 1 to 4 and the thickness of the dike is $4a$. Figure 2-17 shows ρ_a/ρ_1 plotted as the ordinate against n as the abscissa and ρ_2/ρ_1 as a parameter. All of these resistivity plots are approaching 1 for all n integer numbers. When n is increased, deeper information is obtained and the resistive peak on the dike becomes narrow. When n is 4, there is a low anomaly

between the two highest points on the dike. The distance between these two points is narrower than the width of the peak for other numbers of n .

These apparent-resistivity curves over the dike model are also interpreted and compared with a hemispherical sink model. Peters (1988) used the integral method to compute the apparent-resistivity curves for a hemi-spherical body. It is shown in Figures 2-8b, 2-10c, 2-13b, and 2-15b that a hemispherical sink can be approximated in its resistivity edge effects by a vertical dike if the sink is not very narrow.

To compare the thin-dike apparent-resistivity curves with Telford's curves, we chose 5.67 for ρ_2/ρ_1 when the width of the half dike is $0.25a$ (Figs. 2-11a and c). When the thickness of the dike is $0.5a$ and a , we also compared our data with Dakhnov's and Ludwig's curves for pole-pole and dipole-dipole arrays (Figs. 2-10 and 2-18). For a thick dike model, each boundary of the dike can be easily seen on the figures by the two discontinuities that occur when the electrodes cross the dike (Fig. 2-13).

Over the thin and thick dikes, a symmetric profile of apparent resistivity is obtained, because the shape of the profile does not depend on the direction from which the array approaches the contact. Another characteristic of the thin-dike model is that, curves for the thin-dike model are the reverse of curves for the thick-dike model, but they all approach 1 at the beginning and ending points.

Finally, the main difference between the conductive and nonconductive dike is that the resistive one shows two anomalously high trends pointing toward the dike, whereas the conductive one shows only one very slightly high trend.

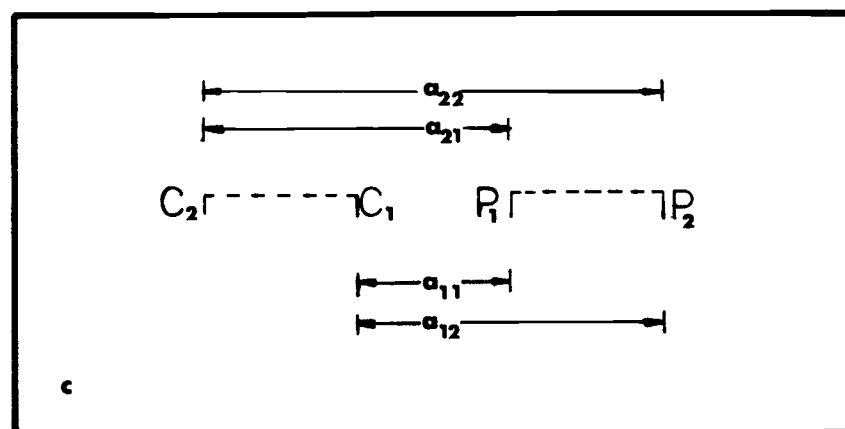
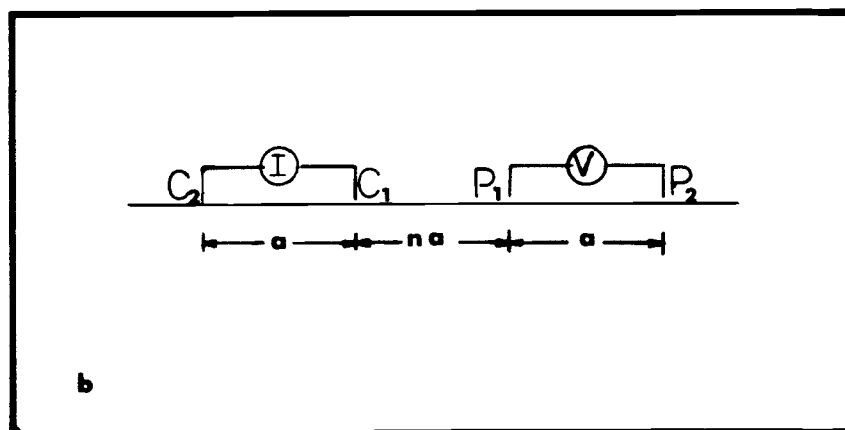
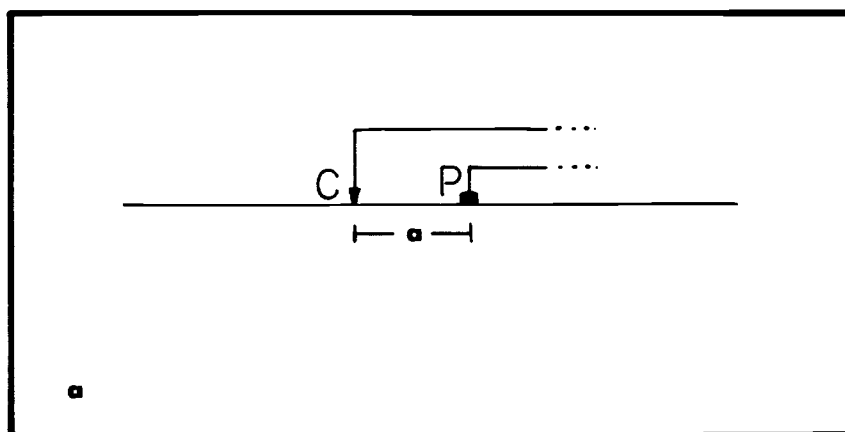


Figure 2-1 a) Pole-pole array, b) Dipole-dipole array,
c) Plan views of the resistivity technique

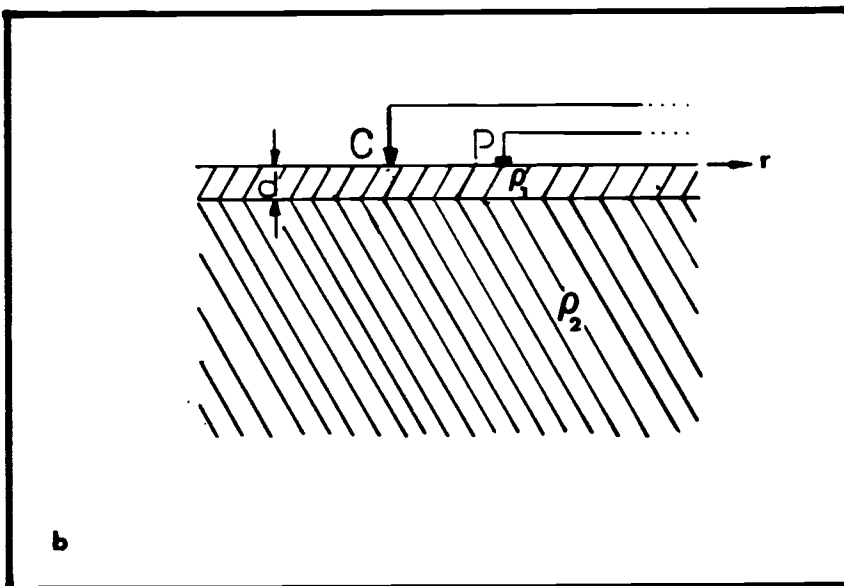
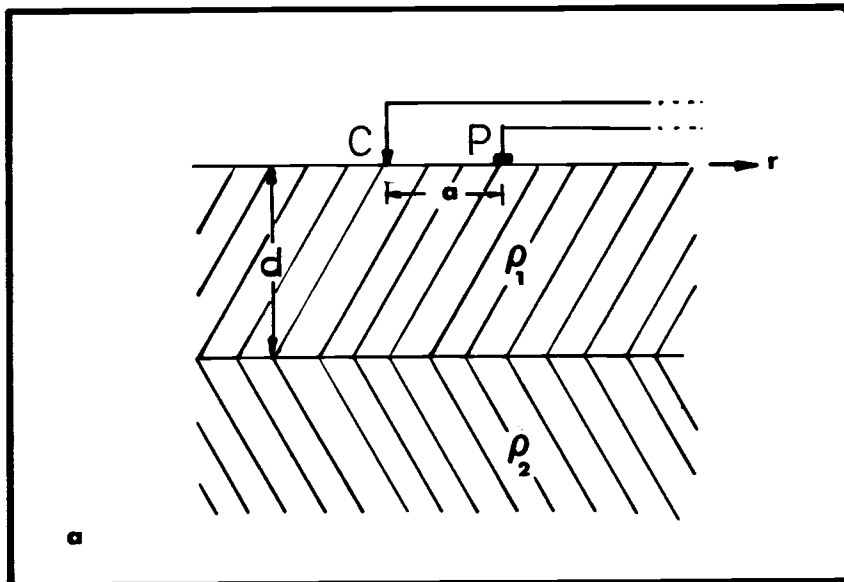


Figure 2-2 a) Two-layer horizontal earth model
b) Thin horizontal layer

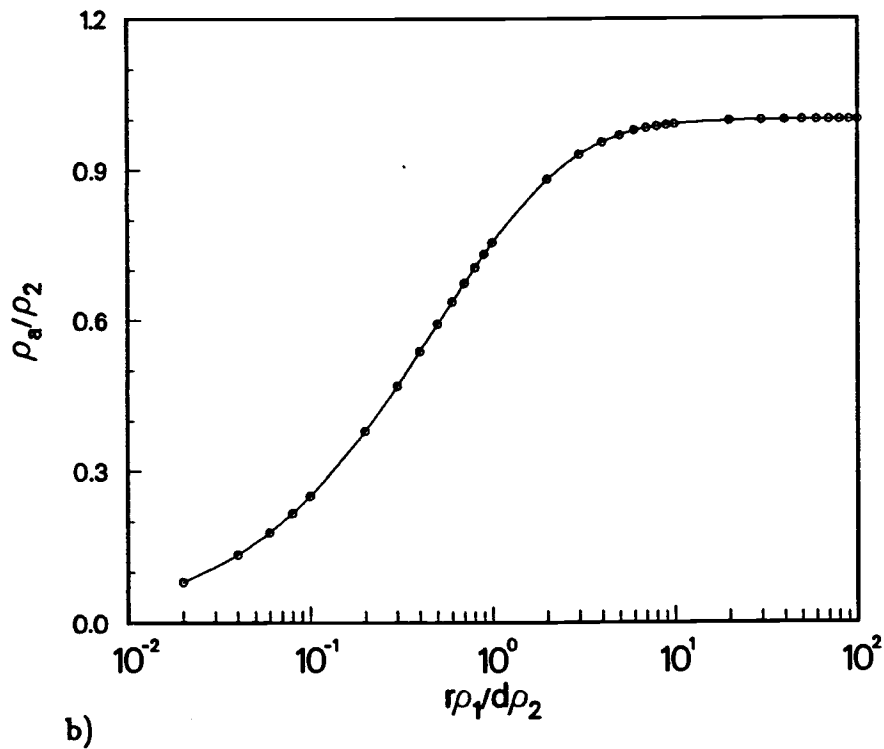
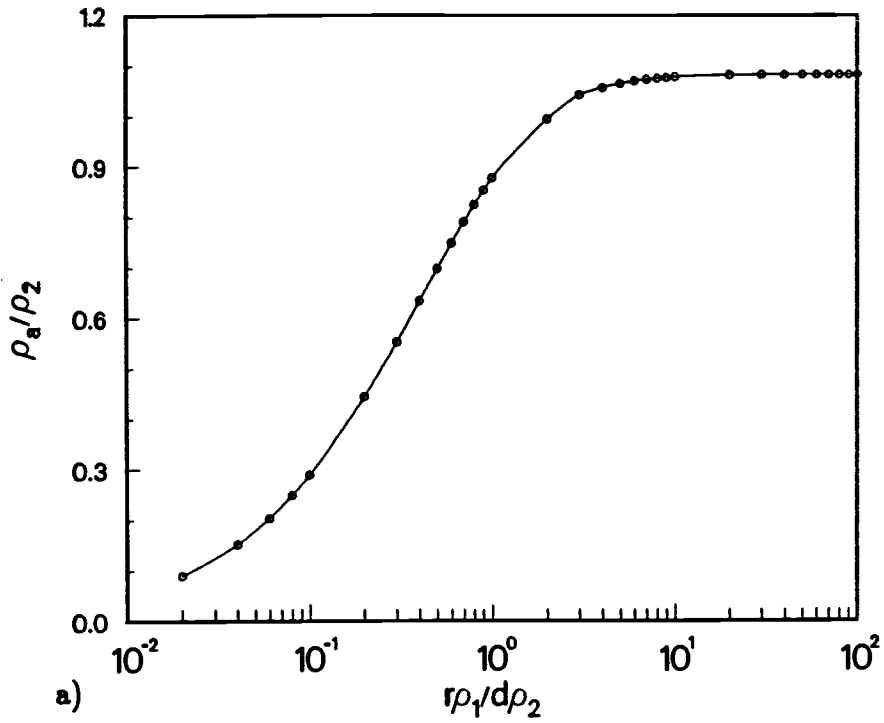


Figure 2-3 The ratio of the apparent resistivity to the second layer resistivity as a function of $r\rho_1/d\rho_2$ over thin horizontal layer
 a) for pole-pole array, b) for dipole-dipole array

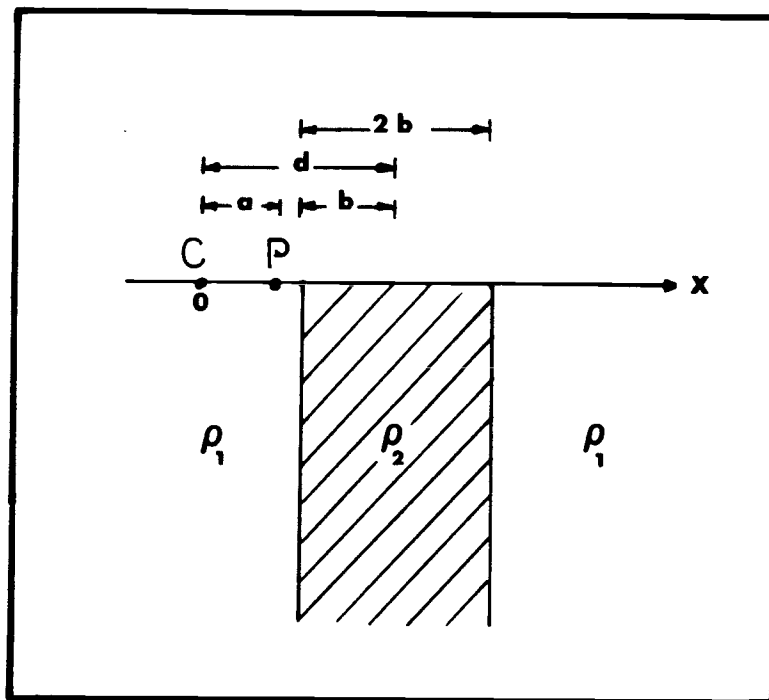


Figure 2-4 Dike model. Parameters: a is the distance between the current and potential electrodes, d is the distance from the current electrode to the midpoint of the dike, $2b$ is the thickness of the dike

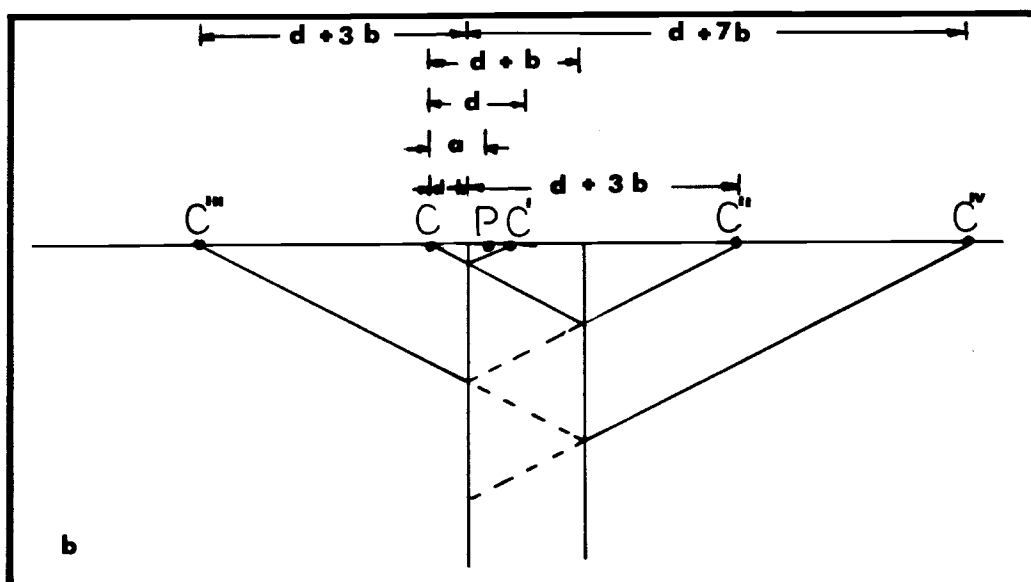
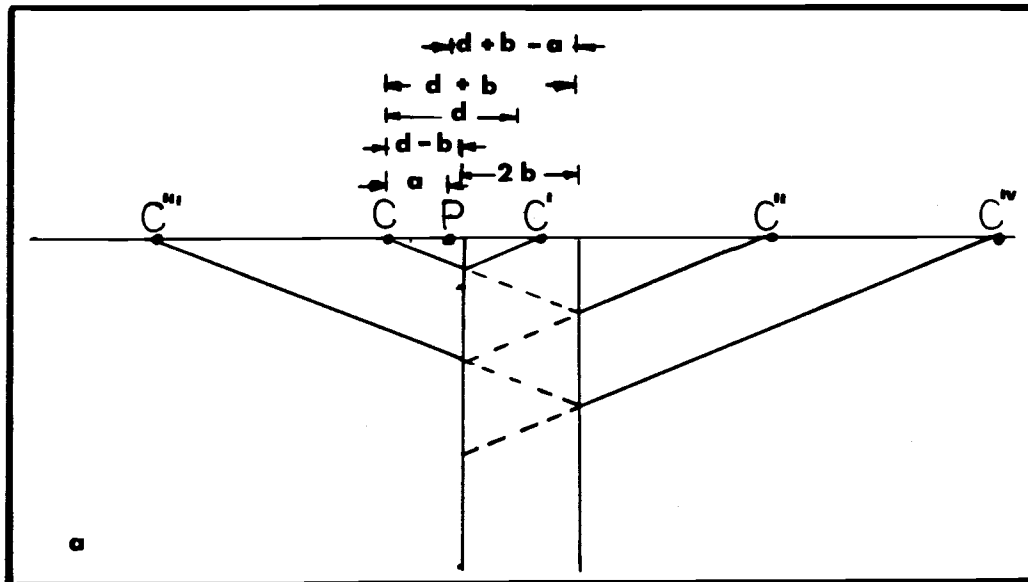


Figure 2-5 Some image points a) when current and potential electrodes are located on the left of the dike b) when current electrode is on the left of the dike and potential electrode is on the dike

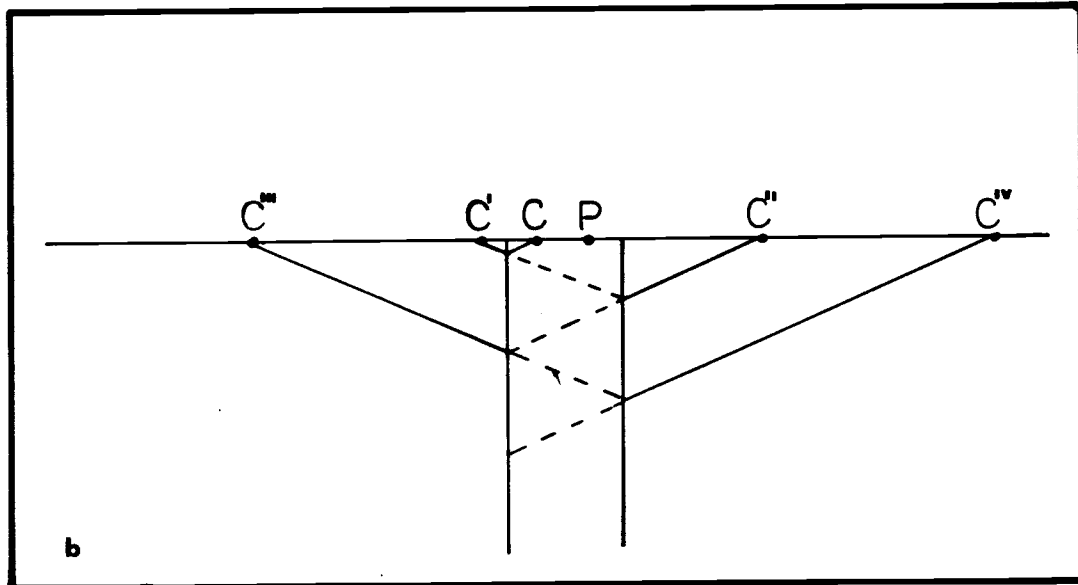
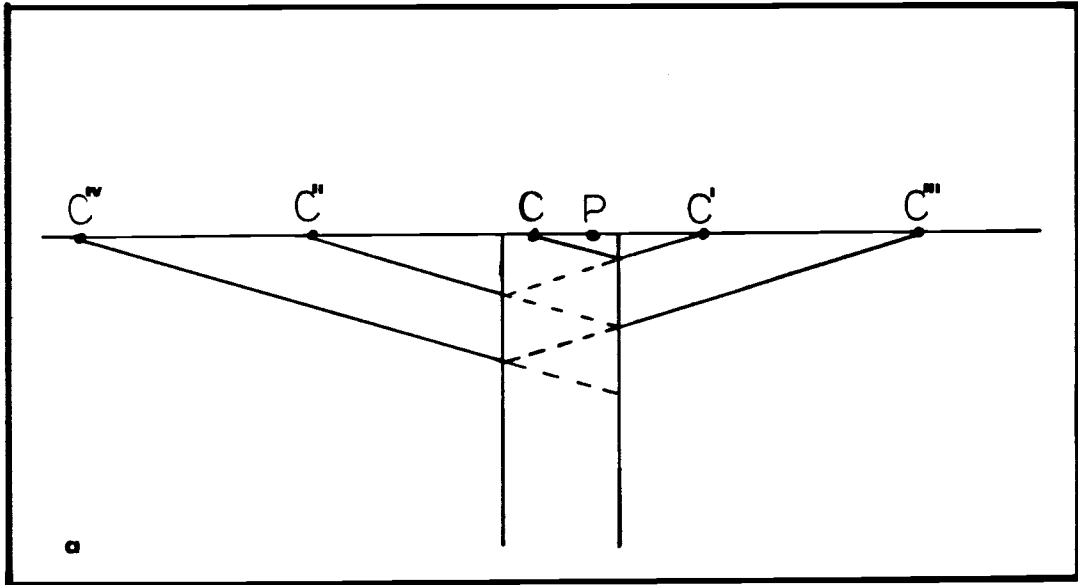


Figure 2-6 Some image points when both electrodes are on the dike

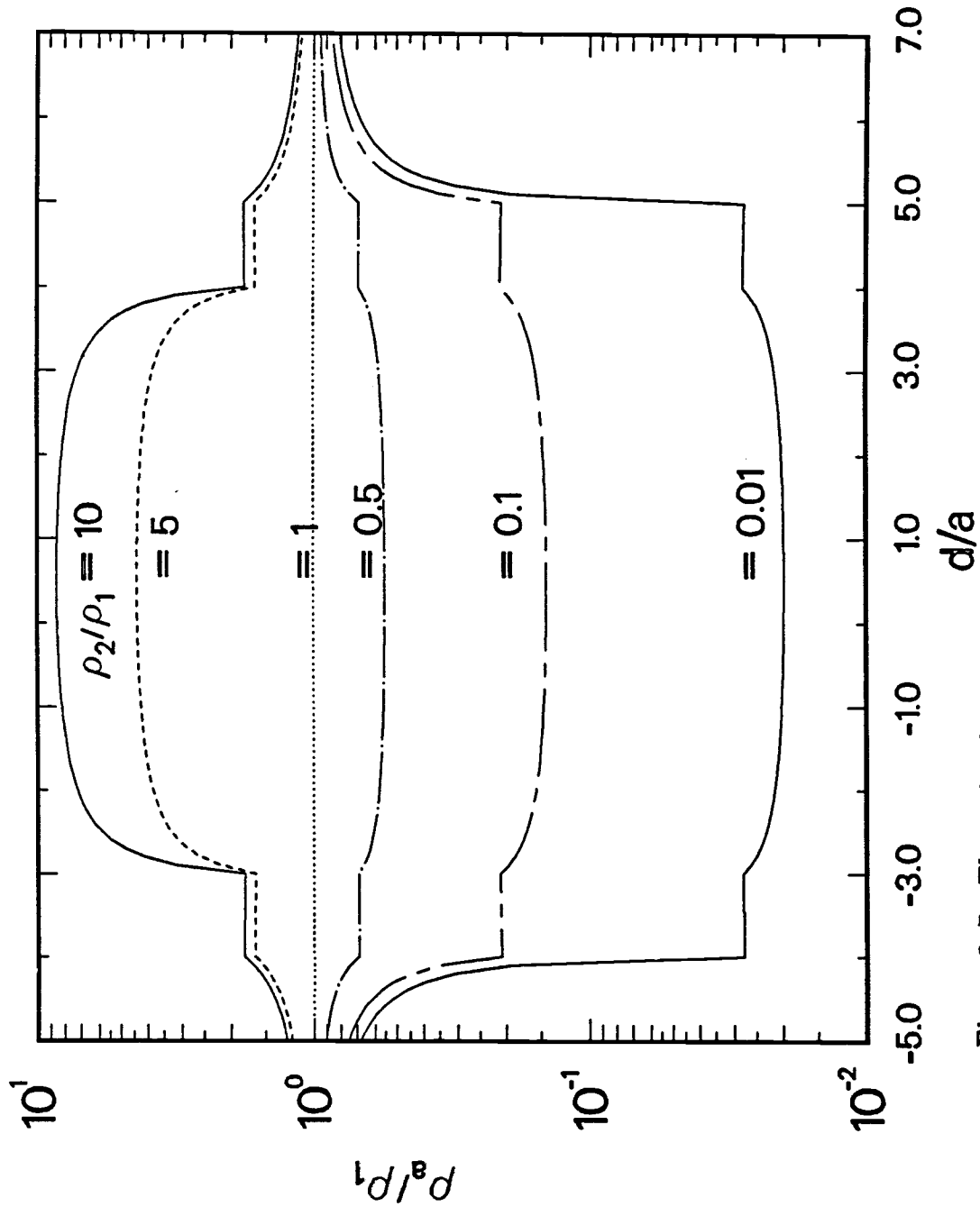


Figure 2-7 The ratio of the apparent resistivity to the resistivity of surrounding material vs. distances d/a for pole-pole array when $b = 4a$

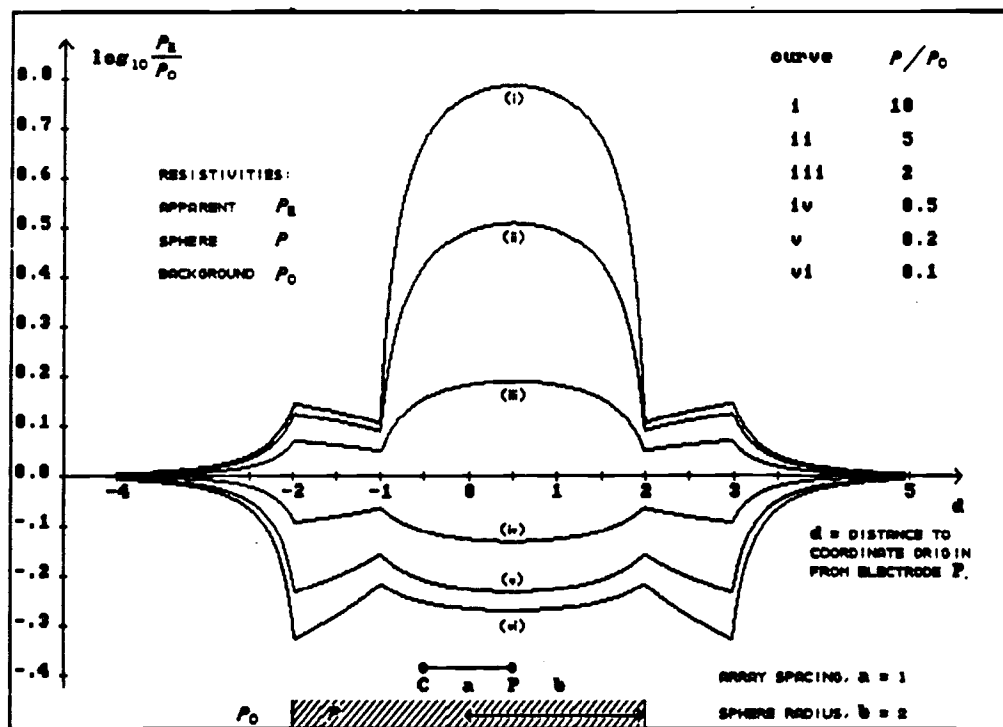
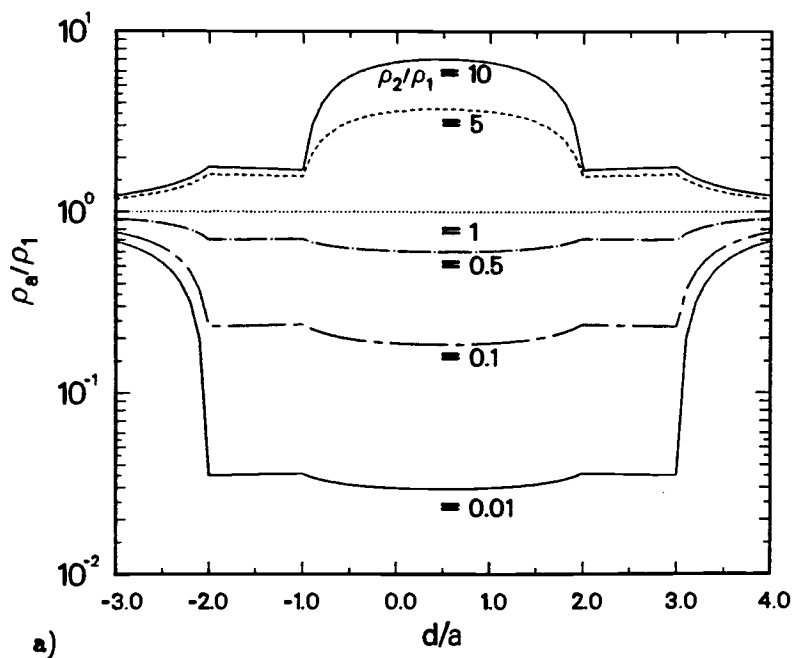


Figure 2-8 The ratio of the apparent resistivity to the resistivity of surrounding material vs. d/a for pole-pole array when $b = 2a$, a) over dike, b) over hemispherical sink (A. Peters, 1988)

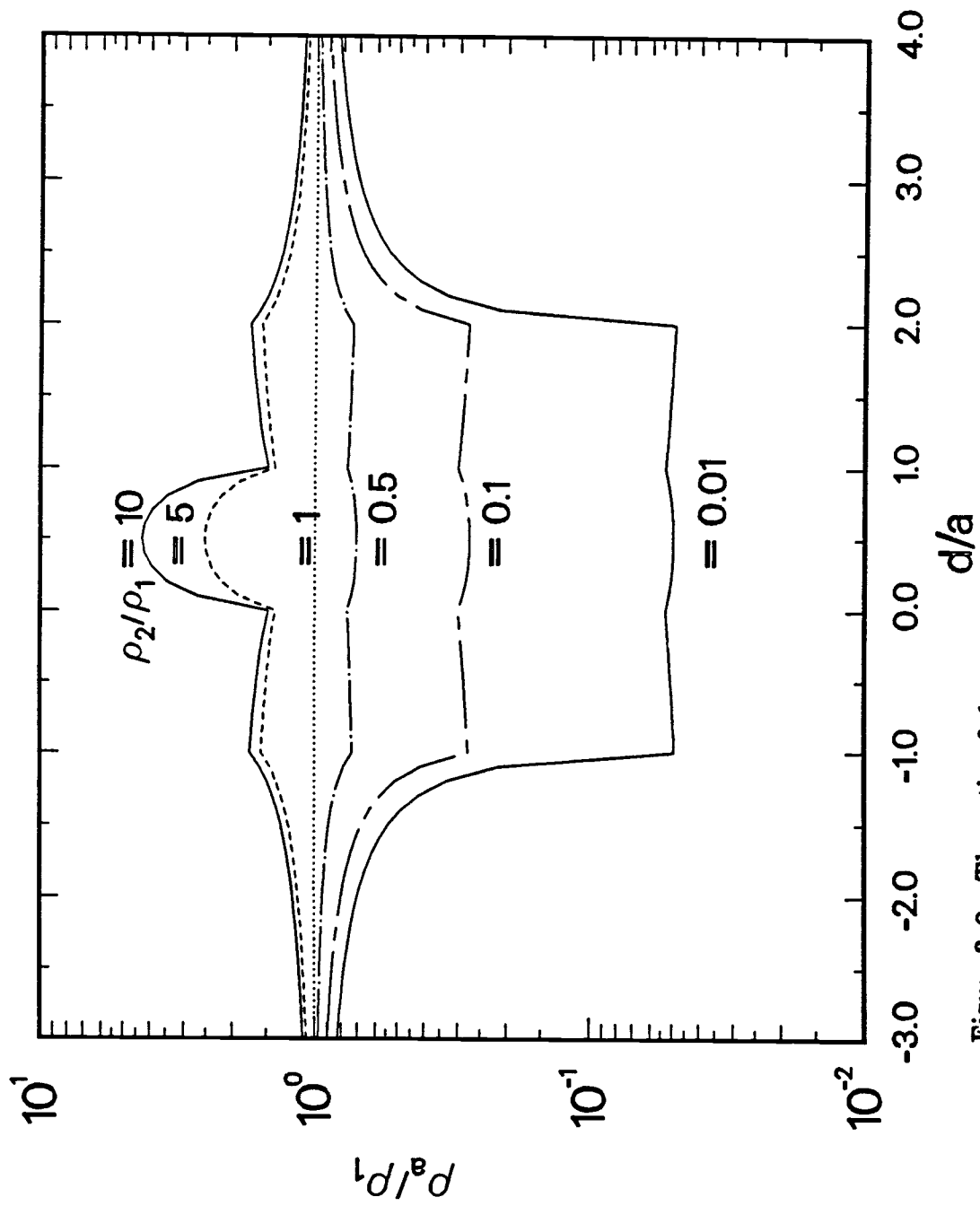


Figure 2-9 The ratio of the apparent resistivity to the resistivity of surrounding material vs. d/a for pole-pole array when $b = a$

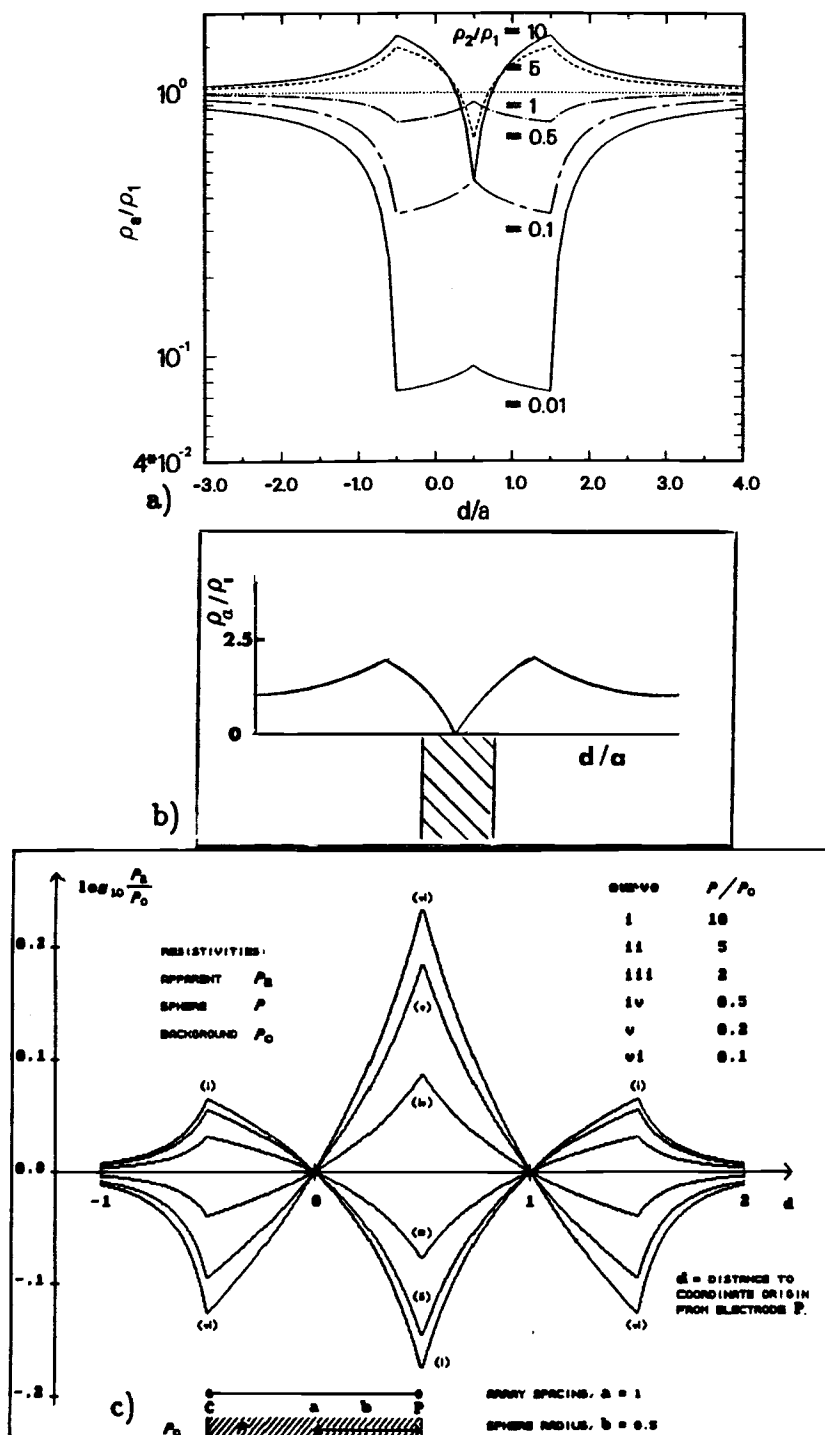


Figure 2-10 The ratio of the apparent resistivity to the resistivity of surrounding material vs. d/a for pole-pole array when $b = 0.5a$ and
 a) $\rho_2/\rho_1 = 10, 5, 1, 0.5, 0.1, 0.01$ over the dike
 b) $\rho_2/\rho_1 = 10$ over the dike (V.N. Dakhnow, 1962)
 c) $\rho_2/\rho_1 = 10, 5, 2, 0.5, 0.2, 0.1$ over hemispherical sink (A. Peters, 1988)

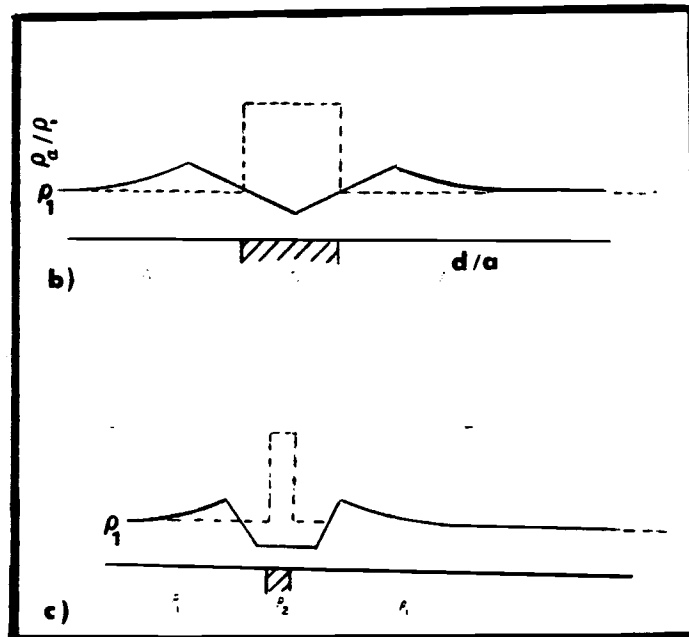
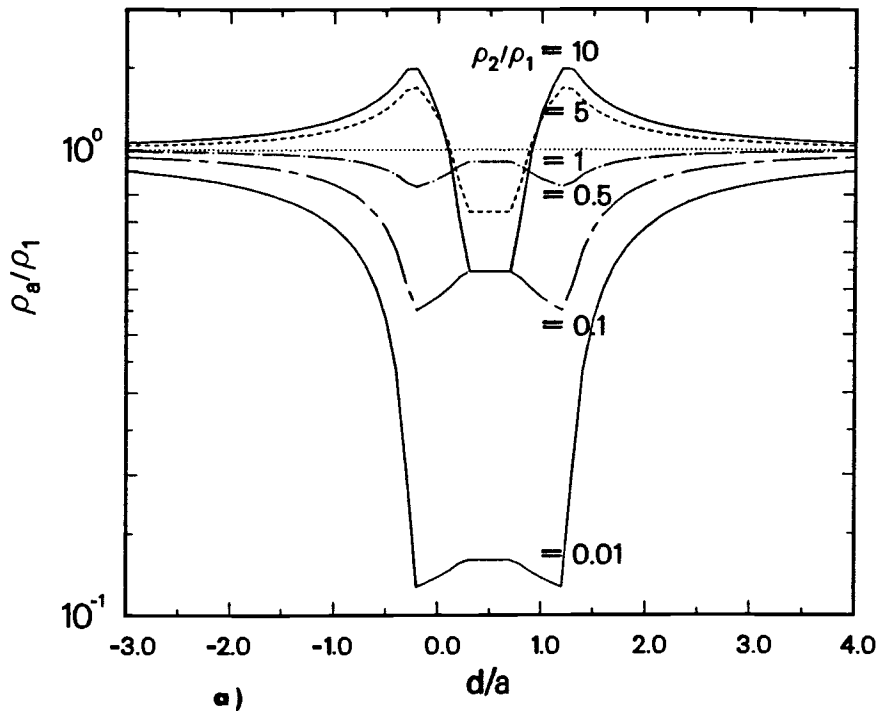


Figure 2-11 The ratio of the apparent resistivity to the resistivity of surrounding material vs. d/a for pole-pole array when

- a) $b = 0.25a$ and $\rho_2/\rho_1 = 10, 5, 1, 0.5, 0.1, 0.01$
- b) $b = 0.5a$ and $\rho_2/\rho_1 = 5.67$ (W.M. Telford, 1976)
- c) $b = 0.25a$ and $\rho_2/\rho_1 = 5.67$ (W.M. Telford, 1976)

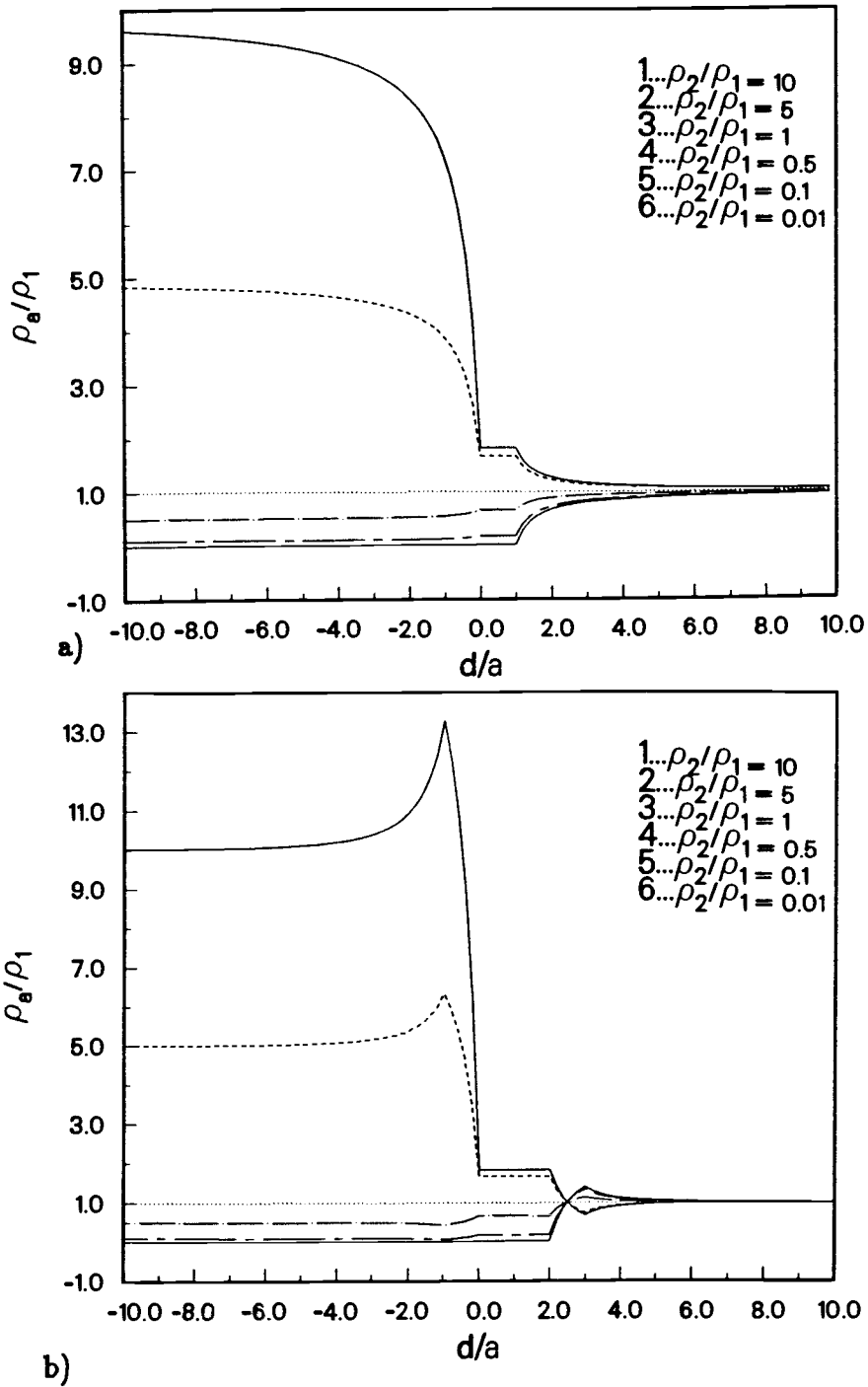


Figure 2-12 The ratio of the apparent resistivity to the resistivity of surrounding material vs. d/a when the thicknesses of dike goes to infinity
 a) for pole-pole array, b) for dipole-dipole array

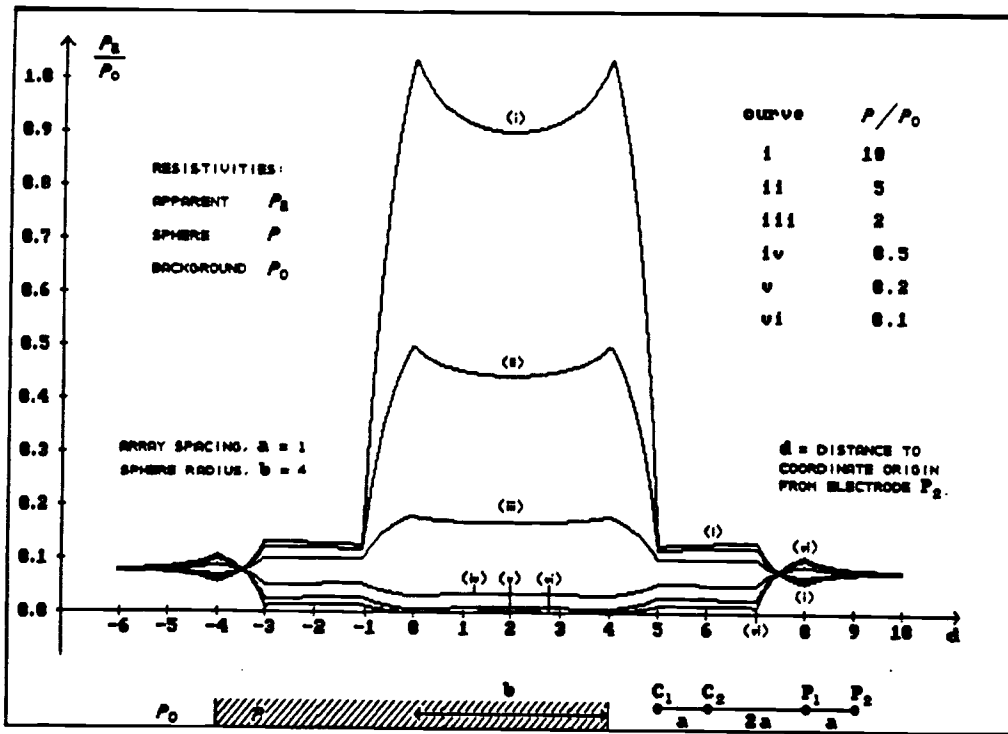
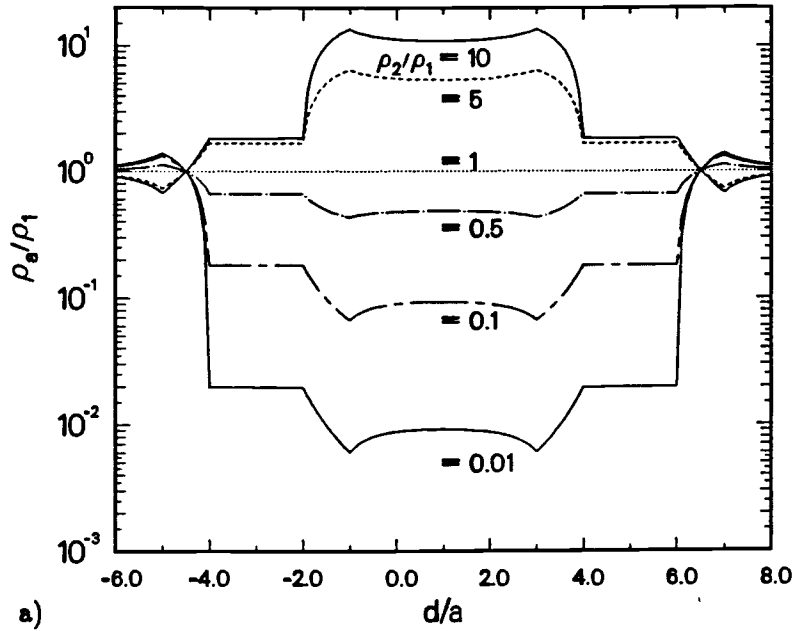


Figure 2-13 The ratio of the apparent resistivity to the resistivity of surrounding material vs. d/a for dipole-dipole array when $b = 4a$ and
 a) $\rho_2/\rho_1 = 10, 5, 1, 0.5, 0.1, 0.01$ over the dike
 b) $\rho_2/\rho_1 = 10, 5, 2, 0.5, 0.2, 0.1$ over hemispherical sink (A. Peters, 1988)

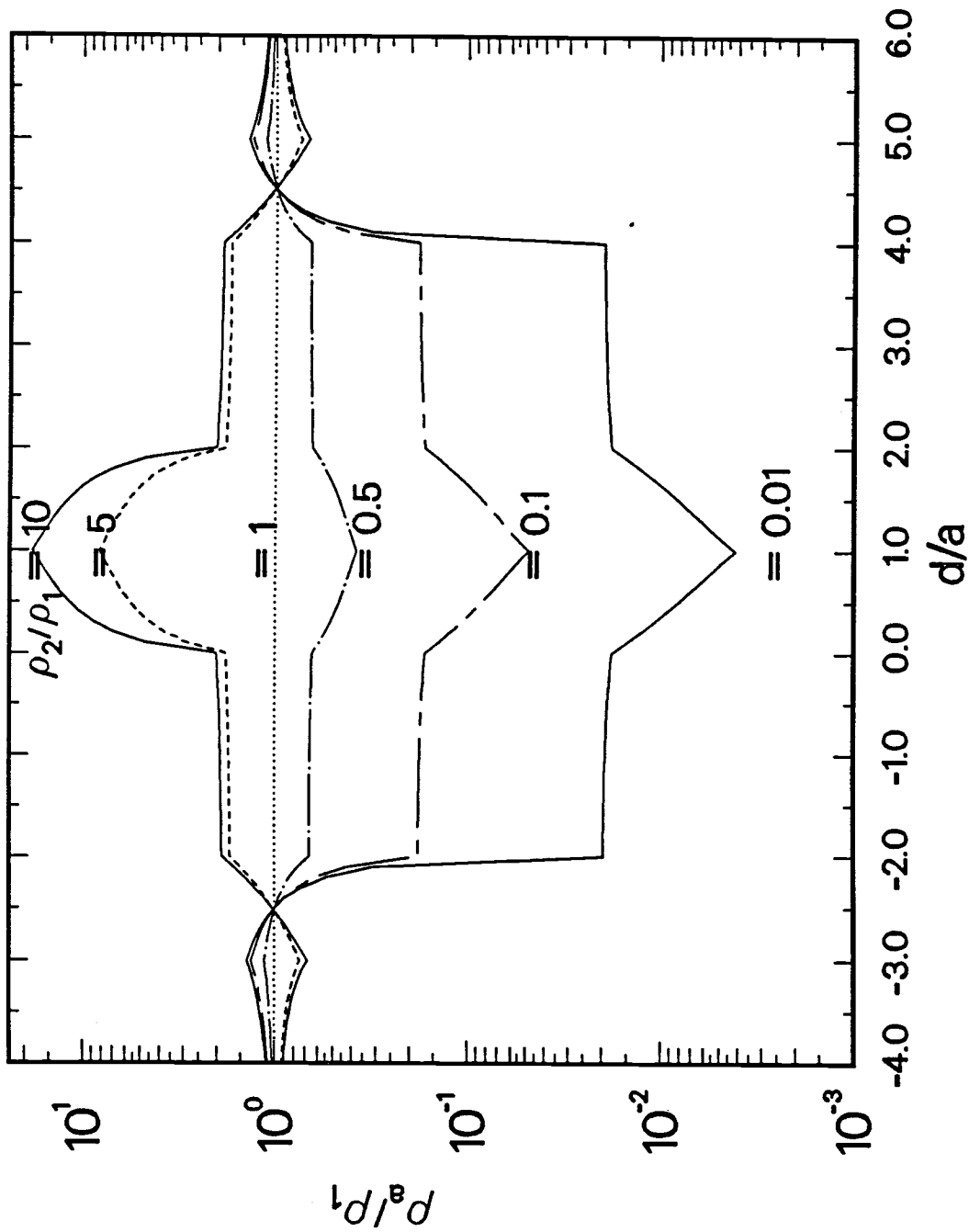
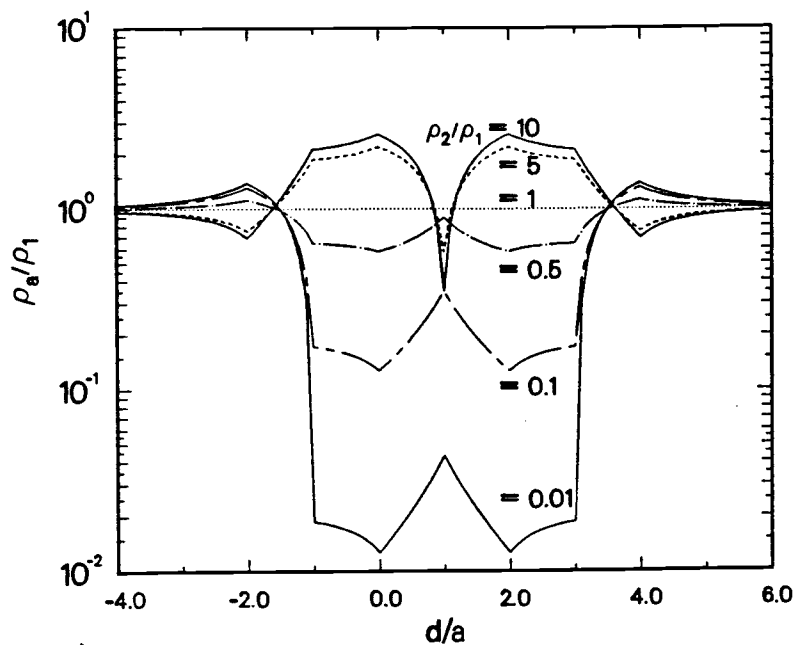
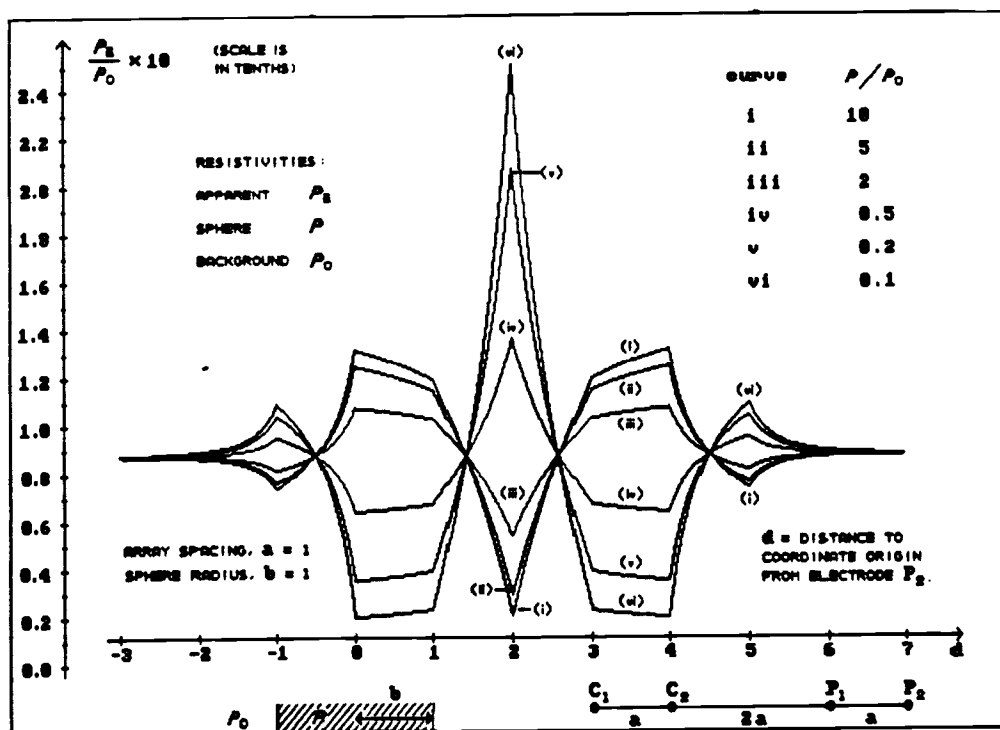


Figure 2-14 The ratio of the apparent resistivity to the resistivity of surrounding material vs. d/a for dipole-dipole array when $b = 2a$



a)



b)

Figure 2-15 The ratio of the apparent resistivity to the resistivity of surrounding material vs. d/a for dipole-dipole array when $b = a$ and

a) $\rho_2/\rho_1 = 10, 5, 1, 0.5, 0.1, 0.01$ over the dike

b) $\rho_2/\rho_1 = 10, 5, 2, 0.5, 0.2, 0.1$ over hemispherical sink (A. Peters, 1988)

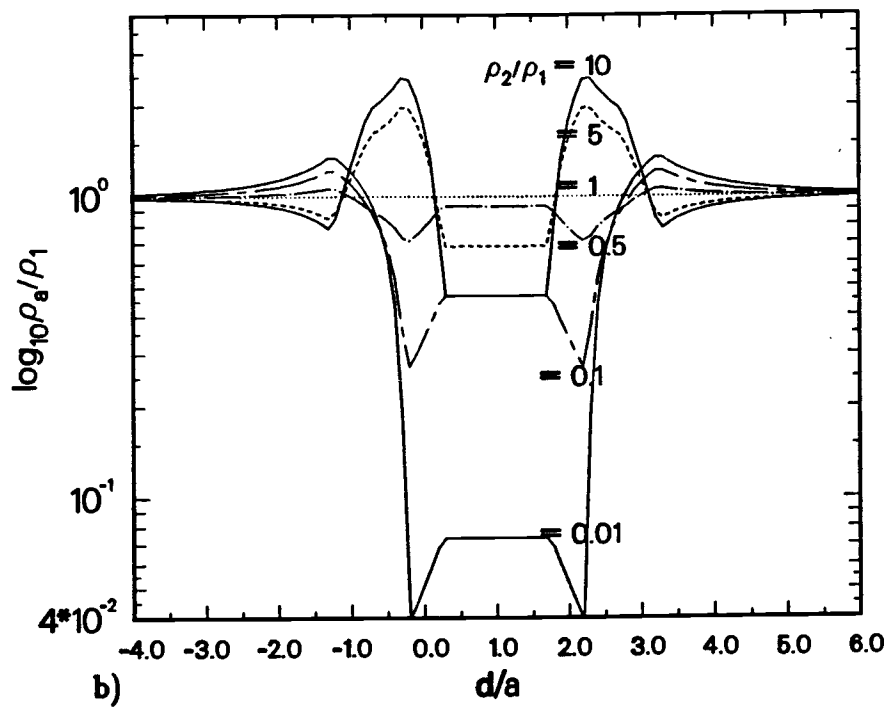
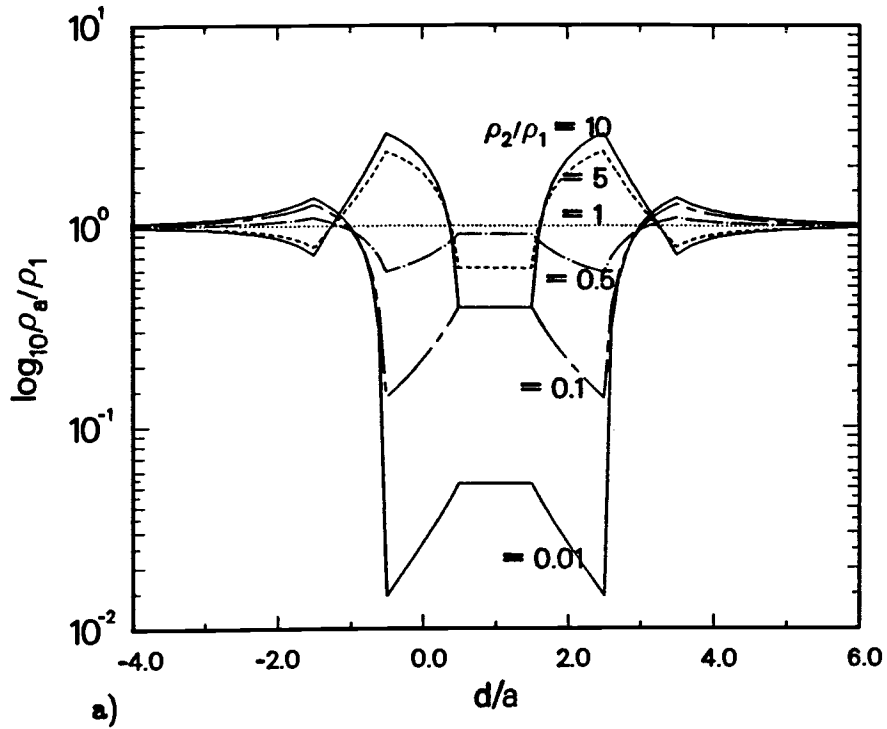


Figure 2-16 The ratio of the apparent resistivity to the resistivity of surrounding material vs. d/a for dipole-dipole array when
 a) $b/a = 0.5$, b) $b/a = 0.25$

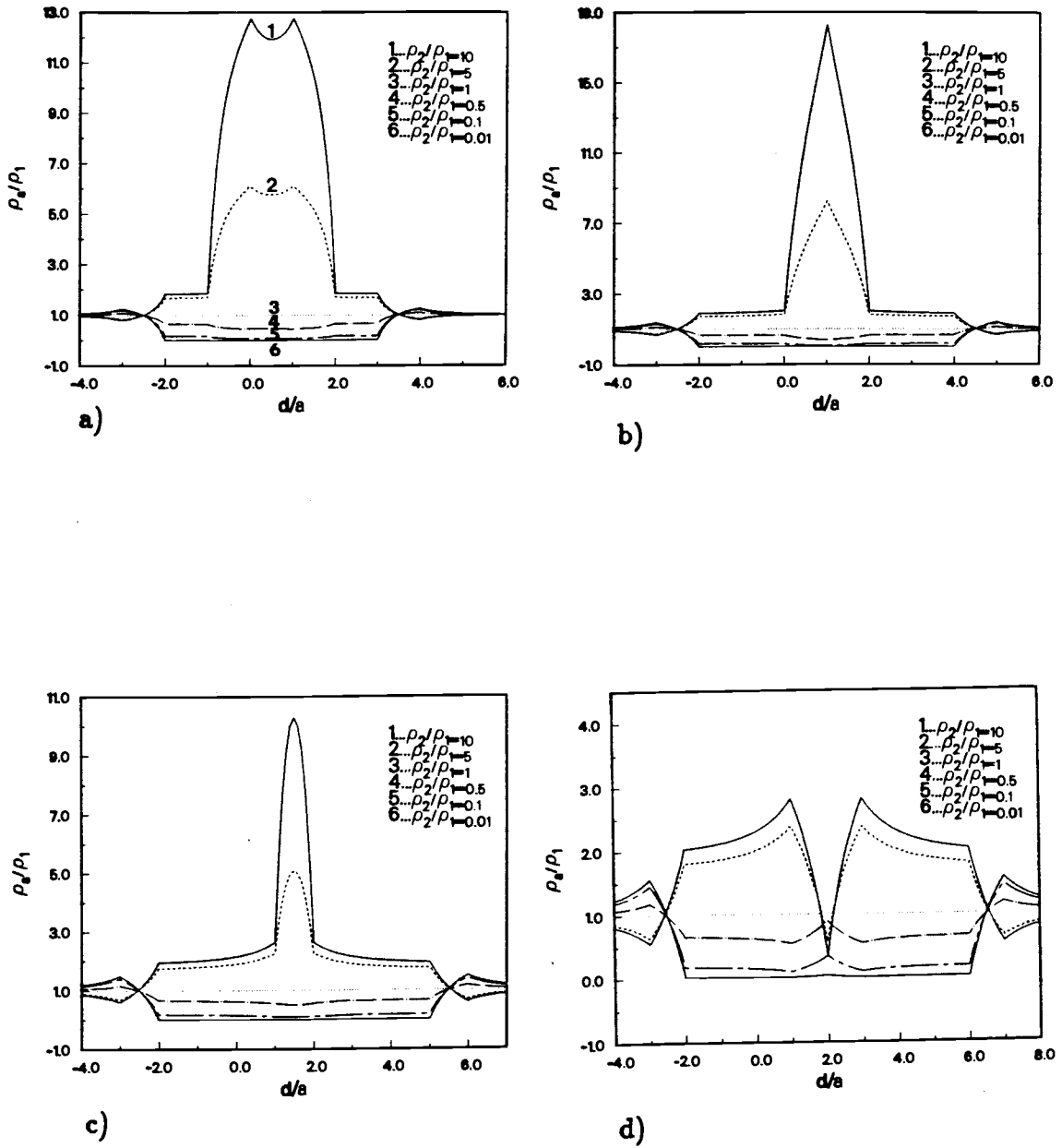


Figure 2-17 The ratio of the apparent resistivity to the resistivity of surrounding material vs. d/a for dipole-dipole array when
 a) $n = 1$, b) $n = 2$, c) $n = 3$, d) $n = 4$

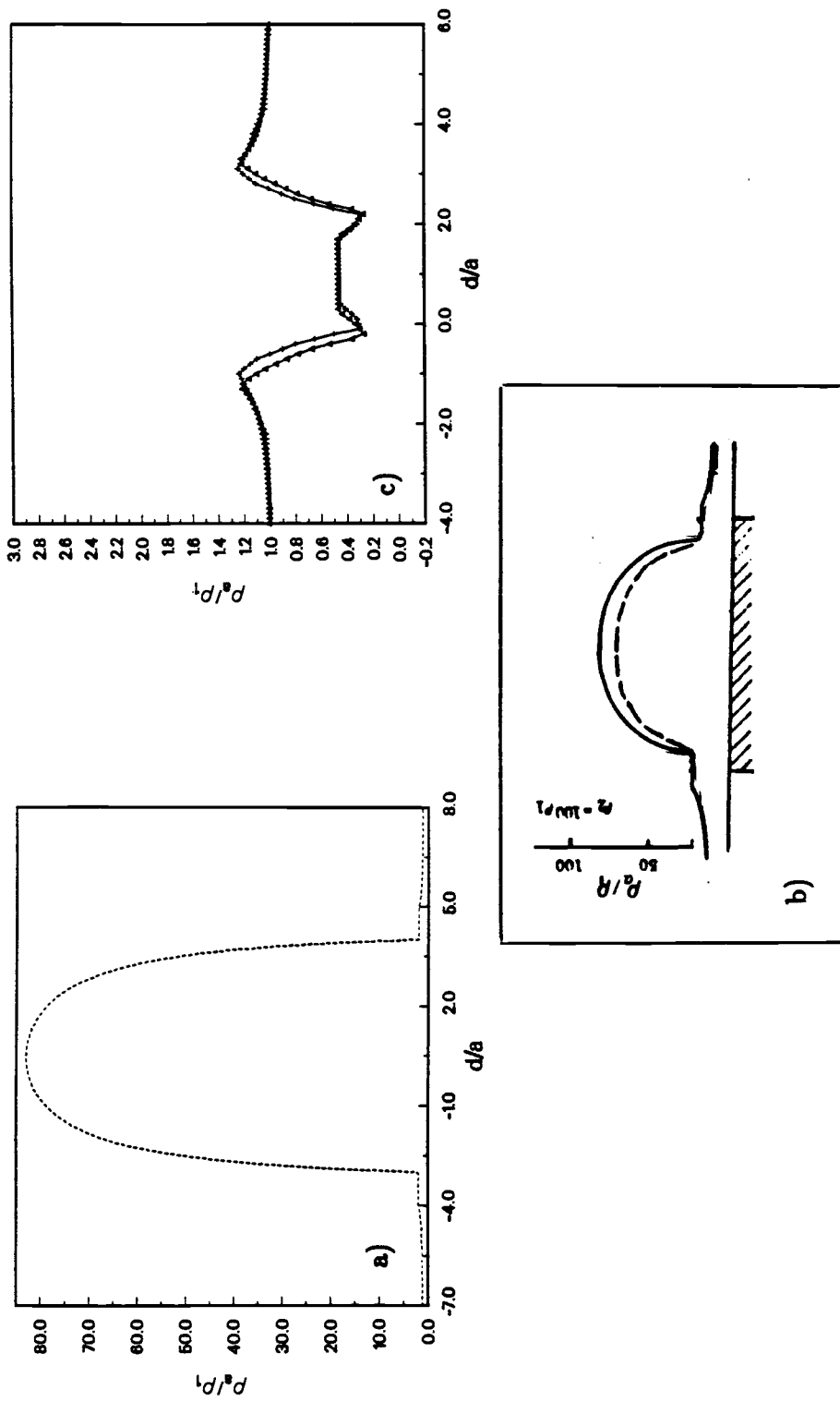


Figure 2-18 The ratio of the apparent resistivity to the resistivity of surrounding material vs. d/a ,
 a) for pole-pole array when $b = a$ and $\rho_2/\rho_1 = 100$,
 b) for pole-pole array when $b = a$ and $\rho_2/\rho_1 = 100$ (V.N. Dakhnow, 1962),
 c) for dipole-dipole array when $b/a = 0.25$ and $\rho_2/\rho_1 = 0.1$
 (x: the curve we obtained, Δ : C.S. Ludwig's curve, 1967)

TABLE 2-1		
$r\rho_1/d\rho_2$	$H_0 - Y_0$	ρ_a/ρ_2
0.001	4.4721900	0.007025
0.002	4.0315500	0.012660
0.003	3.7740590	0.017780
0.004	3.5915470	0.022560
0.005	3.4501206	0.027090
0.007	3.2371747	0.035590
0.010	3.0119900	0.047310
0.015	2.7569870	0.064959
0.020	2.5769510	0.080957
0.025	2.4379900	0.095739
0.030	2.3250060	0.109560
0.040	2.1480070	0.134960
0.050	2.0120659	0.158020
0.060	1.9020909	0.179267
0.070	1.8016108	0.200927
0.080	1.7310917	0.217535
0.090	1.6621670	0.234980
0.100	1.6011469	0.251507
0.150	1.3733142	0.323579
0.200	1.2105346	0.387906
0.250	1.1095386	0.435714
0.300	1.0248970	0.482971
0.400	0.9064760	0.569550
0.500	0.8019320	0.623397
1.000	0.4804000	0.750000
1.500	0.3542800	0.830000
2.000	0.2804800	0.880000
2.500	0.2318800	0.910000
3.000	0.1974500	0.930000
3.500	0.1718000	0.940000
4.000	0.1519500	0.950000
4.500	0.1361600	0.962000
5.000	0.1233010	0.968000
5.550	0.1155600	0.973000
6.250	0.0996550	0.978000
7.143	0.0876020	0.983000
8.330	0.0754040	0.987000
9.090	0.0692540	0.988000
10.00	0.0630720	0.990000
12.50	0.0506200	0.994000
16.66	0.0380640	0.996000
20.00	0.0317530	0.997000

Table 2-1 Numerical values of Struve function and Bessel function of second kind of order zero as a function of $x = r\rho_1/d\rho_2$

TABLE-2-2

x^*	$H_0(2x)$	$H_0(3x)$	$H_0(4x)$	$Y_0(2x)$	$Y_0(3x)$	$Y_0(4x)$
0.1	0.12675	0.18908	0.25014	-1.08110	-0.8073	-0.60602
0.2	0.25014	0.36691	0.47399	-0.60602	-0.3085	-0.08680
0.3	0.36691	0.52303	0.64855	-0.30850	0.00562	0.228080
0.4	0.47399	0.64855	0.75702	-0.08680	0.22808	0.420420
0.5	0.56865	0.73672	0.79085	0.088250	0.38244	0.510370
0.6	0.64855	0.78345	0.75064	0.228080	0.47743	0.510410
0.8	0.71179	0.78752	0.64586	0.337890	0.51829	0.435910
1.0	0.79085	0.57430	0.13501	0.510370	0.37685	-0.01694
1.5	0.57430	-0.05854	-0.1846	0.376850	-0.1947	-0.28819
2.0	0.13501	-0.18460	0.30200	-0.01694	-0.2882	0.223520
2.5	-0.18521	0.20090	0.11870	-0.30851	0.11731	0.055670
3.0	-0.18460	0.31990	-0.1725	-0.28819	0.24993	-0.22523
3.5	0.06340	-0.00740	0.17240	-0.02594	-0.0675	0.127190
4.0	0.30200	-0.17250	0.13387	0.223520	-0.3252	0.095810
5.0	0.11870	0.24770	—	0.055670	0.20546	—

* $x = r\rho_1/d\rho_2$

$$H_0(z) = \frac{2}{\pi} \left(z - \frac{z^3}{1^2 \cdot 3^2} + \frac{z^5}{1^2 \cdot 3^2 \cdot 5^2} - \dots \right)$$

$$H_0(z) - Y_0(x) = \frac{2}{\pi} \left(\frac{1}{z} - \frac{1}{z^3} + \frac{1^2 3^2}{z^5} - \frac{1^2 3^2 5^2}{z^7} + \dots \right) \quad \text{when } |\arg z| < \pi.$$

$$H_1(z) - Y_1(z) = \frac{2}{\pi} \left(1 + \frac{1}{z^2} - \frac{1^2 3}{z^4} + \frac{1^2 3^2 5}{z^6} - \dots \right) \quad \text{when } |\arg z| < \pi.$$

Table 2-2 Numerical values of Struve function and Bessel function of second kind of order zero as a function of $2x$, $3x$, $4x$

TABLE 2-3 (a)	
d/a	ρ_a/ρ_1^*
-3.00	0.9162300
-2.00	0.8612926
-1.00	0.7060637
0.00	0.0966198
1.00	0.0966198
2.00	0.6593027
3.00	0.8205653
4.00	0.8801572

* (M = 10)

TABLE 2-3 (b)	
d/a	ρ_a/ρ_1^*
-3.00	0.8993995
-2.00	0.8412656
-1.00	0.6817372
0.00	0.1194307
1.00	0.1194307
2.00	0.6793550
3.00	0.8389693
4.00	0.8971830

* (M = 50)

TABLE 2-3 (c)	
d/a	ρ_a/ρ_1^*
-3.00	0.8988515
-2.00	0.8406844
-1.00	0.6811196
0.00	0.1211177
1.00	0.1211177
2.00	0.6809529
3.00	0.8405209
4.00	0.8986910

* (M = 100)

TABLE 2-3 (d)	
d/a	ρ_a/ρ_1^*
-3.00	0.8988245
-2.00	0.8406565
-1.00	0.6810908
0.00	0.1212594
1.00	0.1212594
2.00	0.6810892
3.00	0.8406550
4.00	0.8988230

* (M = 200)

TABLE 2-3 (e)	
d/a	ρ_a/ρ_1^*
-3.00	0.8988243
-2.00	0.8406564
-1.00	0.6810906
0.00	0.1212608
1.00	0.1212608
2.00	0.6810906
3.00	0.8406564
4.00	0.8988243

* (M = 300)

TABLE 2-3 (f)	
d/a	ρ_a/ρ_1^*
-3.00	0.8988243
-2.00	0.8406564
-1.00	0.6810906
0.00	0.1212608
1.00	0.1212608
2.00	0.6810906
3.00	0.8406564
4.00	0.8988243

* (M = 350)

 $b/a = 0.25, \rho_2/\rho_1 = 0.01$

M = Number of terms

Table 2-3 Numerical convergence of ρ_a/ρ_1 for pole-pole array

TABLE 2-4 (a)	
d/a	ρ_a/ρ_1^*
-4.00	1.022798
-2.00	1.132518
0.00	0.050687
2.00	0.050687
4.00	1.135903
6.00	1.024561

* (M = 10)

TABLE 2-4 (b)	
d/a	ρ_a/ρ_1^*
-4.00	1.024119
-2.00	1.135186
0.00	0.051584
2.00	0.051584
4.00	1.135203
6.00	1.024132

* (M = 50)

TABLE 2-4 (c)	
d/a	ρ_a/ρ_1^*
-4.00	1.024126
-2.00	1.135195
0.00	0.051590
2.00	0.051590
4.00	1.135196
6.00	1.024126

* (M = 100)

TABLE 2-4 (d)	
d/a	ρ_a/ρ_1^*
-4.00	1.024126
-2.00	1.135195
0.00	0.051591
2.00	0.051591
4.00	1.135195
6.00	1.024126

* (M = 200)

TABLE 2-4 (e)	
d/a	ρ_a/ρ_1^*
-4.00	1.024126
-2.00	1.135195
0.00	0.051591
2.00	0.051591
4.00	1.135195
6.00	1.024126

* (M = 300)

TABLE 2-4 (f)	
d/a	ρ_a/ρ_1^*
-4.00	1.024126
-2.00	1.135195
0.00	0.051591
2.00	0.051591
4.00	1.135195
6.00	1.024126

* (M = 500)

Table 2-4 Numerical convergence of ρ_a/ρ_1 for dipole-dipole array

$$b/a = 0.25, \rho_2/\rho_1 = 0.01$$

M = Number of terms

CHAPTER 3

IP DILUTION AND DISTORTION PARAMETERS FOR DIFFERENT EARTH GEOMETRIES

Seigel in 1959 formulated a relationship based on the proportionality of polarization with current density and defined IP response chargeability, m , in terms of a charge in resistivity. Then, he determined the apparent chargeability, m_a , for any polarizable body and any electrode array. The total apparent chargeability is a summation of all chargeabilities, m_i times the dilution factor or the weighting function, B_i . The dilution factor is the relative IP response of the layer in any earth geometry. This term is formulated to understand how the polarizable structure masks the measurement of the apparent chargeability of the formation. This important parameter describes the departure of the apparent resistivity from its dc value. It could also be developed in the frequency domain by admitting the possibility that the complex resistivities of the region are complex and frequency dependent (Wait, 1982; Wait and Gruszka, 1987). The apparent complex resistivity can be written for a specific configuration of the source dipole and receiving circuit by assuming quasistatic electrical conditions, so that the problem can be solved using potential fields. In this formulation, the higher order effects can also be incorporated. The second-order term is called the distortion factor by J.R. Wait (1981). This factor shows how the frequency response is modified. The higher order terms are not included in Seigel's (1959) formulation. However, they may be present, and it could lead to a misleading diagnosis of the observed data if simply ignored (Wait, 1981).

The purpose here is to present explicit results for the IP responses for a pole-pole (half-Wenner) and dipole-dipole arrays located on a two-layer earth and dike models by using the apparent complex resistivity formulation.

3.1 IP Parameters over Thin Horizontal Layer

The earth's resistivity is not simply resistive. It is in general complex. The term "complex resistivity" is more frequently being invoked to describe the total nature of the earth's resistivity (Wait, 1959; Synder, 1977). To simplify the discussion, we will deal with a thin-layer problem where the constitutive parts are characterized by a complex-resistivity formulation. An attempt is made here to show how the apparent complex resistivity is related to the properties of the medium. We consider that the two-layer earth is characterized by two different complex resistivities $\rho_1(i\omega)$ and $\rho_2(i\omega)$, first and second layer complex resistivities, respectively. Following Wait (1981), we can write

$$\rho_a(i\omega) = \rho_a[\rho_1(i\omega), \rho_2(i\omega)] \quad (3.1)$$

where,

$$\rho_1(i\omega) = \rho_1[1 + \delta_1(i\omega)] \quad (3.2)$$

$$\rho_2(i\omega) = \rho_2[1 + \delta_2(i\omega)] \quad (3.3)$$

where $\rho_1 = \rho_1(0)$ and $\rho_2 = \rho_2(0)$ are the dc resistivities of the first and the second layers or zero frequency solutions and δ_1 and δ_2 are the complex-frequency-dependent departures from the dc resistivities of the two constitutive regions. They can be regarded as dispersion functions which vanish as ω goes to zero (Wait, 1987). Using Wait's idea, we can write the apparent complex resistivity formulation for a horizontal thin-layer earth model which is polarizable. The apparent complex resistivity is a function of the complex resistivities of each layer. By employing a MacLaurin series expansion, we can write equation (3.1) as

$$\begin{aligned} \rho_a(i\omega) = & \rho_a(1 + B_1\delta_1(i\omega) + B_2\delta_2(i\omega) \\ & + B_{1,1}\delta_1^2(i\omega) + B_{1,2}\delta_1(i\omega)\delta_2(i\omega) + B_{2,2}\delta_2^2(i\omega) + \dots) \end{aligned} \quad (3.4)$$

where ρ_a is the dc apparent resistivity for a horizontal thin layer. The coefficients B_1 and B_2 involve only dc resistivity functions and such a convention was first conceived by Seigel (1959). Higher order terms, defined as $B_{1,1}, B_{2,2}, B_{1,2}$, etc. called distortion factors, are neglected in his paper. However, these terms produce a more complicated change of the apparent complex resistivity as shown by Wait (1981), who indicated it could cause a misleading diagnosis of the IP response data if simply ignored.

The following definitions and identities have been established previously (Wait, 1986):

$$B_1 = \frac{\rho_1}{\rho_a} \frac{\partial \rho_a}{\partial \rho_1} = \frac{\partial \ln \rho_a}{\partial \ln \rho_1}, \quad (3.5)$$

$$B_2 = \frac{\rho_2}{\rho_a} \frac{\partial \rho_a}{\partial \rho_2} = \frac{\partial \ln \rho_a}{\partial \ln \rho_2}, \quad (3.6)$$

$$B_{1,1} = \frac{1}{2} \frac{\rho_1^2}{\rho_a} \frac{\partial^2 \rho_a}{\partial \rho_1^2}, \quad (3.7)$$

$$B_{2,2} = \frac{1}{2} \frac{\rho_2^2}{\rho_a} \frac{\partial^2 \rho_a}{\partial \rho_2^2}, \quad (3.8)$$

and,

$$B_{1,2} = \frac{\rho_1 \rho_2}{\rho_a} \frac{\partial^2 \rho_a}{\partial \rho_1 \partial \rho_2}. \quad (3.9)$$

The dilution and distortion factors are derived simply from the real dc resistivity functions $\rho_a(0), \rho_1(0), \rho_2(0)$ and their useful relationships taken from Wait (1986) are:

$$B_1 + B_2 = 1, \quad (3.10)$$

$$B_{1,1} = B_{2,2}, \quad (3.11)$$

and,

$$B_{1,2} = -2B_{2,2}. \quad (3.12)$$

We checked that our computer values satisfy the identities equations (3.10) and (3.11).

The mathematical resistivity solution of the two-layer case has been shown in section 2.1. In induced polarization, it is assumed that the upper thin and lower layers are polarizable. Here, we will formulate the dilution and distortion factors to understand how the polarizable structure masks the measurement of the apparent chargeability of the two-layer horizontal formation, by using the apparent complex resistivity and the complex resistivities of each layer of the formation. Using equation (3.6) and the analytical expression for dc apparent resistivity for pole-pole (half-Wenner) array given by equation (2.39), it follows that

$$B_2 = -\frac{a\rho_1}{d\rho_2} \frac{\mathbf{H}'_0 - Y'_0}{\mathbf{H}_0 - Y_0}. \quad (3.13)$$

where,

$$\mathbf{H}'_0 = \frac{2}{\pi} - \mathbf{H}_1, \quad (3.14)$$

and,

$$Y'_0 = -Y_1. \quad (3.15)$$

\mathbf{H}_1 is the first-order Struve function, and Y_1 is the first-order Bessel function of the second kind (Abramowitz and Stegun, 1964). From equation (3.14) and (3.15), the dilution factor of the upper layer is

$$B_2 = -x \left(\frac{\frac{2}{\pi} - \mathbf{H}_1(x) + Y_1(x)}{\mathbf{H}_0(x) - Y_0(x)} \right), \quad (3.16)$$

where x is $r\rho_1/d\rho_2$. The dilution factor of the lower layer, B_1 , can also be written by definition in equation (3.5). Similarly

$$B_1 = 1 + x \left(\frac{\mathbf{H}'_0(x) - Y'_0(x)}{\mathbf{H}_0(x) - Y_0(x)} \right). \quad (3.17)$$

In Figure 3-1a, the dilution factors B_1 and B_2 are plotted as a function of $r\rho_1/d\rho_2$ for a pole-pole array.

In a similar manner, the higher order terms are obtained by taking a logarithmic derivative of the dc apparent resistivity twice. These terms produce a more complicated change of equation (3.4) (Wait, 1981). The distortion factor is calculated from equation (3.8) and (2.39)

$$B_{2,2} = x \left(\frac{\mathbf{H}_0'(x) - Y_0'(x)}{\mathbf{H}_0(x) - Y_0(x)} \right) + \frac{x^2}{2} \left(\frac{\mathbf{H}_0''(x) - Y_0''(x)}{\mathbf{H}_0(x) - Y_0(x)} \right). \quad (3.18)$$

By using the following identity of Struve and Bessel functions (Abramowitz and Stegun, 1964)

$$\mathbf{H}_0''(x) = -\frac{a}{d\rho_2} \mathbf{H}_1'(2x) = -\frac{a}{d\rho_1\rho_2} (\rho_1 \mathbf{H}_0(x) - \mathbf{H}_1(x)), \quad (3.19)$$

and,

$$Y_0''(x) = -Y_1'(x) = -Y_0(x) + \frac{1}{x} Y_1(x), \quad (3.20)$$

the distortion factor of the upper layer is obtained

$$B_{2,2} = x \frac{\frac{2}{\pi} - \mathbf{H}_1 + Y_1 + \frac{x^2}{2} \left(\frac{\mathbf{H}_1 - Y_1}{x} - \mathbf{H}_0 + Y_0 \right)}{\mathbf{H}_0 - Y_0}. \quad (3.21)$$

In Figure 3-2a, we show the distortion factor of upper layer for pole-pole array.

We also calculated dilution and distortion factors for a dipole-dipole array located on the thin horizontal sheet. The dilution factor is obtained as the analytical expression for ρ_a given by equation (2.47)

$$B_2 = -x \frac{S'}{S}, \quad (3.22)$$

where,

$$S = 2\mathbf{H}_0(3x) - 2Y_0(3x) - \mathbf{H}_0(2x) + Y_0(2x) - \mathbf{H}_0(4x) + Y_0(4x), \quad (3.23)$$

$$S' = 6\mathbf{H}_0(3x) - 6Y_0(3x) - 2\mathbf{H}'_0(2x) + 2Y'_0(2x) - 4\mathbf{H}'_0(4x) + 4Y'_0(4x). \quad (3.24)$$

The derivative of Struve functions is given by Abramowitz and Stegun (1965):

$$\mathbf{H}'_0(2x) = \frac{2}{\pi} - \mathbf{H}_1(2x), \quad (3.25)$$

$$\mathbf{H}'_0(3x) = \frac{2}{\pi} - \mathbf{H}_1(3x), \quad (3.26)$$

$$\mathbf{H}'_0(4x) = \frac{2}{\pi} - \mathbf{H}_1(4x), \quad (3.27)$$

and the derivative of Bessel functions is given by Watson (1966):

$$Y'_0(2x) = -Y_1(2x), \quad (3.28)$$

$$Y'_0(3x) = -Y_1(3x), \quad (3.29)$$

$$Y'_0(4x) = -Y_1(4x). \quad (3.30)$$

Then the distortion factor for dipole-dipole array is obtained by taking the second derivative of apparent resistivity equation (2.47)

$$B_{2,2} = x \frac{S'}{S} - \frac{1}{2} x^2 \frac{S''}{S}, \quad (3.31)$$

where,

$$\begin{aligned} S'' = & 8(\mathbf{H}_0(3x) - Y_0(3x)) + \frac{6}{x}(\mathbf{H}_1(3x) - Y_1(3x)) + 16(\mathbf{H}_0(4x) - Y_0(4x)) \\ & - \frac{4}{x}(\mathbf{H}_1(4x) - Y_1(4x)) + 4(\mathbf{H}_0(2x) - Y_0(2x)) - \frac{2}{x}(\mathbf{H}_1(2x) - Y_1(2x)). \end{aligned} \quad (3.32)$$

Figures 3-1a and 3-1b show IP coefficients B_1 and B_2 over the thin horizontal layer with the pole-pole and dipole-dipole arrays. Like the apparent-resistivity anomalies for the thin-sheet model, they increase rapidly towards 1. Figures 3-2a and 3-2b show $B_{2,2}$ IP coefficients for pole-pole and dipole-dipole arrays as a function of $r\rho_1/d\rho_2$. They give negative IP distortion effects for both arrays. These

anomalies begin at -0.1 for small values of x , decrease rapidly, and reach a negative minimum of -0.25 and finally increase toward zero.

3.2 IP Parameters over Dike Model

In order to give a closed analytical solution for the IP dilution and distortion factors, it has been assumed that the dike and surrounding media are polarizable. These IP responses were obtained for pole-pole and dipole-dipole arrays from the first and second differentiation in the dc formulations. The mathematical dc resistivity solutions of the dike model for a pole-pole array have been derived in section 2.2.1.

If the potential measuring and current source electrodes are to the left of the dike, the apparent-resistivity formula is given by equation (2.57). Since the apparent resistivity has already been found by using equation (3.5) one can write

$$B_1 = 1 - \frac{(1 - k^2)}{2f_1(k)} \frac{\partial f_1}{\partial k}. \quad (3.33)$$

where,

$$f_1(k) = 1 + \frac{k}{2\left(\frac{d}{a} - \frac{b}{a}\right) - 1} - k(1 - k^2) \sum_{m=0}^{\infty} \frac{k^{2m}}{2\left((2m+1)\frac{b}{a} + \frac{d}{a}\right) - 1}, \quad (3.34)$$

and

$$\frac{\partial f_1}{\partial k} = \frac{1}{2\left(\frac{d}{a} - \frac{b}{a}\right) - 1} - \sum_{m=0}^{\infty} \frac{(2m+1)k^{2m}}{2\left((2m+1)\frac{b}{a} + \frac{d}{a}\right) - 1} + \sum_{m=0}^{\infty} \frac{(2m+3)k^{2m+2}}{2\left((2m+1)\frac{b}{a} + \frac{d}{a}\right) - 1}. \quad (3.35)$$

Using equation (3.7), we obtain the distortion factor

$$B_{11} = \frac{(1+k)^2(1-k)}{4f_1(k)} \left(-\frac{\partial f_1}{\partial k} + \frac{(1-k)}{2} \frac{\partial^2 f_1}{\partial k^2} \right), \quad (3.36)$$

where,

$$\frac{\partial^2 f_1}{\partial k^2} = - \sum_{m=0}^{\infty} \frac{(2m+1)2mk^{2m-1}}{2\left((2m+1)\frac{b}{a} + \frac{d}{a}\right) - 1} + \sum_{m=0}^{\infty} \frac{(2m+3)(2m+2)k^{2m+1}}{2\left((2m+1)\frac{b}{a} + \frac{d}{a}\right) - 1}. \quad (3.37)$$

By using equation (2.62), which is obtained when the potential electrode is in medium 2 and the current electrode is in medium 1, the dilution factor is

$$B_1 = 1 - \frac{(1-k^2)}{2f_2(k)} \frac{\partial f_2}{\partial k}, \quad (3.38)$$

where,

$$f_2(k) = (1+k) \left(\sum_{m=0}^{\infty} \frac{k^{2m}}{4m\frac{b}{a} + 1} - k \sum_{m=0}^{\infty} \frac{k^{2m}}{2\left((2m+1)\frac{b}{a} + \frac{d}{a}\right) - 1} \right), \quad (3.39)$$

and

$$\frac{\partial f_2}{\partial k} = \sum_{m=0}^{\infty} \frac{2mk^{2m-1} + (2m+1)k^{2m}}{4m\frac{b}{a} + 1} - \sum_{m=0}^{\infty} \frac{((2m+1)k^{2m} + (2m+2)k^{2m+1})}{2\left((2m+1)\frac{b}{a} + \frac{d}{a}\right) - 1}. \quad (3.40)$$

The distortion factor is

$$B_{11} = \frac{(1+k)^2(1-k)}{4f_2(k)} \left(-\frac{\partial f_2}{\partial k} + \frac{(1-k)}{2} \frac{\partial^2 f_2}{\partial k^2} \right), \quad (3.41)$$

where,

$$\begin{aligned} \frac{\partial^2 f_2}{\partial k^2} &= \sum_{m=0}^{\infty} \frac{2m((2m-1)k^{2m-2} + (2m+1)k^{2m-1})}{4m\frac{b}{a} + 1} \\ &\quad - \sum_{m=0}^{\infty} \frac{(2m+1)(2mk^{2m-1} + (2m+2)k^{2m})}{2\left((2m+1)\frac{b}{a} + \frac{d}{a}\right) - 1}. \end{aligned} \quad (3.42)$$

For the case in which the current electrode is on the first medium and the potential electrode is on the third medium, by using equation (2.63), the dilution factor can be computed

$$B_1 = 1 - \frac{(1-k^2)}{2f_3(k)} \frac{\partial f_3}{\partial k}, \quad (3.43)$$

where,

$$f_3(k) = (1 - k^2) \sum_{m=0}^{\infty} \frac{k^{2m}}{4m^{\frac{b}{a}} + 1}, \quad (3.44)$$

$$\frac{\partial f_3}{\partial k} = \sum_{m=0}^{\infty} \frac{2mk^{2m-1}}{4m^{\frac{b}{a}} + 1} - \sum_{m=0}^{\infty} \frac{(2m+2)k^{2m+1}}{4m^{\frac{b}{a}} + 1}. \quad (3.45)$$

The distortion factor is obtained as

$$B_{1,1} = \frac{(1+k)^2(1-k)}{4f_3(k)} \left(-\frac{\partial f_3}{\partial k} + \frac{(1-k)}{2} \frac{\partial^2 f_3}{\partial k^2} \right), \quad (3.46)$$

where,

$$\frac{\partial^2 f_3}{\partial k^2} = \sum_{m=0}^{\infty} \frac{2m(2m-1)k^{2m-2}}{4m^{\frac{b}{a}} + 1} - \sum_{m=0}^{\infty} \frac{(2m+2)(2m+1)k^{2m}}{4m^{\frac{b}{a}} + 1}. \quad (3.47)$$

When both the current and potential electrodes are on the dike, from equation (2.65), the dilution factor is written

$$B_1 = -\frac{(1-k^2)}{2f_4(k)} \frac{\partial f_4}{\partial k}, \quad (3.48)$$

where,

$$f_4(k) = 1 + \sum_{m=0}^{\infty} \frac{k^{2m+2}}{4(m+1)^{\frac{b}{a}} + 1} + \sum_{m=0}^{\infty} \frac{k^{2m+2}}{4(m+1)^{\frac{b}{a}} - 1} - \sum_{m=0}^{\infty} \frac{k^{2m+1}}{2\left((2m+1)^{\frac{b}{a}} + \frac{d}{a}\right) - 1} - \sum_{m=0}^{\infty} \frac{k^{2m+1}}{2\left((2m+1)^{\frac{b}{a}} - \frac{d}{a}\right) + 1}, \quad (3.49)$$

$$\begin{aligned} \frac{\partial f_4}{\partial k} &= \sum_{m=0}^{\infty} \frac{(2m+2)k^{2m+1}}{4(m+1)^{\frac{b}{a}} + 1} + \sum_{m=0}^{\infty} \frac{(2m+2)k^{2m+1}}{4(m+1)^{\frac{b}{a}} - 1} \\ &- \sum_{m=0}^{\infty} \frac{(2m+1)k^{2m}}{2\left((2m+1)^{\frac{b}{a}} + \frac{d}{a}\right) - 1} - \sum_{m=0}^{\infty} \frac{(2m+1)k^{2m}}{2\left((2m+1)^{\frac{b}{a}} - \frac{d}{a}\right) + 1}, \end{aligned} \quad (3.50)$$

The distortion factor is

$$B_{1,1} = \frac{(1-k^2)(1-k)}{4f_4(k)} \left(\frac{(1+k)}{2} \frac{\partial^2 f_4}{\partial k^2} + \frac{\partial f_4}{\partial k} \right), \quad (3.51)$$

where,

$$\begin{aligned}
\frac{\partial^2 f_4}{\partial k^2} &= \sum_{m=0}^{\infty} \frac{(2m+2)(2m+1)k^{2m}}{4(m+1)^{\frac{b}{a}} + 1} \\
&+ \sum_{m=0}^{\infty} \frac{(2m+2)(2m+1)k^{2m}}{4(m+1)^{\frac{b}{a}} - 1} \\
&- \sum_{m=0}^{\infty} \frac{(2m+1)2mk^{2m-1}}{2\left((2m+1)^{\frac{b}{a}} + \frac{d}{a}\right) - 1} \\
&- \sum_{m=0}^{\infty} \frac{(2m+1)2mk^{2m-1}}{2\left((2m+1)^{\frac{b}{a}} - \frac{d}{a}\right) + 1}. \tag{3.52}
\end{aligned}$$

By a similar analysis, we obtain the dilution and distortion factors when the current electrode is on the dike and the potential electrode is on the right side of the dike.

$$B_1 = 1 - \frac{(1-k^2)}{2f_5(k)} \frac{\partial f_5}{\partial k}, \tag{3.53}$$

and

$$B_{1,1} = \frac{(1+k)^2(1-k)}{4f_5(k)} \left(-\frac{\partial f_5}{\partial k} + \frac{(1-k)}{2} \frac{\partial^2 f_5}{\partial k^2} \right), \tag{3.54}$$

where,

$$\begin{aligned}
f_5(k) &= \sum_{m=0}^{\infty} \frac{k^{2m}}{4m^{\frac{b}{a}} + 1} - \sum_{m=0}^{\infty} \frac{k^{2m+1}}{2\left((2m+1)^{\frac{b}{a}} - \frac{d}{a}\right) + 1} \\
&+ \sum_{m=0}^{\infty} \frac{k^{2m+1}}{4m^{\frac{b}{a}} + 1} - \sum_{m=0}^{\infty} \frac{k^{2m+2}}{2\left((2m+1)^{\frac{b}{a}} - \frac{d}{a}\right) + 1}, \tag{3.55}
\end{aligned}$$

$$\begin{aligned}
\frac{\partial f_5(k)}{\partial k} &= \sum_{m=0}^{\infty} \frac{2mk^{2m-1}}{4m^{\frac{b}{a}} + 1} - \sum_{m=0}^{\infty} \frac{(2m+1)k^{2m}}{2\left((2m+1)^{\frac{b}{a}} - \frac{d}{a}\right) + 1} \\
&+ \sum_{m=0}^{\infty} \frac{(2m+1)k^{2m}}{4m^{\frac{b}{a}} + 1} - \sum_{m=0}^{\infty} \frac{(2m+2)k^{2m+1}}{2\left((2m+1)^{\frac{b}{a}} - \frac{d}{a}\right) + 1}, \tag{3.56}
\end{aligned}$$

$$\begin{aligned} \frac{\partial^2 f_5}{\partial k^2} &= \sum_{m=0}^{\infty} \frac{2m(2m-1)k^{2m-2}}{4m\frac{b}{a}+1} - \sum_{m=0}^{\infty} \frac{(2m+1)2mk^{2m-1}}{2\left((2m+1)\frac{b}{a}-\frac{d}{a}\right)+1} \\ &+ \sum_{m=0}^{\infty} \frac{(2m+1)2mk^{2m-1}}{4m\frac{b}{a}+1} - \sum_{m=0}^{\infty} \frac{(2m+2)(2m+1)k^{2m}}{2\left((2m+1)\frac{b}{a}-\frac{d}{a}\right)+1}. \end{aligned} \quad (3.57)$$

Finally, the dilution and distortion factors for the last case in which both electrodes are at the right side of the dike are obtained from the dc apparent resistivity equation (2.69) which are

$$B_1 = 1 - \frac{(1-k^2)}{2f_6(k)} \frac{\partial f_6}{\partial k}, \quad (3.58)$$

$$B_{1,1} = \frac{(1+k)^2(1-k)}{4f_6(k)} \left(-\frac{\partial f_5}{\partial k} + \frac{1-k}{2} \frac{\partial^2 f_6}{\partial k^2} \right), \quad (3.59)$$

where,

$$f_6(k) = 1 + \sum_{m=0}^{\infty} \frac{k^{2m+1}}{2\left((2m-1)\frac{b}{a}-\frac{d}{a}\right)+1} - \sum_{m=0}^{\infty} \frac{k^{2m+1}}{2\left((2m+1)\frac{b}{a}-\frac{d}{a}\right)+1}, \quad (3.60)$$

$$\frac{\partial f_6}{\partial k} = \sum_{m=0}^{\infty} \frac{(2m+1)k^{2m}}{2\left((2m-1)\frac{b}{a}-\frac{d}{a}\right)+1} - \sum_{m=0}^{\infty} \frac{(2m+1)k^{2m}}{2\left((2m+1)\frac{b}{a}-\frac{d}{a}\right)+1}, \quad (3.61)$$

$$\frac{\partial^2 f_6}{\partial k^2} = \sum_{m=0}^{\infty} \frac{(2m+1)2mk^{2m-1}}{2\left((2m-1)\frac{b}{a}-\frac{d}{a}\right)+1} - \sum_{m=0}^{\infty} \frac{(2m+1)2mk^{2m-1}}{2\left((2m+1)\frac{b}{a}-\frac{d}{a}\right)+1}. \quad (3.62)$$

By following the same identities, the dilution and distortion factors are also calculated for a dipole-dipole array located on the dike by taking the first and second derivatives of ρ_a/ρ_1 obtained in section 2.2.1.2.

3.3 Numerical Examples

Consideration will now be given to investigating how the distortion and dilution factors change with the resistivity contrast, electrode arrays, amount of polarizable material, and size of body. The dimensionless dilution and distortion factors are obtained for pole-pole and dipole-dipole arrays when the dike and surrounding rocks are polarizable. Then these factors are plotted as a function of d/a for various values of ρ_2/ρ_1 and thickness of the dike ($2b$). The results are presented in Figures 3-3 through 3-10.

In numerical examples, we used 10, 20, 30, 40, 50, 60, and 80 terms to check the convergence of the series for the thick-dike model. Finally, we saw that the results did not change after about 30 terms. However, results changed until 300 terms for the dilution factor and about 500 terms for the distortion factor when $b/a = 0.25$ and $\rho_2/\rho_1 = 0.01$ (Table 3-1). Here we computed the series with 600 terms to obtain dilution and distortion curves by using the Fortran computer program given in Appendix B. The numerical convergence of B_2 and B_{22} are given in Table 3-1. The dilution factors for all cases approach 1 as the electrodes move far from the dike. As the electrodes get far away from the dike, $\rho_a \rightarrow \rho_1$, using the definition of B_1 equation (3.2), we see that $B_1 \rightarrow 1$. Following the same procedure, we can easily show that $B_{1,1} \rightarrow 0$, as the electrodes are away from the dike.

We first consider the case for $b = 4a$. The dilution and distortion factors as functions of the position of electrodes (d/a) are plotted in Figure 3-3 for pole-pole and dipole-dipole arrays. The dilution factor of a dike for the pole-pole array shows low anomalies over the dike on the logarithmic scale when the dike is both resistive and conductive, as shown in Figure 3-3a. The highest anomaly is obtained when the dike has high resistivity ($\rho_2/\rho_1 = 10\Omega m$). The dilution curves for dipole-dipole arrays show pronounced polarization highs over the dike and a barely perceptible

paradoxical minimum in the central region of the dike on the linear scale (Fig. 3-3c). The highest peaks are obtained when there is no resistivity contrast between the dike and the surrounding rocks ($\rho_2/\rho_1 = 1$). As the dike becomes resistive or conductive, the peaks become smaller and the dilution factors over the dike approach one. On both sides of the dike, there are regions in which the dilution factor does not change with d/a . When the dike is very resistive, the dilution factor in this flat region approaches zero. As the dike becomes conductive, the dilution factor in this flat region approaches one. The distortion factor for pole-pole array shows the lowest anomaly on both sides of the dike and a paradoxical maximum in the center of the dike, as shown in Figure 3-3b. When the dike is very resistive, the distortion factor approaches zero over the dike. On the other hand, the distortion factor for the dipole-dipole array shows four positive peaks over the dike and both sides of the dike (Fig. 3-3d). These peaks are flanked by two lower anomalies on the right and left side of the dike. Although the distortion factor for pole-pole shows negative anomalies over the dike, the positive anomalies are obtained at the center of the dike for dipole-dipole array.

Attention next is given to the case $b = 2a$. The dilution and distortion factors for pole-pole and dipole-dipole arrays as a function of d/a plots are shown in Figures 3-4 and 3-5. The dilution and distortion factors for the pole-pole array are similar to those for the case $b = 4a$. However, in this case, the width of anomalies over the dike is smaller than the width of anomalies in the case $b = 4a$. The dilution factor for the dipole-dipole array shows high anomalies over the dike with a sharp highest point in the center of the dike. The highest value of dilution factor is approximately 1.4 when $\rho_2/\rho_1 = 1, 0.5\Omega m$. As the dike becomes resistive and conductive the peak values approach one. Unlike four peaks for the case $b = 4a$,

the distortion factor has three positive peaks in this case for the dipole-dipole array. These peaks are flanked by adjacent low anomalies, as shown in Figure 3-5b.

The dilution and distortion factors as functions of d/a plots are shown in Figures 3-6 and 3-7 for pole-pole and dipole-dipole arrays. In this case, the width of dike is $2a$. The dilution and distortion factors show anomalies similar to those in case $b = 4a$ for pole-pole array as shown in Figures 3-6a and 3-6c. When the dike is very conductive ($\rho_2/\rho_1 = 0.01$), the dilution and distortion factors for dipole-dipole arrays are almost the same. As the dike becomes resistive, three peaks for distortion and three low values for dilution are obtained; one is in the center of the dike and the other two are on both sides of the dike. The low values in the center of the dike become larger when the dike becomes more conductive. Since these three low values are flanked by two high anomalies, upside-down W-shaped anomalies are obtained as shown in Figure 3-7a. When the dike is resistive, the distortion factors for dipole-dipole array have also three high peaks. The peak in the middle is the highest ($B_{2,2} = 0.45$ for $\rho_2/\rho_1 = 10$). When the dike is conductive, distortion factors show a low peak on the center of the dike instead of a high peak. The W-shape structure becomes upside down (as shown in Figure 3-7b). When the dike is very conductive ($\rho_2/\rho_1 = 0.01$), the distortion factor shows a very small variation about zero.

We also considered the case $b = 0.5a$ and present the results in Figures 3-8 and 3-9. The dilution factors show one lowest value in the center and two peaks at both sides of the dike when the dike is resistive. As the dike becomes conductive, the low at the center of dike becomes high. As the dike gets more conductive, the distortion factors over the dike approach zero. When the dike is resistive, the distortion factor shows a high positive peak in the center of the dike. The peak gets sharper and the value of the peak gets larger as the dike becomes more resistive

($B_{2,2} = 0.4$ for $\rho_2/\rho_1 = 10.$). For a dipole-dipole array, instead of a peak, there is a region in which the dilution factor does not change with d/a as shown in Figure 3-9a. The value of the distortion factor in this flat region becomes smaller as the dike becomes conductive. Two positive peaks at each side of the dike are still obtained, and the flat region and the two peaks are flanked by two adjacent low anomalies. The distortion factor for the dipole-dipole array as a function of d/a is shown in Figure 3-9b. Over the dike, the distortion factor does not change with d/a and the values of distortion are largest for the resistive dike and smallest for the conductive dike. For both conductive and resistive dikes, there are two positive peaks on each side of the dike. Two peaks and the flat region are flanked by low anomalies.

To complete the numerical results, we also calculated the case $b = 0.25a$ for pole-pole and dipole-dipole arrays and present the results in Figure 3-10. The distortion and dilution factors for both arrays show similar anomalies. The dilution and distortion factors for both arrays have a flat area over the dike.

The IP dilution factor anomalies over the dike model are also interpreted and compared with the anomalies over the hemispherical sink model. They are shown in Figures 3-4b, 3-6b, and 3-8b. Like resistivity effects, we have a nice correlation between dike and hemispherical sink models especially when the dike is thick. It is shown that a hemi-spherical sink can also be approximated in its polarization effects by a vertical dike if the sink is not very narrow.

The expression for the apparent complex resistivity $\rho_a(iw)$ is given by equation (3.4) when both regions are polarizable. If we assume that the surrounding material is nonpolarizable (i.e., $\rho_1(iw) = \rho_1$, $\delta_1 = 0$), equation (3.4) can be written in simpler form as

$$\rho_a(iw) = \rho_a[1 + B_2\delta_2(iw) + B_{22}\delta_2^2(iw) + \dots], \quad (3.63)$$

where the distortion factor can be important if δ_2 is not very small (Wait, 1987). If the higher order terms are neglected, the apparent complex resistivity is

$$\rho_a(iw) = \rho_a[1 + B_2\delta_2(iw)] = \rho_2(iw). \quad (3.64)$$

When the magnitude of the apparent complex resistivity approaches ρ_2 , the phase of $\rho_a(iw)$ is equal to $[1 + \delta_2(iw)]$ from the definition of $\rho_2(iw)$. However, from equation (3.63), we see that both the magnitude and phase of $\rho_a(iw)$ will not have the same frequency dependence on the dike resistivity $\rho_2(iw)$ (Wait, 1987) because of the $B_{22}\delta_2^2$ term. Therefore, we should not ignore the distortion factor in the apparent complex resistivity equation for some cases.

We also adopt the Cole-Cole model to characterize the frequency dependence of the complex resistivity of the dike model.

$$\rho_j(iw) = \rho_j(0) \left[1 - \frac{1}{1 + (iw\tau_j)^{k_j}} \right], \quad (3.64)$$

$$\rho_j(iw) = \rho_j(0)[1 + \delta_j(iw)], \quad (3.65)$$

where, j is the number of layers ($j=1,2$), $\rho(iw)$ is the complex resistivity, $\rho(0)$ is the limiting zero frequency (i.e., dc) value of the resistivity, m is the chargeability, τ is the time constant, k is the dispersion index and frequency dependence, w is the angular frequency ($w = 2 \pi f$), and f is the frequency. For a simple Debye model $k = 1$, but more typically k is the order of 0.5 for geophysical applications (Gruszka and Wait, 1985).

We used real field data, measured by W. H. Pelton et al. (1978) on North America massive sulfide and graphite deposits, to show the effect of distortion factor for the complex apparent resistivity of the dike. Table 3-2 shows some numerical

values of $\rho_a(i\omega)$ including the first-order terms in equation (3.4) and of $\rho_a(i\omega)$ including the first- and second-order terms into equation (3.4) when d/a is 2, n is 2, f is 0.5 Hz, k_1 is 0.218, k_2 is 0.349, τ_1 is 4170 sec, and τ_2 is 0.00000252 sec., the chargeability of dike is 0.794, and the chargeability of surrounding material is 0.686. Table 3-3 shows the result of apparent complex-resistivity for different parameters. Finally, the second-order terms are important when δ is not very small and regions are polarizable.

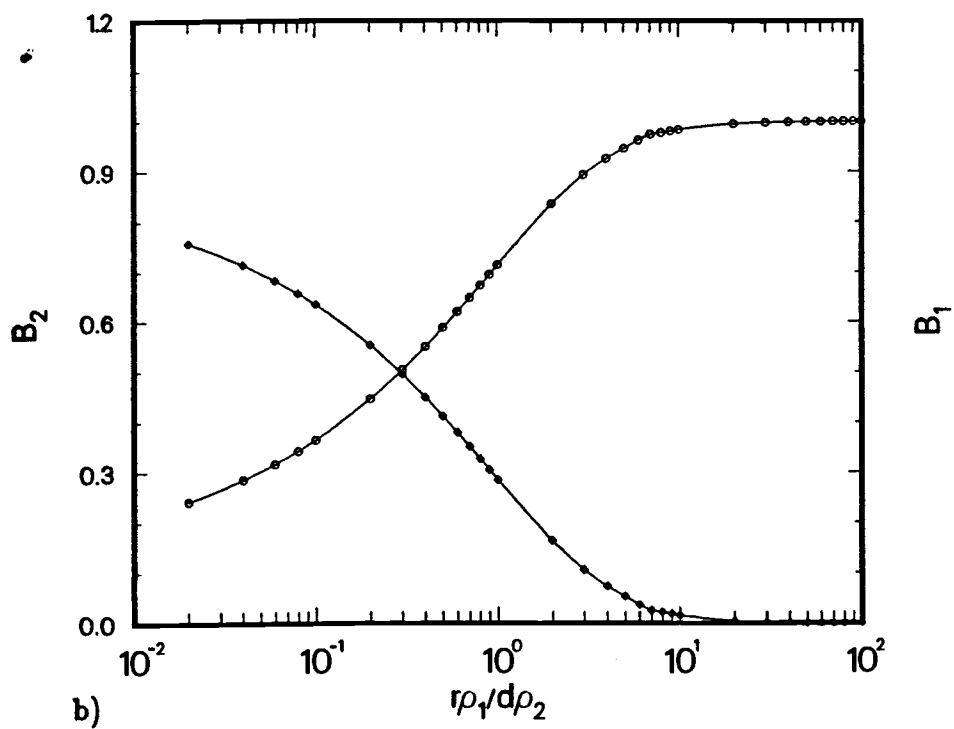
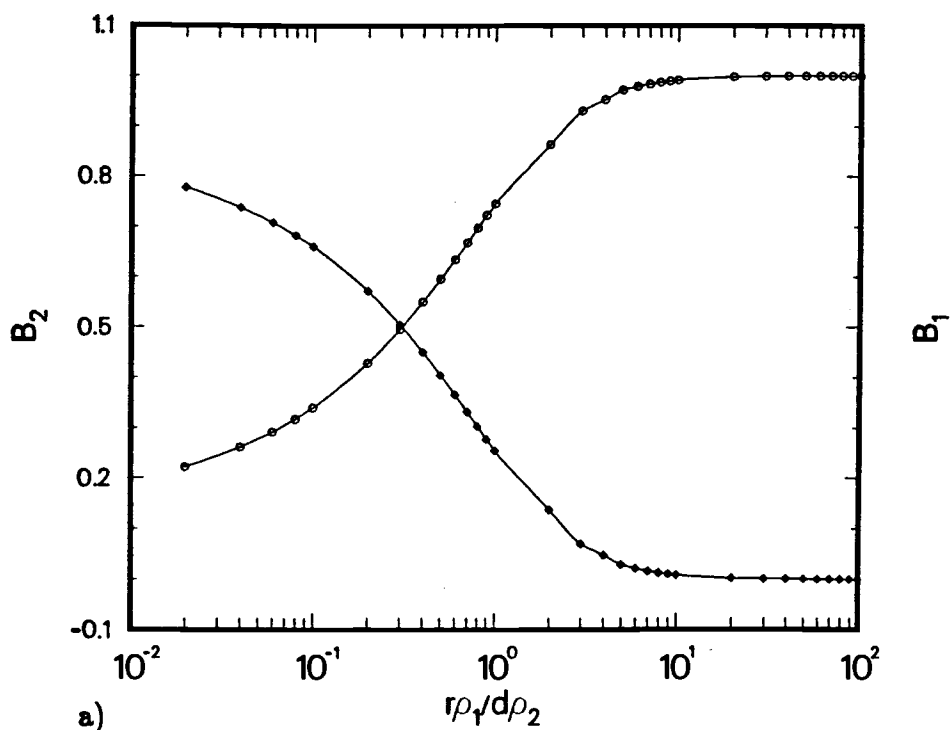


Figure 3-1 Dilution factor of thin layer, B_1 , and of second layer, B_2 , vs. $r\rho_1/d\rho_2$
 a) for pole-pole array, b) for dipole-dipole array

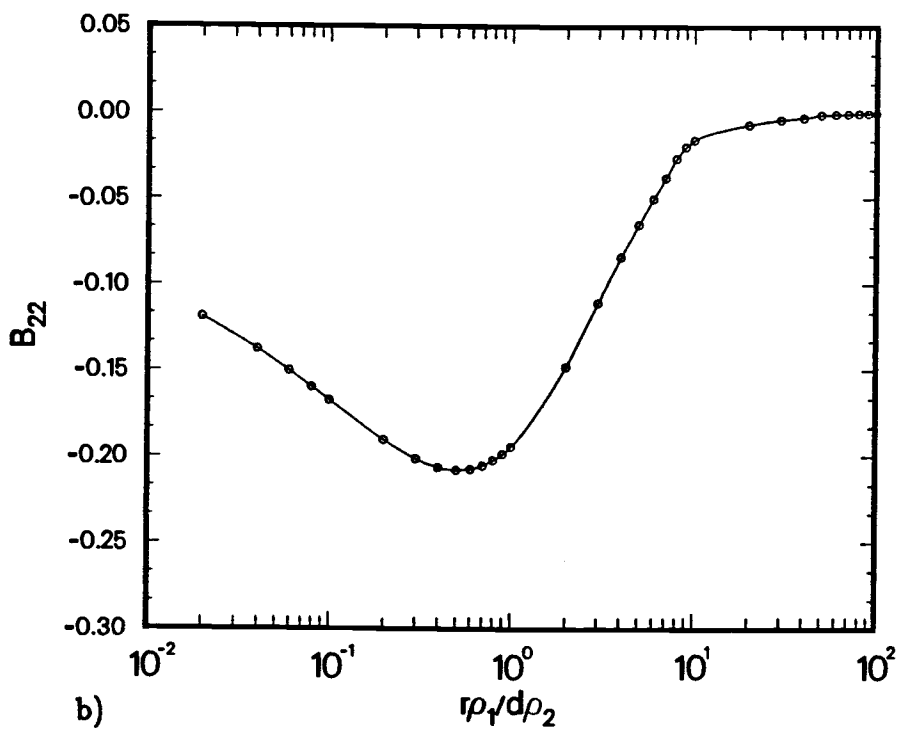
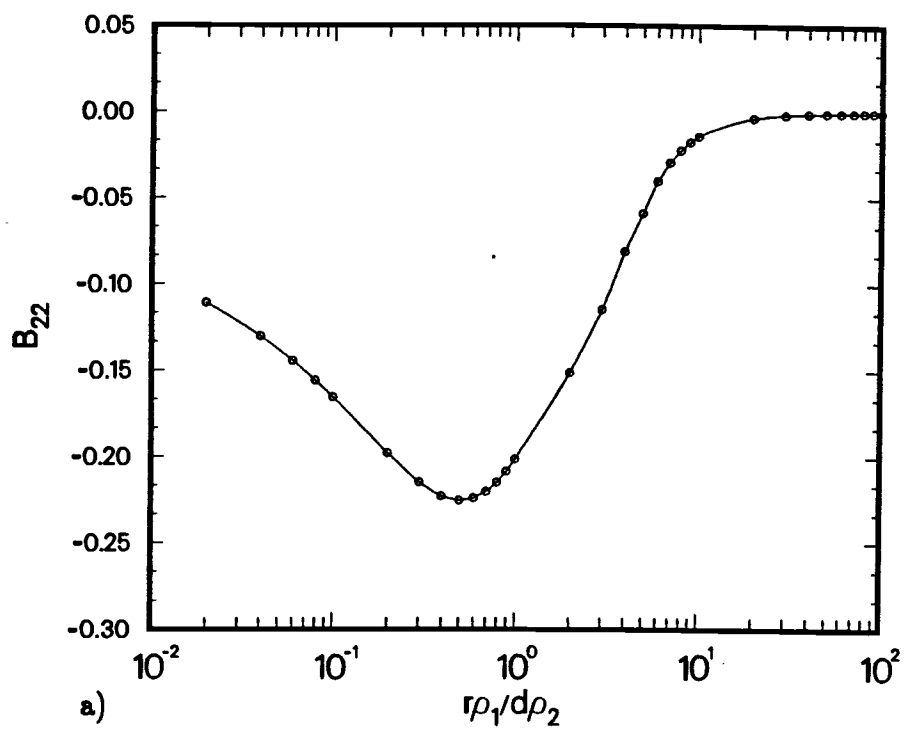


Figure 3-2 Distortion factor, a) for pole-pole array, b) for dipole-dipole array

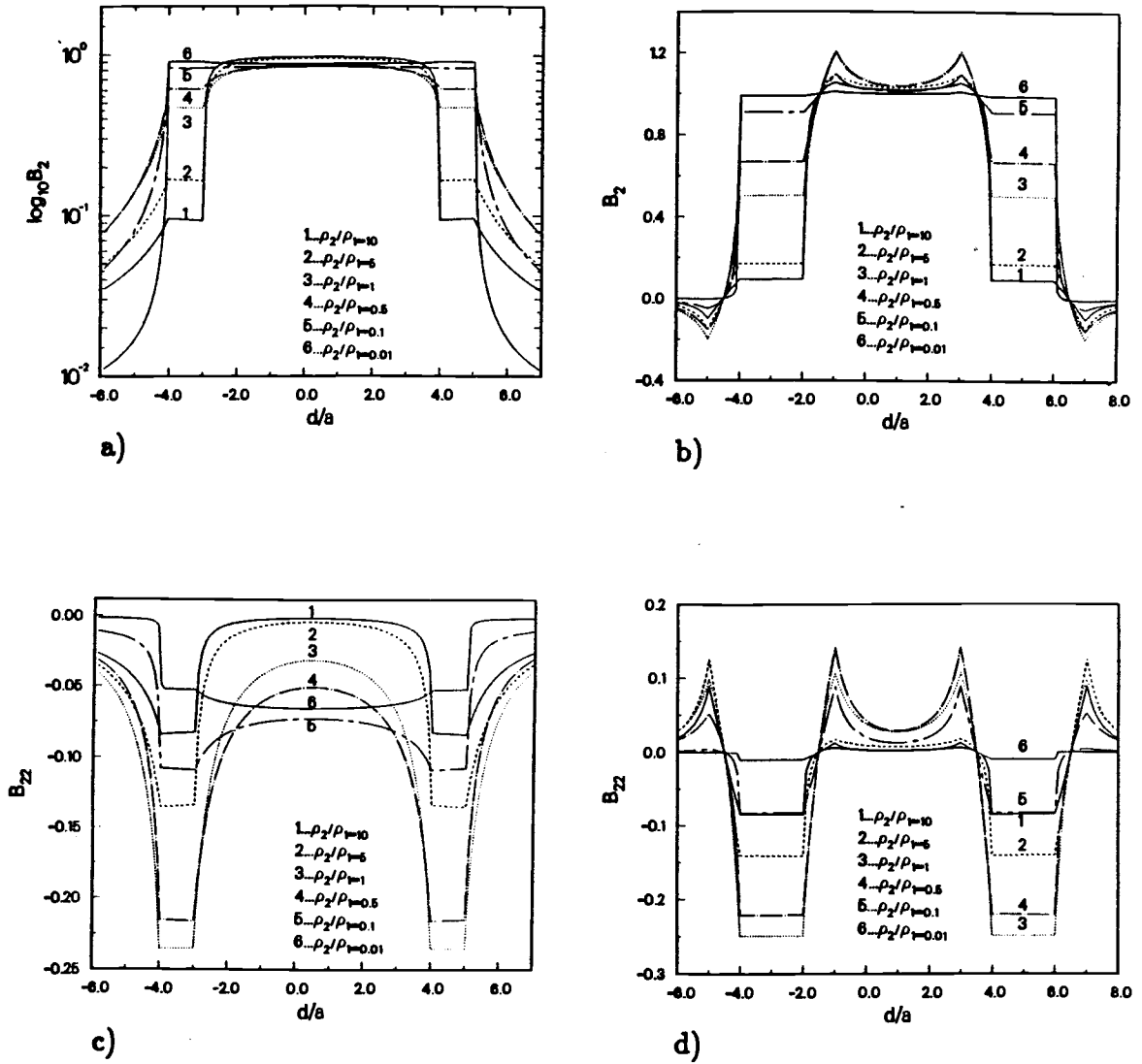


Figure 3-3 When $b/a = 4$,

- a) dilution factor of dike for pole-pole array
- b) distortion factor of dike for pole-pole array
- c) dilution factor of dike for dipole-dipole array
- d) distortion factor of dike for dipole-dipole array

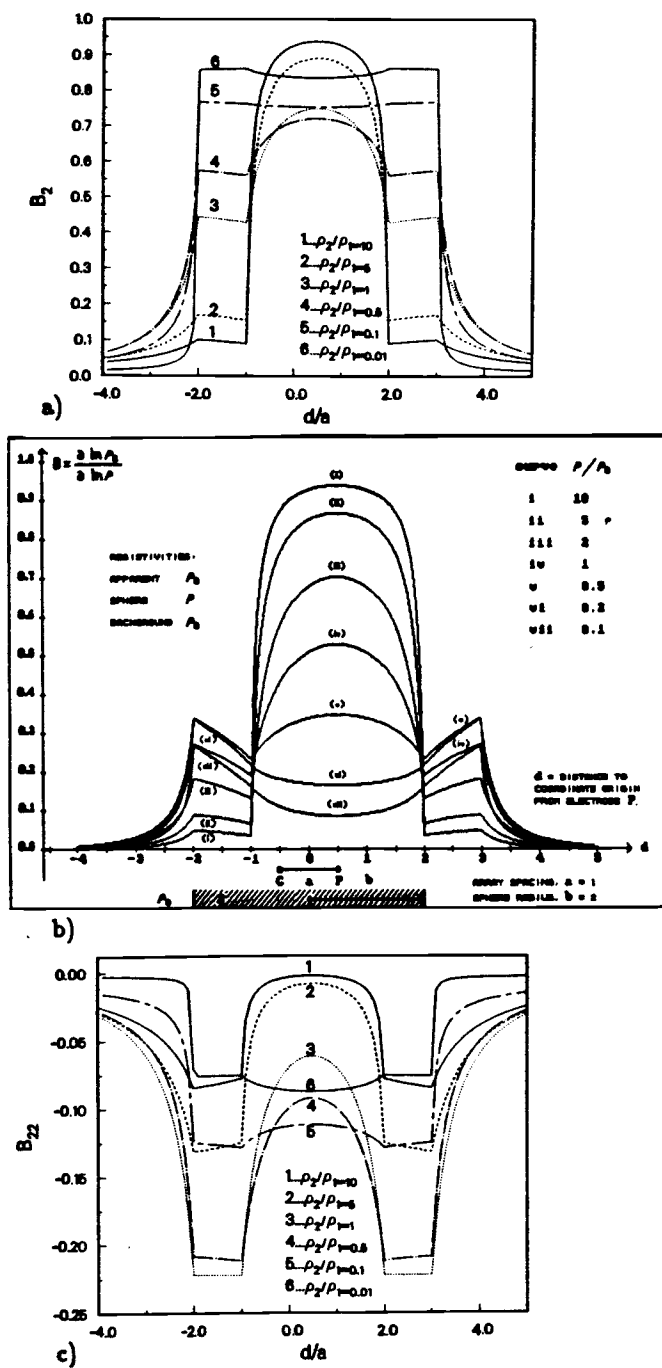


Figure 3-4 When $b/a = 2$,

- a) dilution factor of dike for pole-pole array
- b) dilution factor of hemispherical sink for pole-pole array
- c) distortion factor of dike for pole-pole array

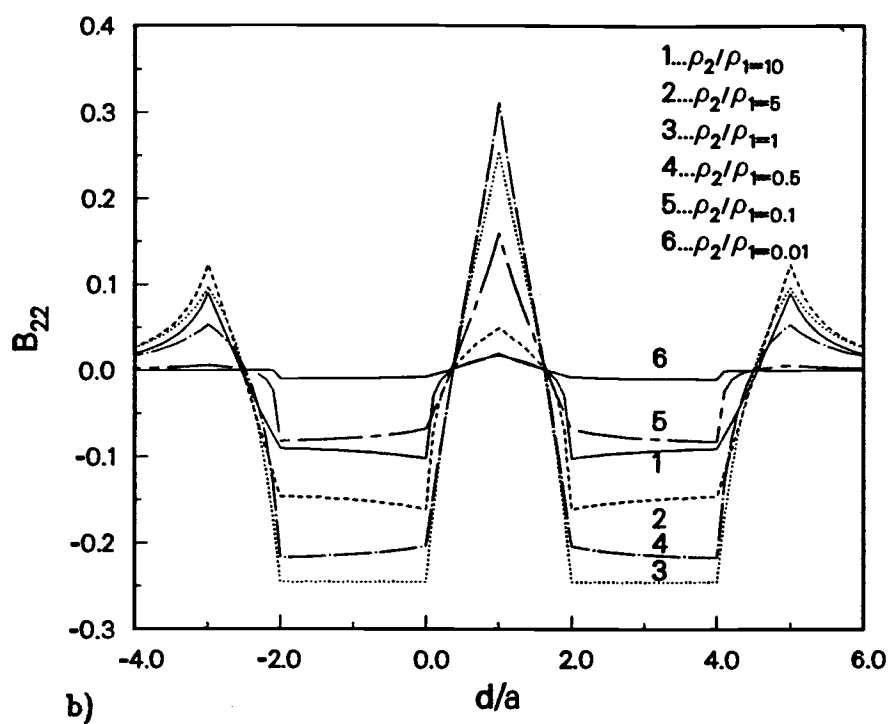
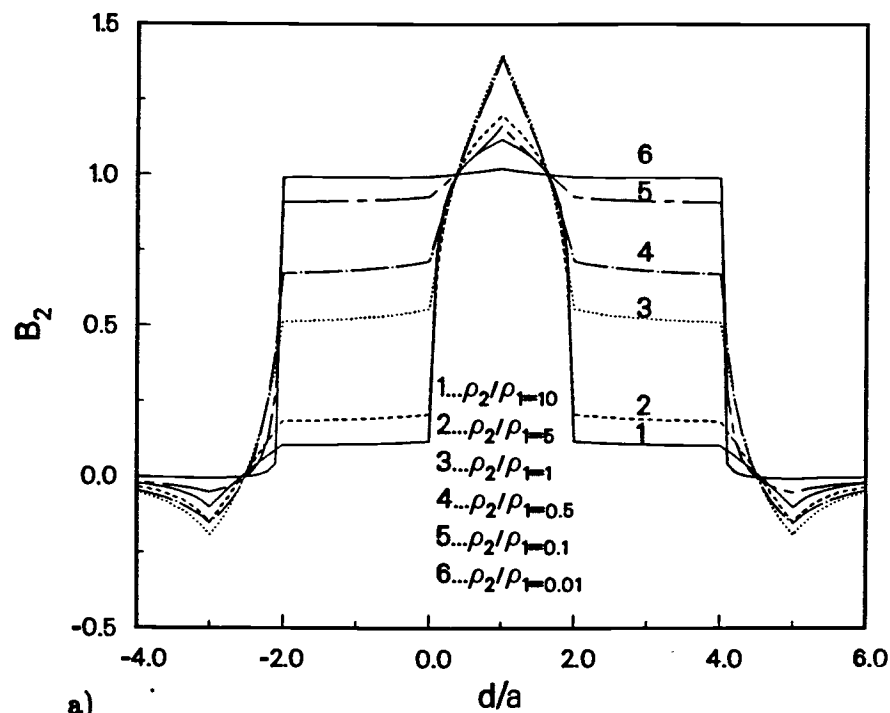


Figure 3-5 When $b/a = 2$

- a) dilution factor of dike for dipole-dipole array
 b) distortion factor of dike for dipole-dipole array

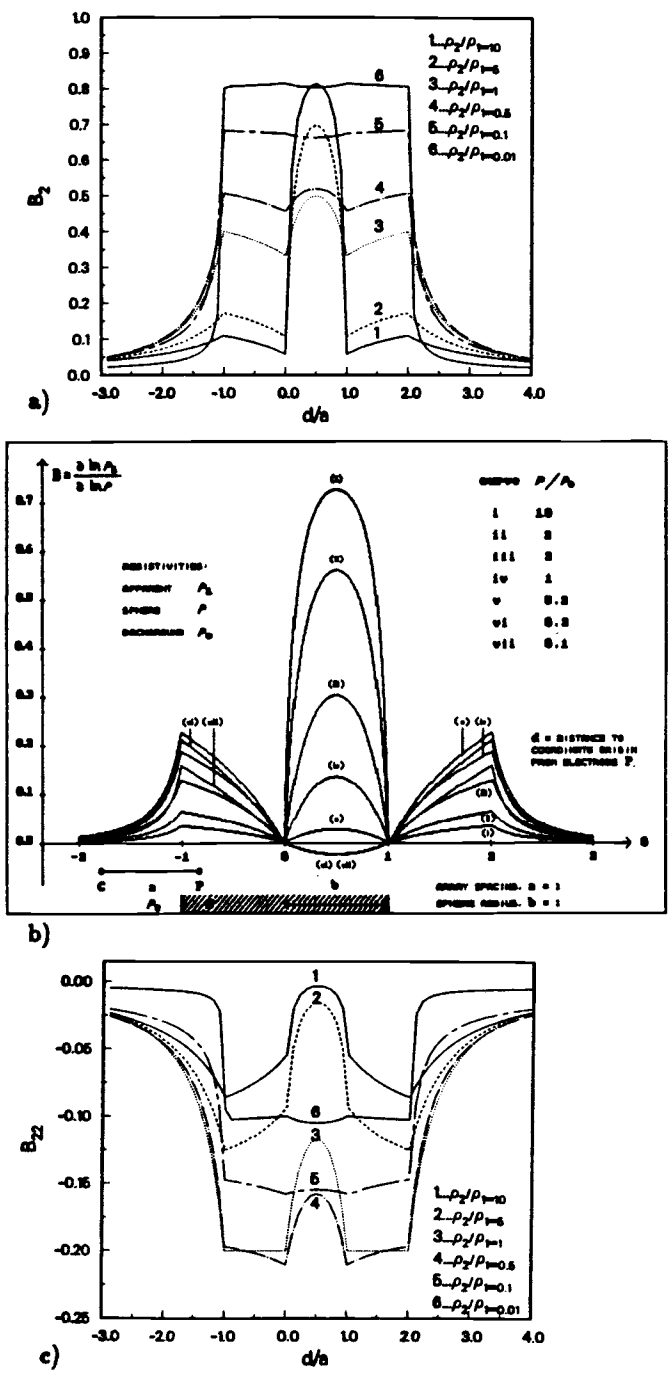


Figure 3-6 When $b/a = 1$,
 a) dilution factor of dike for pole-pole array
 b) dilution factor of hemispherical sink for pole-pole array (A. Peters, 1988)
 c) distortion factor of dike for pole-pole array

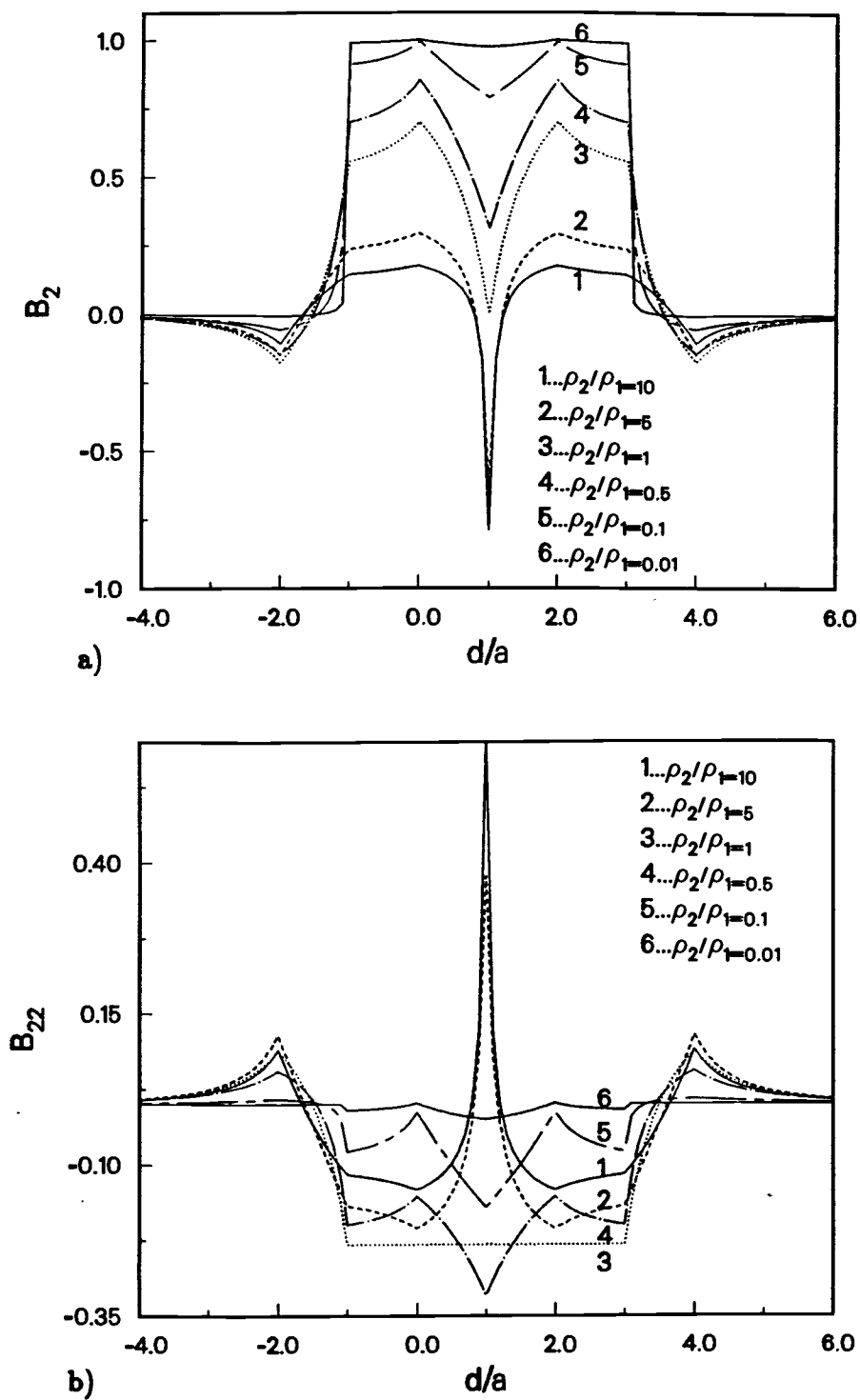


Figure 3-7 When $b/a = 1$,

- a) dilution factor of dike for dipole-dipole array
- b) distortion factor of dike for dipole-dipole array

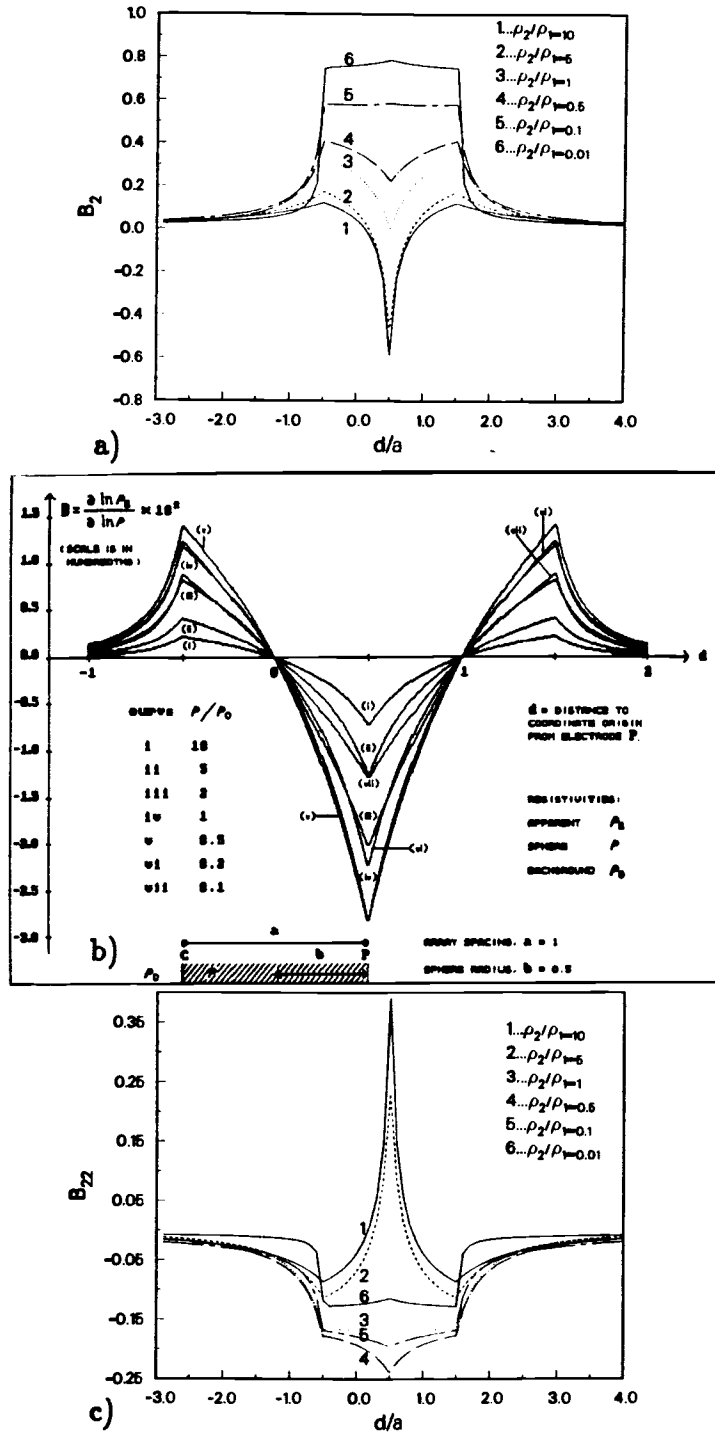
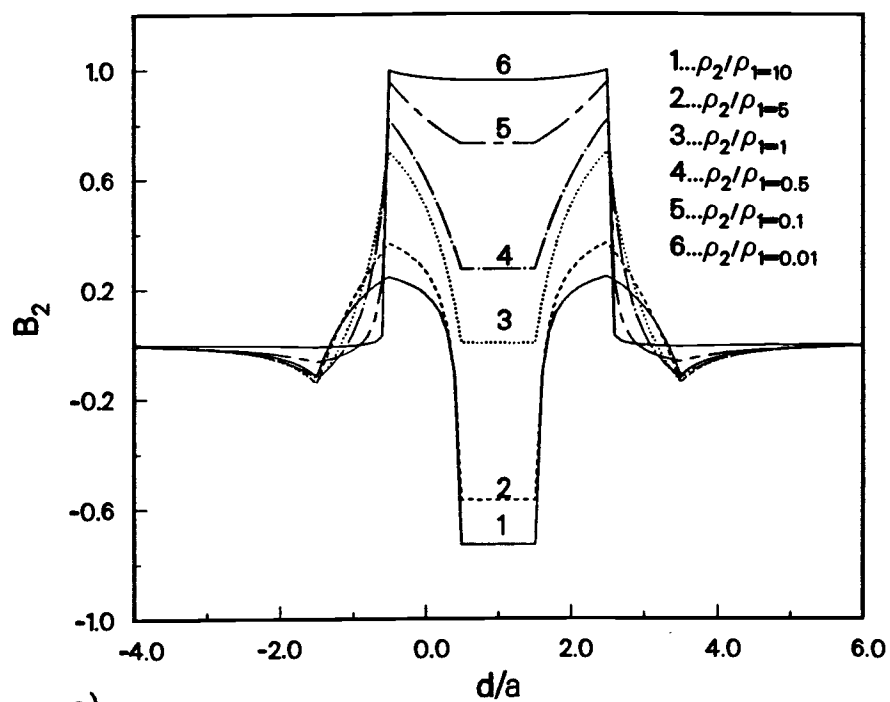
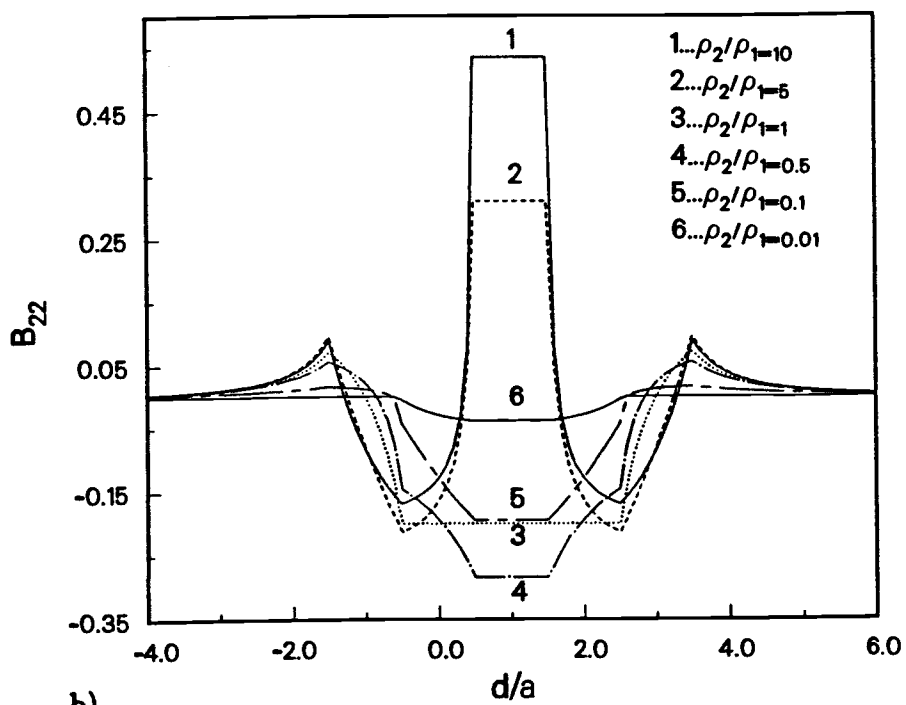


Figure 3-8 When $b/a = 0.5$,
 a) dilution factor of dike for pole-pole array
 b) dilution factor of hemispherical sink for pole-pole array
 c) distortion factor of dike for pole-pole array



a)



b)

Figure 3-9 When $b/a = 0.5$,

a) dilution factor of dike for dipole-dipole array

b) distortion factor of dike for dipole-dipole array

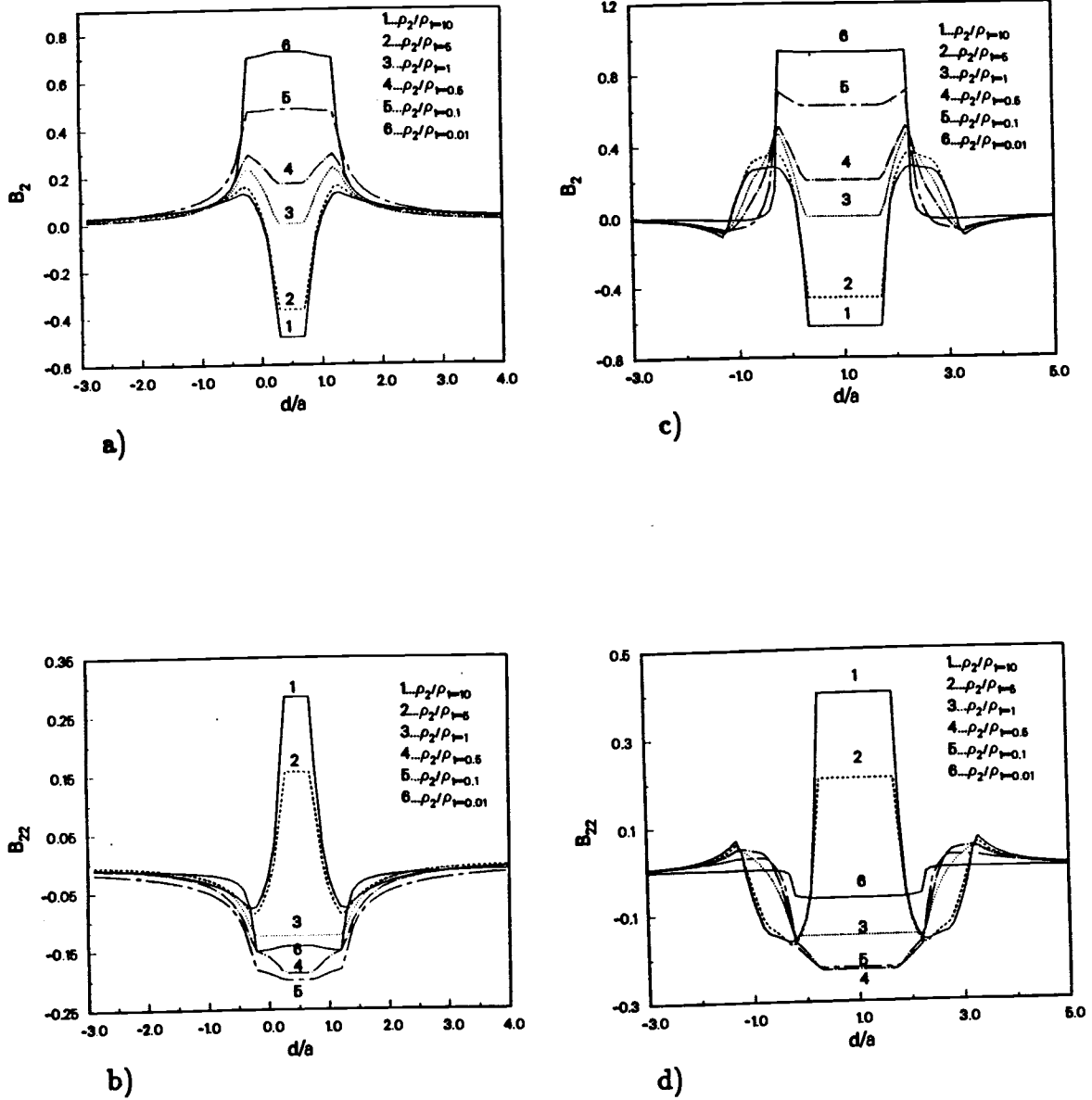


Figure 3-10 When $b/a = 0.25$,

- a) dilution factor of dike for pole-pole array
- b) distortion factor of dike for pole-pole array
- c) dilution factor of dike for dipole-dipole array
- d) distortion factor of dike for dipole-dipole array

TABLE 3-1 (a)		
d/a	B_2^*	B_{22}^*
6.00	-0.0031844	0.0004174
4.00	-0.0105285	0.0010475
2.00	0.9387321	-0.0566383
0.00	0.9387321	-0.0566383
-2.00	-0.0091848	0.0007344
-4.00	-0.0023970	0.0002358

* (M = 10)

TABLE 3-1 (b)		
d/a	B_2^*	B_{22}^*
6.00	-0.0032789	0.0005905
4.00	-0.0106941	0.0013039
2.00	0.9277940	-0.0627287
0.00	0.9277940	-0.0627287
-2.00	-0.0106929	0.0013014
-4.00	-0.0032776	0.0005880

* (M = 100)

TABLE 3-1 (c)		
d/a	B_2^*	B_{22}^*
6.00	-0.0032782	0.0005893
4.00	-0.0106934	0.0013027
2.00	0.9277785	-0.0627069
0.00	0.9277785	-0.0627069
-2.00	-0.0106934	0.0013027
-4.00	-0.0032782	0.0005892

* (M = 200)

TABLE 3-1 (d)		
d/a	B_2^*	B_{22}^*
6.00	-0.0032782	0.0005892
4.00	-0.0106934	0.0013027
2.00	0.9277784	-0.0627066
0.00	0.9277784	-0.0627066
-2.00	-0.0106934	0.0013027
-4.00	-0.0032782	0.0005892

* (M = 300)

TABLE 3-1 (e)		
d/a	B_2^*	B_{22}^*
6.00	-0.0032782	0.0005892
4.00	-0.0106934	0.0013027
2.00	0.9277784	-0.0627066
0.00	0.9277784	-0.0627066
-2.00	-0.0106934	0.0013027
-4.00	-0.0032782	0.0005893

* (M = 500)

TABLE 3-1 (f)		
d/a	B_2^*	B_{22}^*
6.00	-0.0032782	0.0005892
4.00	-0.0106934	0.0013027
2.00	0.9277784	-0.0627066
0.00	0.9277784	-0.0627066
-2.00	-0.0106934	0.0013027
-4.00	-0.0032782	0.0005893

* (M = 550)

$$b/a = 0.25, \rho_2/\rho_1 = 0.01$$

M = Number of terms

Table 3-1 Numerical convergence of B_2 and B_{22} for dipole-dipole array

b/a	$\rho(0)$	B_1	B_2
4.00	9.00	-0.02	1.02
1.00	12.5	0.05	0.95
0.25	35.0	0.36	0.64

B_{11}	B_{22}	B_{12}
0.02500	0.02500	-0.0500
-0.00625	-0.00625	0.0125
-0.19000	-0.19000	0.3800

$\rho_a(i\omega)^*$	$\rho_a(i\omega)^\#$
1.004 - i0.005	1.016 - i0.004
0.955 - i0.006	0.952 - i0.007
0.738 - i0.013	0.646 - i0.018

Table 3-2 Numerical example to show effect of distortion term to apparent complex resistivity

Data: $d/a = 3$, $n = 2$, $\rho_1 = 0.2$, $\rho_2 = 2$, $m_1 = 0.794$, $m_2 = 0.911$, $f = 0.5$, $k = 0.306$, $\tau = 0.0308$

* with first-order terms

† with first- and second-order terms

TABLE 3-3			
b/a	$\rho(0)$	B_1	B_2
4.00	1.30	-0.05	1.05
1.00	0.25	0.85	0.15
0.25	0.20	0.80	0.20

B_{11}	B_{22}	B_{12}
0.01	0.01	-0.02
-0.11	-0.11	0.22
-0.05	-0.05	0.10

$\rho_a(i\omega)^*$	$\rho_a(i\omega)^\#$
$1.031 + i0.004$	$1.035 + i0.006$
$0.448 - i0.091$	$0.403 - i0.107$
$0.480 - i0.086$	$0.460 - i0.093$

Table 3-3 Numerical example to show effect of distortion term to apparent complex resistivity

Data: $d/a = 2$, $n = 2$, $\rho_1 = 100$, $\rho_2 = 10$, $m_1 = 0.4$, $m_2 = 0.2$, $f = 0.1$, $k = 0.5$,

$\tau = 0.5$

*with first-order terms

^\#with first- and second-order terms

CHAPTER 4

CONCLUSIONS

In this thesis, the solutions of Laplace's equation for two different earth geometries, two horizontal layers and a dike, are derived. The Bessel integral formulation is used to obtain the potential over two horizontal layers. Apparent resistivity for the dike model is found by using the image method. The series obtained by the image method converges poorly when b/a is less than 1 where b is half of dike thickness and a is electrode spacing. The thin dike and thin horizontal layer representations are obtained by employing the Bessel integral method with thin-sheet boundary conditions. We see that such an idealization is justifiable in the dike model, but further corrections are needed if the dike is highly conductive or resistive. The results for the thin dike are similar to those reported by Aguirre and Wait (1985), who employed a simplified thin conductive sheet boundary conditions.

The numerical results of apparent resistivity for the conductive and resistive dike models are presented in section 2.2. The main distinguishing feature between the conductive and nonconductive thin dikes is that the resistive dike gives two anomalously anomalies, whereas the conductive dike gives only a very slight response. The corresponding results for the dilution and distortion factors relevant to the IP response are given in chapter 3. In all cases, ρ_a/ρ_1 approaches 1 as the spacing parameter d/a becomes sufficiently large while B_2 and B_{22} , in this limiting case, vanish. It can also be shown that the higher order terms in the expansion in equation (3.63) also vanish in this limiting case. It is shown that the apparent resistivity and dilution and distortion factors are constant when the potential and the current electrodes straddle the dike ($b/a < 0.5$ for pole-pole array and < 1

for dipole-dipole array), but there is a characteristic decrease or increase as the electrodes move away from the dike.

The results of the apparent resistivity for pole-pole and dipole-dipole arrays agree with the results of Telford (1976), Keller (1970), and Ludwig (1967). They also used the image method to obtain the apparent-resistivity curve over the dike. Our results for the dike model are consistent with the results of Peters (1988) for a hemispherical sink model. It is shown that a hemispherical sink can be approximated in its resistivity and polarization edge effects by a vertical dike if the sink is not very narrow. This point was also made by Cook and Van Nostrand in 1966.

One of the important results is that the magnitude and phase of the apparent-complex resistivity will not have the same frequency dependence of the dike complex resistivity because of the higher order interaction. Therefore, we should not ignore the distortion factor in the prediction of the IP response.

APPENDIX A

Calculation of Potential by Using Image Method

When the current electrode is in the medium with resistivity ρ_1 and the potential electrode is in the third medium with same resistivity, we should write the potential equations of each image points. The potential is obtained when the current is transmitted from the first medium to the second medium and also from the second medium to the third medium which is

$$V_1^0 = \frac{I\rho_1}{2\pi} \frac{\tau\tau'}{a}, \quad (A.1)$$

where $\tau\tau'$ is equal to $1 - k^2$. The first image point is located in the second medium which has a distance $a + 4b$ from the potential electrode. Then, the potential equation for this first image point is

$$V_1' = \frac{I\rho_1}{2\pi} \frac{\tau\tau'(-k)^2}{a + 4b}. \quad (A.2)$$

The second image point is on the third medium and this gives a similar potential equation. When we add all of image sources potential equations into the real current source potential equation, V_1^0 , we can calculate the potential equation for this case.

$$V_1 = \frac{I\rho_1}{2\pi} (1 - k^2) \sum_{m=0}^{\infty} \frac{k^{2m}}{4mb + a}. \quad (A.3)$$

Then, the apparent resistivity from the relation between V and ρ_a is obtained.

$$\frac{2\pi a}{\rho_1} \frac{V_1}{I} = (1 - k^2) \sum_{m=0}^{\infty} \frac{k^{2m}}{4m\frac{b}{a} + 1}, \quad (A.4)$$

or

$$\frac{\rho_a}{\rho_1} = (1 - k^2) \sum_{m=0}^{\infty} \frac{k^{2m}}{4m\frac{b}{a} + 1}. \quad (A.5)$$

The fourth case we will consider is that in which the current and potential electrodes are on the dike (Fig. 2-6). The real current potential as the earth were homogeneous is

$$V_{2a}^0 = \frac{I\rho_2}{2\pi a}. \quad (\text{A.6})$$

The potential equation for the right side of the first image point can be written when the current source is first reflected from the second boundary (Fig. 2-6a).

$$V_{2a}' = \frac{I\rho_2}{2\pi} \frac{-k}{2(b+d) - a}. \quad (\text{A.7})$$

Then, we can write potential equation for each image point which are first reflected from the second boundary by similar way.

$$V_{2a}'' = \frac{I\rho_2}{2\pi} \frac{(-k)^2}{4b + a}. \quad (\text{A.8})$$

$$V_{2a}''' = \frac{I\rho_2}{2\pi} \frac{(-k)^3}{2(3b+d) - a}. \quad (\text{A.9})$$

$$V_{2a}' = \frac{I\rho_2}{2\pi} \frac{(-k)^4}{8b + a}. \quad (\text{A.10})$$

The potential equations obtained from the image points for the left side of the dike which is the first reflected from the first boundary (Fig. 2-6b) are written as

$$V_{2b}^0 = \frac{I\rho_2}{2\pi} \frac{-k}{2b - 2d + a}. \quad (\text{A.11})$$

$$V_{2b}' = \frac{I\rho_2}{2\pi} \frac{(-k)^2}{4b - a}. \quad (\text{A.12})$$

$$V_{2b}'' = \frac{I\rho_2}{2\pi} \frac{(-k)^3}{2(3b-d) + a}. \quad (\text{A.13})$$

$$V_{2b}''' = \frac{I\rho_2}{2\pi} \frac{(-k)^4}{8b - a}. \quad (\text{A.14})$$

The real current potential and image current potentials are added together to calculate the potential for this case.

$$V_2 = \frac{I\rho_2}{2\pi} \frac{\rho_1}{\rho_1} \left[\frac{1}{a} + k^2 \left[\sum_{m=0}^{\infty} \frac{k^{2m}}{4(m+1)b+a} + \sum_{m=0}^{\infty} \frac{k^{2m}}{4(m+1)b-a} \right] - k \left[\sum_{m=0}^{\infty} \frac{k^{2m}}{2[(2m+1)b+d]-a} + \sum_{m=0}^{\infty} \frac{k^{2m}}{2[(2m+1)b-d]+a} \right] \right], \quad (A.15)$$

where,

$$\frac{\rho_2}{\rho_1} = \frac{1+k}{1-k}. \quad (A.16)$$

Then,

$$V_2 = \frac{I\rho_1}{2\pi} \left(\frac{1+k}{1-k} \right) \left[\frac{1}{a} + k^2 \left[\sum_{m=0}^{\infty} \frac{k^{2m}}{4(m+1)b+a} + \sum_{m=0}^{\infty} \frac{k^{2m}}{4(m+1)b-a} \right] - k \left[\sum_{m=0}^{\infty} \frac{k^{2m}}{2[(2m+1)b+d]-a} + \sum_{m=0}^{\infty} \frac{k^{2m}}{2[(2m+1)b-d]+a} \right] \right]. \quad (A.17)$$

When the current electrode is on the dike and the potential electrode is on the third medium, we should write the potential equation by following the same method. If image points are located on the left of the dike, the current source is first transmitted from the second medium to the third medium.

$$V_{3a}^0 = \frac{I\rho_2}{2\pi} \frac{\tau'}{a}, \quad (A.18)$$

$$V_{3a}' = \frac{I\rho_2}{2\pi} \frac{\tau'(-k)^2}{4b+a}, \quad (A.19)$$

$$V_{3a}'' = \frac{I\rho_2}{2\pi} \frac{\tau'(-k)^4}{8b+a}. \quad (A.20)$$

If the image points are located on the right side of the dike, the current source is first reflected from the first boundary and then transmitted from the second medium to the third medium.

$$V_{3b}^0 = \frac{I\rho_2}{2\pi} \frac{\tau'(-k)}{(a+2b-2d)}, \quad (A.21)$$

$$V'_{3b} = \frac{I\rho_2}{2\pi} \frac{\tau'(-k)^3}{2(3b-d)+a}. \quad (A.22)$$

When we add these potential equations for infinite image points, we obtain potential equation for this case.

$$V_3 = \frac{I\rho_2}{2\pi} \frac{\rho_1}{\rho_1} \tau' \left[\frac{1}{a} + k^2 \sum_{m=0}^{\infty} \frac{k^{2m}}{4(m+1)b+a} - k \sum_{m=0}^{\infty} \frac{k^{2m}}{2[(2m+1)b-d]+a} \right], \quad (A.23)$$

or

$$V_3 = \frac{I\rho_1}{2\pi} (1+k) \left[\sum_{m=0}^{\infty} \frac{k^{2m}}{4mb+a} - k \sum_{m=0}^{\infty} \frac{k^{2m}}{2[(2m+1)b-d]+a} \right]. \quad (A.24)$$

APPENDIX B
Computer Programs

```

*****
***** APPENDIX B
*****
* 1. COMPUTER PROGRAM TO COMPUTE APPARENT RESISTIVITY,DILUTION,
*   AND DISTORTION FACTORS FOR THIN SHEET(PL-PL,DIP-DIP)
-----
* SX =  $r_1 / d_2$ 
* SRA = Ratio Of apparent resistivity to first layer resistivity,
* SB2 = Dilution factor,
* SB22 = Distortion factor,
* H0 = Struve function of zore Order,
* H1 = Struve function of first order.
*****
  IMPLICIT REAL*8 (A-H,O-Z)
  REAL SX,SRA,SB2,SB22
  DIMENSION H0(500),H1(500)
  COMMON PI
  H0(2)=2.5766872D0
  H0(4)=2.1473609D0
  H0(6)=1.9008083D0
  H0(8)=1.7289188D0
  H0(10)=1.5978300D0
  H0(12)=1.4924691D0
  H0(16)=1.3300407D0
  H0(18)=1.2650962D0
  H0(20)=1.2078643D0
  H0(24)=1.1109352D0
  H0(30)=0.9963565D0
  H0(32)=0.9641303D0
  H0(40)=0.8561743D0
  H0(50)=0.7540746D0
  H0(60)=0.6754213D0
  H0(70)=0.6125073D0
  H0(80)=0.5607967D0
  H0(90)=0.5174067D0
  H0(100)=0.4803996D0
  H0(120)=0.4204665D0
  H0(140)=0.3738974D0
  H0(150)=0.3542746D0
  H0(160)=0.3365986D0
  H0(180)=0.3060206D0
  H0(200)=0.2804831D0
  H0(210)=0.2692285D0
  H0(240)=0.2402338D0
  H0(270)=0.2167942D0
  H0(280)=0.2099486D0
  H0(300)=0.1974561D0
  H0(320)=0.1863424D0
  H0(360)=0.1674340D0
  H0(400)=0.1519553D0
  H0(500)=0.1233008D0

```

```

*****
H1(2)=31.8598977D0
H1(4)=15.9646484D0
H1(6)=10.6765530D0
H1(8)=8.0390271D0
H1(10)=6.4610718D0
H1(12)=5.4124930D0
H1(16)=4.1084779D0
H1(18)=3.6764644D0
H1(20)=3.3322907D0
H1(24)=2.8193039D0
H1(30)=2.3120894D0
H1(32)=2.1865686D0
H1(40)=1.8144645D0
H1(50)=1.5236461D0
H1(60)=1.3349710D0
H1(70)=1.2038816D0
H1(80)=1.1082667D0
H1(90)=1.0359441D0
H1(100)=0.9796701D0
H1(120)=0.8985582D0
H1(140)=0.8436750D0
H1(150)=0.8225971D0
H1(160)=0.8046252D0
H1(180)=0.7757670D0
H1(200)=0.7537961D0
H1(210)=0.7447204D0
H1(240)=0.7230309D0
H1(270)=0.7072633D0
H1(280)=0.7029544D0
H1(300)=0.6954352D0
H1(320)=0.6891190D0
H1(360)=0.6791798D0
H1(400)=0.6718010D0
H1(500)=0.6599488D0
*****
IR=0
PI=3.14159265357989D0
WRITE(6,*)'READ NE, 1=POLE-POLE, 2=DIP-DIP'
READ(5,*)NE
GO TO(10,20)NE
10 OPEN(UNIT=70,FILE='THPP.DAT',STATUS='NEW')
X=0.02D0
1 X2=X*X
N=IIDNNT(X*100.0D0)
RA=PI*.5D0*X*H0(N)
B2=-X*(2.0D0/PI-H1(N))/H0(N)
B22=(X*(2.0D0/PI-H1(N))+X2*.5D0*(H1(N)/X-H0(N)))/H0(N)
SX=SNGL(DLOG10(X))
SRA=SNGL(RA)
SB2=SNGL(B2)
SB22=SNGL(B22)
WRITE(6,*)SX,SRA,SB2,SB22
WRITE(70,*)SX,SRA,SB2,SB22
IF(X.LT..1D0)GO TO 100
IF(X.LT.1.0D0)GO TO 200
GO TO 300
100 X=X+.02
GO TO 1
200 X=X+.10D0

```

```

GO TO 1
300 X=X+1.0D0
    IF(X.LE.5.01D0)GO TO 1
    GO TO 400
400 X2=X*X
    RA=PI*.5D0*X*HOS(X)
    B2=-X*(2.0D0/PI-H1S(X))/HOS(X)
    B22=(X*(2.0D0/PI-H1S(X))+X2*.5D0*(H1S(X)/X-HOS(X)))/HOS(X)
    SX=SNGL(DLOG10(X))
    SRA=SNGL(RA)
    SB2=SNGL(B2)
    SB22=SNGL(B22)
    WRITE(6,*)SX,SRA,SB2,SB22
    WRITE(70,*)SX,SRA,SB2,SB22
    IF(X.LT.10.0D0)GO TO 500
    X=X+10.0D0
    GO TO 600
500 X=X+1.0D0
    GO TO 400
600 IF(X.LT.100.10D0)GO TO 400
    CLOSE(UNIT=70)
    GO TO 1000
20  OPEN(UNIT=71,FILE='THDD.DAT',STATUS='NEW')
    X=.02
30  N=IIDNNT(X*100.0D0)
    IF(N.LE.500)THEN
        A10=H0(N)
        A11=H1(N)
    ELSE
        A10=HOS(X)
        A11=H1S(X)
    END IF
    IF(2*N.LT.500)THEN
        A20=H0(2*N)
        A21=H1(2*N)
    ELSE
        A20=HOS(2.0D0*X)
        A21=H1S(2.0D0*X)
    END IF
    IF(3*N.LT.500)THEN
        A30=H0(3*N)
        A31=H1(3*N)
    ELSE
        A30=HOS(3.0D0*X)
        A31=H1S(3.0D0*X)
    END IF
    IF(4*N.LT.500)THEN
        A40=H0(4*N)
        A41=H1(4*N)
    ELSE
        A40=HOS(4.0D0*X)
        A41=H1S(4.0D0*X)
    END IF
C   WRITE(6,*)'X=',X
C   WRITE(6,*)'A20=',A20,'A21',A21
C   WRITE(6,*)'A30=',A30,'A31',A31
C   WRITE(6,*)'A40=',A40,'A41',A41
    S=-2.0D0*A30/3.0D0+A40/4.0D0+A20/2.0D0
    SD=2.0D0*A31-A41-A21
    SDD=-6.0D0*A30+4.0D0*A40+2.0D0*A20+(2.0D0*A31-A41

```

```

C      -A21)/X
C      WRITE(6,*)'s=',S
C      WRITE(6,*)'SD=',SD
C      WRITE(6,*)'SDD=',SDD
C      WRITE(6,*)'*****'
      RA=PI*X*S*6.0D0
      B2=-X*SD/S
      B22=X*SD/S-.5D0*X*X*SDD/S
      SX=SNGL(DLOG10(X))
      SRA=SNGL(RA)
      SB2=SNGL(B2)
      SB22=SNGL(B22)
      IR=IR+1
      WRITE(6,*)IR,SX,SRA,SB2,SB22
      WRITE(71,*)SX,SRA,SB2,SB22
      IF(X.LT..1D0)GO TO 25
      IF(X.LT.1.0D0)GO TO 50
      IF(X.LT.10.0D0)GO TO 75
      X=X+10.0D0
      IF(X.LT.100.10D0)GO TO 30
      CLOSE(UNIT=71)
      GO TO 1000
25     X=X+.02
      GO TO 30
50     X=X+.1
      GO TO 30
75     X=X+1.0D0
      GO TO 30
1000  STOP
      END

```

```

*****
      FUNCTION H0S(Z)
      IMPLICIT REAL*8(A-H,O-Z)
      COMMON PI
      Y=1.0D0/Z
      Y2=Y*Y
      Y3=Y2*Y
      Y5=Y3*Y2
      Y7=Y5*Y3
      H0S=2.0D0*(Y-Y3+9.0D0*Y5-225.0D0*Y7)/PI
      RETURN
      END
*****
      FUNCTION H1S(Z)
      IMPLICIT REAL*8(A-H,O-Z)
      COMMON PI
      Y=1.0D0/Z
      Y2=Y*Y
      Y4=Y2*Y2
      Y6=Y4*Y2
      H1S=2.0D0*(1.0D0+Y2-3.0D0*Y4+45.0D0*Y6)/PI
      RETURN
      END
*****

```

```

*****
*      2. COMPUTER PROGRAM FOR APPARENT RESISTIVITY
*      FOR POLE-POLE ARRAY
-----
*      BA = b/a,
*      R1R0 =  $\rho_2/\rho_1$ ,
*      R = k = reflection coefficient,
*      DA = d/a,
*      RAR0 =  $\rho_a/\rho_1$ .
*****
      IMPLICIT REAL*8(A-H,O-Z)
      REAL SR
      OPEN(UNIT=59,FILE='PW0.DAT',STATUS='NEW')
      BA=0.250D0
      R1R0=.01D0
      R=(R1R0-1.0D0)/(R1R0+1.0D0)
      WRITE(59,*)'R2/R1= ',R1R0,'B/A= ',BA
112  WRITE(6,*)'ENTER M1'
      READ(5,*)M1
      IF(M1.EQ.0)GO TO 111
      WRITE(6,*)'M= ',M1
      WRITE(59,*)'M= ',M1
      WRITE(59,*)'D/A=.....,RA/R0=.....'
      DA=-3.0D0
      IR=1
*****
***** When the current and potential electrodes are
***** located on the left of the dike:
*****
      6  IF(DA.GE.1.250D0.AND.DA.LE.4.0D0)THEN
          RAR0=1.0D0+R/(2.0D0*(DA-BA)-1.0D0)
          DO 1 M=0,M1
              M2=2*M
              FM2=DFLOAT(2*M+1)
          1  RAR0=RAR0-R*(1.0D0-R*R)*R**M2/(2.0D0*(FM2*BA+DA)-1.0D0)
*****
***** When the current electrode is on the left of dike
***** and the potential electrode is on the dike:
*****
          ELSE IF(DA.GT.0.750D0.AND.DA.LT.1.250D0)THEN
              RAR0=0.0D0
              DO 2 M=0,M1
                  FM=DFLOAT(M)
                  FM2=DFLOAT(2*M+1)
                  M2=M*2
          2  RAR0=RAR0-R*R**M2/(2.0D0*(FM2*BA+DA)-1.0D0)+R**M2/
              C  (FM*4.0D0*BA+1.0D0)
              RAR0=RAR0*(1.0D0+R)
*****
***** When the current electrode is on the left of the dike
***** and the potential electrode is on the right of the dike:
*****
          ELSE IF(DA.GE.0.250D0.AND.DA.LE..750D0)THEN
              C  RAR0=1.0D0
              C  DO 3 M=0,M1
              C  FM4=DFLOAT(4*(M+1))
              C  FM2=DFLOAT(2*M+1)
              C  M2=M*2

```

```

C 3  RAR0=RAR0+R*R*(R**M2/(FM4*BA+1.0D0)+R**M2/(FM4*BA-1.0D0))
C  C  -R*(R**M2/(2.0D0*(FM2*BA+DA)-1.0D0)+R**M2/(2.0D0*(FM2
C  C  *BA-DA)+1.0D0))
C  RAR0=RAR0*((1.0D0+R)/(1.0D0-R))
RAR0=.0D0
DO 3 M=0,M1
FM=DFLOAT(M)
M2=M*2
FM4=DFLOAT(M*4)
3  RAR0=RAR0+R**M2/(FM4*BA+1.0D0)
RAR0=RAR0*(1.0D0-R*R)
*****
***** When the current electrode is on the dike and
***** the potential electrode is on the right side of the dike:
*****
ELSE IF(DA.GE.-.250D0.AND.DA.LT.0.250D0)THEN
RAR0=0.0D0
DO 4 M=0,M1
M2=M*2
FM4=DFLOAT(M*4)
FM2=DFLOAT(2*M+1)
4  RAR0=RAR0+R**M2/(FM4*BA+1.0D0)-R*(R**M2/(2.0D0*(FM2*BA-DA)+
C  1.0D0))
RAR0=RAR0*(1.0D0+R)
*****
***** When both electrodes are on the right of the dike:
*****
ELSE
RAR0=1.0D0
DO 5 M=0,M1
FM2=DFLOAT(2*M+1)
FM3=DFLOAT(2*M-1)
M2=M*2
5  RAR0=RAR0+R*R**M2/(2*(FM3*BA-DA)+1)-R*R**M2/(2*(FM2*BA-DA)+1)
END IF
SR= SNGL(RAR0)
SDA=SNGL(DA)
WRITE(6,*)'IR=',IR,'DA=',DA,'RAR0=',RAR0
WRITE(59,*)SR,SDA
DA=DA+.5D0
IR=IR+1
IF(DA.GT.4.0D0)GO TO 8
GO TO 6
8  GO TO 112
111 CLOSE(UNIT=59)
STOP
END

```

```

*****
* 3. COMPUTER PROGRAM FOR APPARENT RESISTIVITY, DILUTION,
* AND DISTORTION FACTORS OVER THE DIKE BY USING DIPOLE-
* DIPOLE ARRAY
-----
* BA = b/a, R = k = reflection coefficient, DA = d/a,
* RAR0 =  $\rho_a/\rho_s$ , B1 = dilution factor of surrounding
* material, B2 = dilution factor of dike, B11 =
* distortion factor of surrounding material.
*****
      IMPLICIT REAL*8(A-H,O-Z)
      COMMON BA,R,IN
      REAL SR,SDA,SB1,SB11,SB2
      OPEN(UNIT=10,FILE='U6.DAT',STATUS='NEW')
C      WRITE(9,*)'D/A=.....,RA/R0=.....'
      IR=1
      DA=6.0D0
      DAM=DA+1.0D0
      BA=.250D0
      R1R0=10.0D0
      R=(R1R0-1.0D0)/(R1R0+1.0D0)
      R2=R*R
      IN=700
      SBA=SNGL(BA)
C      WRITE(10,*)' M=',IN,'          B/A=',SBA,'   R2/R1=100.'
C      write(10,*)' D/A=','          RA/R0=','       B1=','
C      &      B11='
c 57 B11=(1.0D0-R2)*(-(1.0D0+R)*D3(1.0D0,DA)+.5D0*DD3(1.0D0,DA)
c      C *(1.0D0-R2))/(4.0D0*F3(1.0D0,DA))
c      WRITE(9,*)DA,B11
c      WRITE(6,*)DA,B11
c      DA=DA-.1D0
c      IF(DA.LT..250D0)GO TO 102
c      GO TO 57
*#####
6      IF(DA.LE.6.0D0.AND.DA.GT.3.250D0)THEN
C      WRITE(6,*)'1'
C      WRITE(9,*)'1'
      RAR0=-F1(3.0D0,DA)-F1(3.0D0,DAM)+F1(2.0D0,DA)+F1(4.0D0,DAM)
      DH=-D1(3.0D0,DA)-D1(3.0D0,DAM)+D1(2.0D0,DA)+D1(4.0D0,DAM)
      SH=-DD1(3.0D0,DA)-DD1(3.0D0,DAM)+DD1(2.0D0,DA)+DD1(4.0D0,DAM)
      B1=-DH*(1.0D0-R2)*.5D0/RAR0+1.0D0
      B11=(1.0D0-R2)*(-(1.0D0+R)*DH+.5D0*(1.0D0-R2)*SH)
C      /(4.0D0*RAR0)
      B2=1.0D0-B1
*#####
      ELSE IF(DA.GT.2.750D0.AND.DA.LE.3.250D0)THEN
C      WRITE(6,*)'1,2'
C      WRITE(9,*)'1,2'
      RAR0=-F1(3.0D0,DAM)+F1(2.0D0,DA)+F2(4.0D0,DAM)-F2(3.0D0,DA)
      DH=-D1(3.0D0,DAM)+D1(2.0D0,DA)+D2(4.0D0,DAM)-D2(3.0D0,DA)
      SH=-DD1(3.0D0,DAM)+DD1(2.0D0,DA)+DD2(4.0D0,DAM)-DD2(3.0D0,DA)
      B1=-DH*(1.0D0-R2)*.5D0/RAR0+1.0D0
      B11=(1.0D0-R2)*(-(1.0D0+R)*DH+.5D0*(1.0D0-R2)*SH)
C      /(4.0D0*RAR0)
      B2=1.0D0-B1
*#####
      ELSE IF(DA.GT.2.250D0.AND.DA.LE.2.750D0)THEN

```

```

RAR0=F1(2.0D0,DA)-F1(3.0D0,DAM)-F3(3.0D0,DA)+F3(4.0D0,DAM)
DH=D1(2.0D0,DA)-D1(3.0D0,DAM)-D3(3.0D0,DA)+D3(4.0D0,DAM)
SH=DD1(2.0D0,DA)-DD1(3.0D0,DAM)-DD3(3.0D0,DA)+DD3(4.0D0,DAM)
B1=-DH*(1.0D0-R2)*.5D0/RAR0+1.0D0
B11=(1.0D0-R2)*(-(1.0D0+R)*DH+.5D0*(1.0D0-R2)*SH)
& /(4.0D0*RAR0)
B2=1.0D0-B1
*#####
C ELSE IF(DA.GT.2.0D0.AND.DA.LE.3.0D0)THEN
C WRITE(6,*)'2'
C WRITE(9,*)'2'
C RAR0=-F2(3.0D0,DAM)+F2(2.0D0,DA)+F2(4.0D0,DAM)-F2(3.0D0,DA)
C DH=-D2(3.0D0,DAM)+D2(2.0D0,DA)+D2(4.0D0,DAM)-D2(3.0D0,DA)
C SH=-DD2(3.0D0,DAM)+DD2(2.0D0,DA)+DD2(4.0D0,DAM)-DD2(3.0D0,DA)
C B1=-DH*(1.0D0-R2)*.5D0/RAR0+1.0D0
C B11=(1.0D0-R2)*(-(1.0D0+R)*DH+.5D0*(1.0D0-R2)*SH)
C C /(4.0D0*RAR0)
C B2=1.0D0-B1
*#####
ELSE IF(DA.GT.1.750D0.AND.DA.LE.2.250D0)THEN
C WRITE(6,*)'2,3'
C WRITE(9,*)'2,3'
C RAR0=-F2(3.0D0,DAM)+F2(2.0D0,DA)+F3(4.0D0,DAM)-F3(3.0D0,DA)
C DH=-D2(3.0D0,DAM)+D2(2.0D0,DA)+D3(4.0D0,DAM)-D3(3.0D0,DA)
C SH=-DD2(3.0D0,DAM)+DD2(2.0D0,DA)+DD3(4.0D0,DAM)-DD3(3.0D0,DA)
C B1=-DH*(1.0D0-R2)*.5D0/RAR0+1.0D0
C B11=(1.0D0-R2)*(-(1.0D0+R)*DH+.5D0*(1.0D0-R2)*SH)
C C /(4.0D0*RAR0)
C B2=1.0D0-B1
*#####
ELSE IF(DA.GT..250D0.AND.DA.LE.1.750D0)THEN
C WRITE(6,*)'3'
C WRITE(9,*)'3'
C RAR0=F3(2.0D0,DA)-F3(3.0D0,DAM)-F3(3.0D0,DA)+F3(4.0D0,DAM)
C DH=D3(2.0D0,DA)-D3(3.0D0,DAM)-D3(3.0D0,DA)+D3(4.0D0,DAM)
C SH=DD3(2.0D0,DA)-DD3(3.0D0,DAM)-DD3(3.0D0,DA)+DD3(4.0D0,DAM)
C B1=-DH*(1.0D0-R2)*.5D0/RAR0+1.0D0
C B11=(1.0D0-R2)*(-(1.0D0+R)*DH+.5D0*(1.0D0-R2)*SH)
& /(4.0D0*RAR0)
C B2=1.0D0-B1
*#####
ELSE IF(DA.GT.-0.250D0.AND.DA.LE..250D0)THEN
C WRITE(6,*)'3,4'
C WRITE(9,*)'3,4'
C RAR0=-F3(3.0D0,DAM)+F3(4.0D0,DAM)+F4(2.0D0,DA)-F4(3.0D0,DA)
C DH=-D3(3.0D0,DAM)+D3(4.0D0,DAM)+D4(2.0D0,DA)-D4(3.0D0,DA)
C SH=-DD3(3.0D0,DAM)+DD3(4.0D0,DAM)+DD4(2.0D0,DA)-DD4(3.0D0,DA)
C B1=-DH*(1.0D0-R2)*.5D0/RAR0+1.0D0
C B11=(1.0D0-R2)*(-(1.0D0+R)*DH+.5D0*(1.0D0-R2)*SH)
& /(4.0D0*RAR0)
C B2=1.0D0-B1
*#####
ELSE IF(DA.GT.-1.0D0.AND.DA.LE.0.0D0)THEN
C WRITE(6,*)'4'
C WRITE(9,*)'4'
C RAR0=-F4(3.0D0,DAM)+F4(2.0D0,DA)+F4(4.0D0,DAM)-F4(3.0D0,DA)
C DH=-D4(3.0D0,DAM)+D4(2.0D0,DA)+D4(4.0D0,DAM)-D4(3.0D0,DA)
C SH=-DD4(3.0D0,DAM)+DD4(2.0D0,DA)+DD4(4.0D0,DAM)-DD4(3.0D0,DA)
C B1=-DH*(1.0D0-R2)*.5D0/RAR0+1.0D0
C B11=(1.0D0-R2)*(-(1.0D0+R)*DH+.5D0*(1.0D0-R2)*SH)

```

```

C      &      /(4.0D0*RAR0)
C      B2=1.0D0-B1
*@@@@@@@@@@@@@@@@
      ELSE IF(DA.GT.-.750D0.AND.DA.LE.-0.250D0)THEN
C      WRITE(6,*)'5,3'
C      WRITE(9,*)'5,3'
      RAR0=F5(2.0D0,DA)-F3(3.0D0,DAM)-F5(3.0D0,DA)+F3(4.0D0,DAM)
      DH=D5(2.0D0,DA)-D3(3.0D0,DAM)-D5(3.0D0,DA)+D3(4.0D0,DAM)
      SH=DD5(2.0D0,DA)-DD3(3.0D0,DAM)-DD5(3.0D0,DA)+DD3(4.0D0,DAM)
      B1=-DH*(1.0D0-R2)*.5D0/RAR0+1.0D0
      B11=(1.0D0-R2)*(-(1.0D0+R)*DH+.5D0*(1.0D0-R2)*SH)
      &      /(4.0D0*RAR0)
      B2=1.0D0-B1
*****
      ELSE IF(DA.GT.-1.250D0.AND.DA.LE.-.750D0)THEN
C      WRITE(6,*)'5,4'
C      WRITE(9,*)'5,4'
      RAR0=F5(2.0D0,DA)-F4(3.0D0,DAM)-F5(3.0D0,DA)+F4(4.0D0,DAM)
      DH=D5(2.0D0,DA)-D4(3.0D0,DAM)-D5(3.0D0,DA)+D4(4.0D0,DAM)
      SH=DD5(2.0D0,DA)-DD4(3.0D0,DAM)-DD5(3.0D0,DA)+DD4(4.0D0,DAM)
      B1=-DH*(1.0D0-R2)*.5D0/RAR0+1.0D0
      B11=(1.0D0-R2)*(-(1.0D0+R)*DH+.5D0*(1.0D0-R2)*SH)
      &      /(4.0D0*RAR0)
      B2=1.0D0-B1
*****
      ELSE
C      WRITE(6,*)'5'
C      WRITE(9,*)'5'
      RAR0=-F5(3.0D0,DAM)-F5(3.0D0,DA)+F5(2.0D0,DA)+F5(4.0D0,DAM)
      DH=-D5(3.0D0,DAM)-D5(3.0D0,DA)+D5(2.0D0,DA)+D5(4.0D0,DAM)
      SH=-DD5(3.0D0,DAM)-DD5(3.0D0,DA)+DD5(2.0D0,DA)+DD5(4.0D0,DAM)
      B1=-DH*(1.0D0-R2)*.5D0/RAR0+1.0D0
      B11=(1.0D0-R2)*(-(1.0D0+R)*DH+.5D0*(1.0D0-R2)*SH)
      &      /(4.0D0*RAR0)
      B2=1.0D0-B1
*@@@@@@@@@@@@@@@@
      END IF
      SDA=SNGL(DA)
      SR=SNGL(RAR0)
      SB1=SNGL(B1)
      SB11=SNGL(B11)
      SB2=SNGL(B2)
      WRITE(10,*)SDA,SR,SB1,SB11,SB2
C      WRITE(6,*)SDA,SR,SB1,SB11,SB2
      DA=DA-.20D0
      DAM=DA+1.0D0
C      WRITE(6,*)'IR',IR
      IF(DA.LT.-4.0D0)GO TO 7
      IR=IR+1
      GO TO 6
7 CLOSE(UNIT=10)
102 STOP
      END
*****
      FUNCTION F1(X,DAY)
      IMPLICIT REAL*8(A-H,O-Z)
      COMMON BA,R,IN
C      WRITE(6,*)'1',BA,DAY,R
      S1=1.0D0/X+R/(2.0D0*(DAY-BA)-X)
      DO 1 M=0,IN

```

```

M2=2*M
FM2=DFLOAT(2*M+1)
1 S1=S1-R*(1.0D0-R*R)*R**M2/(2.0D0*(FM2*BA+DAY)-X)
F1=S1*12.0D0
C WRITE(6,*)'F1=',F1
RETURN
END
*****
FUNCTION F2(X,DAY)
IMPLICIT REAL*8(A-H,O-Z)
COMMON BA,R,IN
C WRITE(6,*)'2',BA,DAY,R
S2=0.0D0
DO 2 M=0,IN
FM=DFLOAT(M)
FM2=DFLOAT(2*M+1)
M2=M*2
2 S2=S2-R*R**M2/(2.0D0*(FM2*BA+DAY)-X)+R**M2/
C (FM*4.0D0*BA+X)
F2=S2*(1.0D0+R)*12.0D0
C WRITE(6,*)'F2=',F2
RETURN
END
*****
FUNCTION F3(X,DAY)
IMPLICIT REAL*8(A-H,O-Z)
COMMON BA,R,IN
C WRITE(6,*)'3',BA,DAY,R
S3=.0D0
DO 3 M=0,IN
FM4=DFLOAT(4*M)
M2=M*2
3 S3=S3+R**M2/(FM4*BA+X)
F3=S3*(1.0D0-R*R)*12.0D0
C WRITE(6,*)'F3=',F3
RETURN
END
*****
FUNCTION F3A(X,DAY)
IMPLICIT REAL*8(A-H,O-Z)
COMMON BA,R,IN
S3A=1.0D0/X
DO 11 M=0,IN
FM4=DFLOAT(4*(M+1))
FM2=DFLOAT(2*M+1)
M2=M*2
11 S3A=S3A+R*R*(R**M2/(FM4*BA+X)+R**M2/(FM4*BA-X))
& -R*(R**M2/(2.0D0*(FM2*BA+DAY)-X)+R**M2/(2.0D0
& *(FM2*BA-DAY)+X))
F3A=S3A*((1.0D0+R)/(1.0D0-R))*12.0D0
C WRITE(6,*)'F3A=',F3A
RETURN
END
*****
FUNCTION F4(X,DAY)
IMPLICIT REAL*8(A-H,O-Z)
COMMON BA,R,IN
C WRITE(6,*)'4',BA,DAY,R
S4=0.0D0
DO 4 M=0,IN

```

```

M2=M*2
FM4=DFLOAT(M*4)
FM2=DFLOAT(2*M+1)
4 S4=S4+R**M2/(FM4*BA+X)-R*(R**M2/(2.0D0*(FM2*BA-DAY)+
C X))
F4=S4*(1.0D0+R)*12.0D0
C WRITE(6,*)'F4=',F4
RETURN
END
*****
FUNCTION F5(X,DAY)
IMPLICIT REAL*8(A-H,O-Z)
COMMON BA,R,IN
C WRITE(6,*)'5',BA,DAY,R
S5=1.0D0/X
DO 5 M=0,IN
FM2=DFLOAT(2*M+1)
FM3=DFLOAT(2*M-1)
M2=M*2
5 S5=S5+R**M2/(2*(FM3*BA-DAY)+X)-R**M2/(2*(FM2*BA-DAY)+X)
F5=S5*12.0D0
C WRITE(6,*)'F5=',F5
RETURN
END
*****
FUNCTION D1(X,DAY)
IMPLICIT REAL*8(A-H,O-Z)
REAL*8 M,M1
COMMON BA,R,IN
S1=1.0D0/(2.0D0*(DAY-BA)-X)
C write(6,*)'5'
DO 2 N=0,IN
M=DFLOAT(2*N)
M1=DFLOAT(2*N+1)
R2=R*R
RM=R**(2*N)
RM0=R**(2*N-1)
S1=S1-(1.0D0-3.0D0*R2)*RM/(2.0D0*(M1*BA+DAY)-X)
& -R*(1.0D0-R2)*M*RM0/(2.0D0*(M1*BA+DAY)-X)
2 CONTINUE
D1=S1*12.0D0
RETURN
END
*****
FUNCTION D2(X,DAY)
IMPLICIT REAL*8(A-H,O-Z)
REAL*8 M,M1
COMMON BA,R,IN
S2=0.0D0
C write(6,*)'4'
DO 3 N=0,IN
M=DFLOAT(2*N)
M1=DFLOAT(2*N+1)
RM=R**(2*N)
RM0=R**(2*N-1)
R2=R*R
S2=S2+RM/(2.0D0*M*BA+X)
& -R*RM/(2.0D0*(M1*BA+DAY)-X)
& +(1.0D0+R)*(M*RM0/(2.0D0*M*BA+X)
& -M1*RM/(2.0D0*(M1*BA+DAY)-X))

```

```

3 CONTINUE
  D2=S2*12.0D0
  RETURN
  END
*****
FUNCTION D3(X, DAY)
  IMPLICIT REAL*8(A-H,O-Z)
  REAL*8 M,M1,M2
  COMMON BA,R,IN
  S3=0.0D0
C   write(6,*)'3'
  DO 4 N=0,IN
    M2=DFLOAT(2*N+2)
    M=DFLOAT(2*N)
    M1=DFLOAT(2*N+1)
    RM=R**(2*N)
    R2=R*R
    RM0=R**(2*N-1)
    S3=S3+(1-R2)*M*RM0/(2.0D0*M*BA+X)
    &   -2.0D0*R*RM/(2.0D0*M*BA+X)
4   continue
  D3=S3*12.0D0
  RETURN
  END
*****
FUNCTION D3A(X, DAY)
  IMPLICIT REAL*8(A-H,O-Z)
  REAL*8 M,M1,M2,M0
  COMMON BA,R,IN
  S3A=2.0D0/((1.0D0-R)**2*X)
C   WRITE(6,*)'3'
  DO 4 N=0,IN
    M2=DFLOAT(2*N+2)
    M=DFLOAT(2*N)
    M1=DFLOAT(2*N+1)
    M0=DFLOAT(N+1)
    RM=R**(2*N)
    R2=R*R
    RM0=R**(2*N-1)
    RM1=R**(2*N+1)
    A=R2*(RM/(2.0D0*M2*BA+X)+RM/(2.0D0*M2*BA-X))
    &   -R*(RM/(2.0D0*(M1*BA+DAY)-X)+RM/(2.0D0*(M1*BA-DAY)+X))
    B=(1.0D0+R)/(1.0D0-R)
    C=(1.0D0-R)**2
    S3A=S3A+2.0D0*A/C+B*(
    &   2.0D0*M0*RM1/(2.0D0*M2*BA+X)
    &   +2.0D0*M0*RM1/(2.0D0*M2*BA-X)
    &   -RM*M1/(2.0D0*(M1*BA+DAY)-X)
    &   -RM*M1/(2.0D0*(M1*BA-DAY)+X))
4   CONTINUE
  D3A=S3A*12.0D0
  RETURN
  END
*****
FUNCTION D4(X, DAY)
  IMPLICIT REAL*8(A-H,O-Z)
  REAL*8 M,M1
  COMMON BA,R,IN
  S4=0.0D0
C   write(6,*)'2'

```

```

DO 5 N=0,IN
M=DFLOAT(2*N)
M1=DFLOAT(2*N+1)
RM=R**(2*N)
RM0=R**(2*N-1)
A=RM/(2.0D0*M*BA+X)-R*RM/(2.0D0*(M1*BA-DAY)+X)
S4=S4+A+(1.0D0+R)*(M*RM0/(2.0D0*M*BA+X)
&      -RM/(2.0D0*(M1*BA-DAY)+X)
& -R*M*RM0/(2.0D0*(M1*BA-DAY)+X))
5 CONTINUE
D4=S4*12.0D0
RETURN
END
*****
FUNCTION D5(X,DAY)
IMPLICIT REAL*8(A-H,O-Z)
REAL*8 M,M1,M0
COMMON BA,R,IN
S5=0.0D0
C   write(6,*)'1'
DO 6 N=0,IN
M=DFLOAT(2*N)
M1=DFLOAT(2*N+1)
M0=DFLOAT(2*N-1)
RM=R**(2*N)
RM0=R**(2*N-1)
S5=S5+R*M*RM0/(2.0D0*(M0*BA-DAY)+X)
&      +RM/(2.0D0*(M0*BA-DAY)+X)
&      -RM/(2.0D0*(M1*BA-DAY)+X)
&      -R*M*RM0/(2.0D0*(M1*BA-DAY)+X)
6 CONTINUE
D5=S5*12.0D0
RETURN
END
*****
FUNCTION DD1(X,DAY)
IMPLICIT REAL*8(A-H,O-Z)
REAL*8 M,M1,M0
COMMON BA,R,IN
S11=0.0D0
C   write(6,*)'5'
DO 2 N=0,IN
M=DFLOAT(2*N)
M1=DFLOAT(2*N+1)
M0=DFLOAT(2*N-1)
R2=R*R
RM=R**(2*N)
RM0=R**(2*N-1)
RM2=R**(2*N-2)
QM1=1.0D0/(2.0D0*(M1*BA+DAY)-X)
S11=S11+6.0D0*R*RM*QM1
&      -2.0D0*(1.0D0-3.0D0*R2)*M*RM0*QM1
&      -R*(1.0D0-R2)*M*M0*RM2*QM1
2 CONTINUE
DD1=S11*12.0D0
RETURN
END
*****
FUNCTION DD2(X,DAY)
IMPLICIT REAL*8(A-H,O-Z)

```

```

REAL*8 M,M1,M0,M2
COMMON BA,R,IN
S22=0.0D0
C   write(6,*)'4'
DO 3 N=0,IN
M=DFLOAT(2*N)
M1=DFLOAT(2*N+1)
M0=DFLOAT(2*N-1)
M2=DFLOAT(N+1)
RM=R**(2*N)
RM0=R**(2*N-1)
RM2=R**(2*N-2)
R2=R*R
S22=S22+2.0D0*M*RM0/(2.0D0*M*BA+X)
&   -2.0D0*M2*RM/(2.0D0*(M1*BA+DAY)-X)
&   -R*M*RM0/(2.0D0*(M1*BA+DAY)-X)
& +(1.0D0+R)*(M*M0*RM2/(2.0D0*M*BA+X)
&   -M1*M*RM0/(2.0D0*(M1*BA+DAY)-X))
3  CONTINUE
DD2=S22*12.0D0
RETURN
END
*****
FUNCTION DD3(X,DAY)
IMPLICIT REAL*8(A-H,O-Z)
REAL*8 M0,M1,M,M2
COMMON BA,R,IN
S33=0.0D0
C   write(6,*)'3'
DO 4 N=0,IN
M2=DFLOAT(2*N+2)
M=DFLOAT(2*N)
M1=DFLOAT(2*N+1)
M0=DFLOAT(2*N-1)
RM=R**(2*N)
R2=R*R
RM0=R**(2*N-1)
RM2=R**(2*N-2)
S33=S33-2.0D0*RM/(2.0D0*M*BA+X)
&   -4.0D0*R*M*RM0/(2.0D0*M*BA+X)
&   +(1.0D0-R2)*M*M0*RM2/(2.0D0*M*BA+X)
4  continue
DD3=S33*12.0D0
RETURN
END
*****
FUNCTION DD3A(X,DAY)
IMPLICIT REAL*8(A-H,O-Z)
REAL*8 M2,M1,M,M3,M4,M0
COMMON BA,R,IN
A=1.0D0/X
B=0.0D0
S=0.0D0
C   WRITE(6,*)'3'
DO 4 N=0,IN
M2=DFLOAT(2*N+2)
M=DFLOAT(2*N)
M1=DFLOAT(2*N+1)
M0=DFLOAT(2*N-1)
M3=DFLOAT(N)

```

```

M4=DFLOAT(N+1)
RM=R**(2*N)
R2=R*R
RM0=R**(2*N-1)
RM2=R**(2*N-2)
RM1=R**(2*N+1)
A=A+R2*(RM/(4.0D0*M4*BA+X)+RM/(4.0D0*M4*BA-X))
C -R*(RM/(2.0D0*(M1*BA+DAY)-X)+RM/(2.0D0*(M1*BA-DAY)+X))
B=B+2.0D0*RM1*(1.0D0/(4.0D0*M4*BA+X)+1.0D0/(4.0D0*M4*BA-X))
C +RM1*M*(1.0D0/(4.0D0*M4*BA+X)+1.0D0/(4.0D0*M4*BA-X))
C -RM/(2.0D0*(M1*BA+DAY)-X)-RM/(2.0D0*(M1*BA-DAY)+X)-
C M*RM*(1.0D0/(2.0D0*(M1*BA+DAY)-X)+1.0D0/(2.0D0*(M1*BA-DAY)+X))
S=S+2.0D0*RM*((1.0D0+2.0D0*M+M*M0*.5D0)/(4.0D0*M4*BA+X)+
C (1.0D0+2.0D0*M+M*M0*.5D0)/(4.0D0*M4*BA-X))
C -2.0D0*M*RM0*(1.0D0/(2.0D0*(M1*BA+DAY)-X)
C +1.0D0/(2.0D0*(M1*BA-DAY)+X))-M*M0*RM0*(1.0D0
C /(2.0D0*(M1*BA+DAY)-X)+1.0D0/(2.0D0*(M1*BA-DAY)+X))
4 CONTINUE
DD3A=(4.0D0*A/(1.0D0-R)**3+4.0D0*B/(1.0D0-R)**2+
C (1.0D0+R)*S/(1.0D0-R))*12.0D0
RETURN
END
*****
FUNCTION DD4(X, DAY)
IMPLICIT REAL*8(A-H, O-Z)
REAL*8 M, M0, M1
COMMON BA, R, IN
S44=0.0D0
C write(6,*)'2'
DO 5 N=0, IN
M=DFLOAT(2*N)
M1=DFLOAT(2*N+1)
M0=DFLOAT(2*N-1)
R2=R*R
RM=R**(2*N)
RM0=R**(2*N-1)
RM2=R**(2*N-2)
A=M*RM0/(2.0D0*M*BA+X)-RM/(2.0D0*(M1*BA-DAY)+X)
& -R*M*RM0/(2.0D0*(M1*BA-DAY)+X)
S44=S44+2.0D0*A+(1.0D0+R)*(M*M0*RM2/(2.0D0*M*BA+X)
& -2.0D0*M*RM0/(2.0D0*(M1*BA-DAY)+X)
& -R*M*M0*RM2/(2.0D0*(M1*BA-DAY)+X))
5 CONTINUE
DD4=S44*12.0D0
RETURN
END
*****
FUNCTION DD5(X, DAY)
IMPLICIT REAL*8(A-H, O-Z)
REAL*8 M, M1, M0
COMMON BA, R, IN
S55=0.0D0
C write(6,*)'1'
DO 6 N=0, IN
M=DFLOAT(2*N)
M1=DFLOAT(2*N+1)
M0=DFLOAT(2*N-1)
R2=R*R
RM=R**(2*N)
RM0=R**(2*N-1)

```

```
RM2=R**(2*N-2)
S55=S55+2.0D0*M*RM0/(2.0D0*(M0*BA-DAY)+X)
&      +R*M*M0*RM2/(2.0D0*(M0*BA-DAY)+X)
&      -2.0D0*M*RM0/(2.0D0*(M1*BA-DAY)+X)
&      -R*M*M0*RM2/(2.0D0*(M1*BA-DAY)+X)
6 CONTINUE
DD5=S55*12.0D0
RETURN
END
*****&***** (*****
```

```

*****
* 4. COMPUTER PROGRAM FOR APPARENT RESISTIVITY WHEN THICKNESSES
*   OF DIKE GOES TO INFINITY (POLE-POLE ARRAY)
*****
  IMPLICIT REAL*8(A-H,O-Z)
  REAL SR,SDA
  OPEN(UNIT=59,FILE='hf6.DAT',STATUS='NEW')
  WRITE(9,*)'D/A=.....,RA/R0=.....'
  DA=-10.0D0
  R1R0=.010D0
  IR=0
  R=(R1R0-1.0D0)/(R1R0+1.0D0)
6  IF(DA.GE.1.0D0.AND.DA.LE.10.0D0)THEN
    RAR0=1.0D0+R/(2.0D0*DA-1.0D0)
  ELSE IF(DA.GT..0D0.AND.DA.LT.1.0D0)THEN
    RAR0=1.0D0+R
  ELSE
    RAR0=(1.0D0-R/(-2.0D0*DA+1.0D0))*(1.0D0+R)/(1.0D0-R)
  END IF
  WRITE(6,*)'IR=',IR,'DA=',DA,'RAR0=',RAR0
  SR=SNGL(RAR0)
  SDA=SNGL(DA)
  WRITE(59,*)SR,SDA
  DA=DA+.2D0
  IR=IR+1
  IF(DA.GT.10.0D0)GO TO 8
  GO TO 6
8  CLOSE(UNIT=59)
  STOP
  END

```

REFERENCES

- Abramowitz, M. and Stegun, I.A., 1970. Handbook of Mathematical Functions with Formulas, Graphs, and Mathematical Tables, National Bureau of Standards, Applied Mathematics Series, No. 55, 1046 pages.
- Aguirre, G., 1986. An Appraisal of the Electrically Thin Conductive Sheet Model in Geophysical Probing, M.S. Thesis, Dept. of Electrical and Computer Engineering, University of Arizona, 103 pages.
- Aguirre, G. and Wait, J.R., 1985. "Resistivity and induced polarization response of a thin sheet," *Pageoph.*, Vol. 123, pp. 882-892.
- Al-Chalabi, M., 1969. "Theoretical resistivity anomalies across a single vertical discontinuity," *Geophysical Prospecting*, Vol. 17, pp. 63-81.
- Al'pin, L.M., Berdichevskii, M.N., Vedrintsev, G.A., and Zagarmistr, A.M. (translated by G. V. Keller), 1966. Dipole Methods for Measuring Earth Conductivity, Consultants Bureau New York, 302 pages.
- Anderson, L.A. and Keller, G.V., 1964. "A study in induced polarization," *Geophysics*, Vol. 29, No. 5, pp. 848-864.
- Brant, A.A., 1981. "A History of Induced Polarization Development as Seen From the Perspective of the Newmont Mining Group, 1946-1960": In Advances in Induced Polarization and Complex Resistivity, edited by J.S. Sumner, University of Arizona, Laboratory of Geophysics, Tucson, pp. 1-19.
- Cook, K.L. and Van Nostrand, R.G., 1954. "Interpretation of resistivity data over filled sinks," *Geophysics*, Vol. 19, No. 4, pp. 761-770.
- Dakhnov, V.N. (translated by G.V. Keller), 1962. "Geophysical well logging," *Quarterly Colorado School of Mines*, Vol. 57, No. 2.
- Das, U.C., 1984. "A single digital linear filter for computations in electrical methods, A unifying approach," *Geophysics*, Vol. 49, pp. 1115-1118.
- Flanagan, P. W., 1982. Induced Polarization Response of Disseminated Mineralization for Spheroidal Geometries, M.S. Thesis, Dept. of Geosciences, University of Arizona.
- Gruszka, T.P. and Wait, J.R., 1985. "Dilution and distortion effects in the induced polarization of a two-layer earth," *IEEE Transactions on Geoscience and Remote Sensing*, Vol. GE-23, No. 4, pp. 606-610.
- Hedstrom, H., 1932. "Electrical prospecting for auriferous quartz veins and reefs," *Mining Magazine*, pp. 201-213.

- Keller, G.V. and Frischknecht, F.C., 1970. Electrical Methods in Geophysical Prospecting, Pergamon Press, 517 pages.
- Koefoed, O., 1979. Geosounding Principles, 1, Resistivity Sounding Measurements, Elsevier Scientific Publishing Company, 276 pages.
- Logn, O., 1954. "Mapping nearly vertical discontinuities by earth resistivities," *Geophysics*, Vol. 19, No. 4, pp. 739-760.
- Ludwig, C.S. and Henson, H.K., 1967. Theoretical Induced Polarization and Resistivity Response for the Dual Frequency System Collinear Dipole-Dipole Array, Vol. 1 and 2, Heinrichs Geoexploration Company, 241 pages.
- Maxwell, C., 1892. A Treatise on Electricity and Magnetism, Vol. 1, The Clarendon Press, 506 pages.
- Nabighian, M.N., 1987. Exploration geophysics, Geos-560 class notes, University of Arizona.
- Nabighian, M.N. and Elliot, C.L., 1976. "Negative induced polarization effects from layered media," *Geophysics*, Vol. 41, pp. 1236-1255.
- Nadiu, P., 1966. "Theoretical analysis of apparent resistivity over a dike of arbitrary shape," *Geophysical Prospecting*, Vol. 14, pp. 168-183.
- Pelton, W.H., Ward, S.H., Hallof, P.G., Sill, W.R., and Nelson, P.H., 1978. "Mineral discrimination and removal of inductive coupling with multifrequency IP," *Geophysics*, Vol. 43, No. 3, pp. 588-609.
- Peters, A., 1986. Hemispherical sink model, Grad. Student Project, ECE-586, University of Arizona.
- Seigel, H.O., 1959. "Mathematical formulation and type curves for induced polarization," *Geophysics*, Vol. 24, No. 3, pp. 547-565.
- Sumner, J. S., 1976. Principles of Induced Polarization for Geophysical Exploration, Elsevier Scientific Publishing Company, 259 pages.
- Synder, D.D., 1977. "Induced parameters, Part 2": In Induced Polarization for Exploration Geologists and Geophysicists, edited by J.S. Sumner, University of Arizona, pp. 79-104.
- Tagg, G.F., 1930. "The earth resistivity method of geophysical prospecting," *Mining Magazine*, pp. 150-158.
- Tagg, G.F., 1964. Earth Resistances, George Newnes Limited, 258 pages.
- Telford, W.M., Geldart, L.P., Sheriff, R.E., and Keys, D.A., 1976. Applied Geophysics, Cambridge University Press, pp. 632-734.

- Van Blaricom, R., 1971. Induced Polarization and Resistivity Modeling of Dikes and Other Selected Structural Features, M.S. Thesis, Dept. of Geosciences, University of Arizona.
- Wait, J.R., 1959. Overvoltage Research and Geophysical Applications, Pergamon Press, 158 pages.
- Wait, J.R., 1981. "Towards a general theory of induced electrical polarization in geophysical exploration," *I.E.E.E. Transactions on Geoscience and Remote Sensing*, Vol. GE-19, No. 4, pp. 231-234.
- Wait, J.R., 1982. Geoelectromagnetism, Academic Press, 268 pages.
- Wait, J.R., 1984a. A Biased Collection of Papers and Unpublished Material Relating to I.P. in Electrical Geophysics.
- Wait, J.R., 1984b. "Relaxation phenomena and induced polarization," *Geoplotation*, Vol. 22, pp. 107-127.
- Wait, J.R., 1986. "Extensions to the phenomenological theory of induced polarization," *I.E.E.E. Transactions on Geoscience and Remote Sensing*, Vol. GE-24, No. 3, pp. 409-414.
- Wait, J.R. and Gruszka, T.P., 1987. "Resistivity and induced polarization response for a borehole model," *I.E.E.E. Transactions on Geoscience and Remote Sensing*, Vol. GE-25, No. 3, pp. 368-371.
- Watson, G.N., 1966. A Treatise on the Theory of Bessel Functions, Cambridge University Press, Series 55, 1046 pages.
- Wilkins, J.R., 1974. An I.P. Survey at Meteor Crater, M.S. Thesis, Dept. of Geosciences, University of Arizona.